

THE ROLE OF EGFR AND JAK/STAT SIGNALING DURING REGENERATIVE
NEUROGENESIS IN THE ZEBRAFISH OLFACTORY EPITHELIUM

by

Aysu Şevval Alkiraz

B.S., Molecular Biology and Genetics, Uludağ University, 2019

Submitted to the Institute for Graduate Studies in
Science and Engineering in partial fulfillment of
the requirements for the degree of
Master of Science

Graduate Program in Molecular Biology and Genetics

Boğaziçi University

2022

ACKNOWLEDGEMENTS

I would like to express my deep and sincere gratitude to my jury members for their endless support, especially to my supervisor, Assoc. Prof. Stefan Fuss, for his guidance throughout this research. It would not be possible for me to finish it without his vision, sincerity and motivation. I would also like to thank all the members of Boğaziçi University MBG Department. Starting with Mehmet Can Demirler and Yiğit Kocagöz for their valuable guidance throughout my time in Fish Lab and being always available for questions. I would like to extend my thanks to rest of the Fish Lab members, especially Zeynep Dokuzluoğlu and Şiran Şireci for their friendship and support both in and outside of the lab. I also would like to express how grateful I am to have Barış Can Mandacı, Ayşe Kahraman, and Emre Pekbilir as my friends.

The work presented in this thesis has been supported by The Scientific and Technological Research Council of Turkey (TÜBİTAK) through research grant 119Z081 to SHF.

ABSTRACT

THE ROLE OF EGFR AND JAK/STAT SIGNALING DURING REGENERATIVE NEUROGENESIS IN THE ZEBRAFISH OLFACTORY EPITHELIUM

The zebrafish olfactory epithelium (OE) has an exceptional neurogenic capacity, which supports the continuous turnover olfactory sensory neurons (OSNs) and efficient regeneration after injury. These processes depend on the presence of a dual stem cell system that is comprised of globose (GBCs) and horizontal basal cells (HBCs), which selectively contribute to maintenance of the intact and repair of the injured OE, respectively. Transcriptome profiling of the injured OE revealed strong upregulation of the HB-EGF. Exogenous stimulation and pharmacological inhibition of HB-EGF signaling show a selective effect on HBCs, suggesting that HB-EGF is a key signal for OE regeneration. Among the known cell surface receptors for HB-EGF, only the transcript levels of ErbB1/EGFR are upregulated in response to injury. EGFR expression localizes to HBCs, suggesting that HB-EGF signals through EGFR to activate injury-responsive HBCs. To investigate the roles of EGFR and JAK/STAT signaling on OSN neurogenesis, the effect of pharmacological inhibition of the pathways on maintenance and repair neurogenesis were evaluated. Inhibition of EGFR signaling resulted in the suppression of basal proliferative activity, which, however, only slightly reduced the rate of OSNs turnover in the intact OE. In the injured tissue, on the other hand, EGFR inhibition resulted in a dramatic impairment of OSN regeneration by preventing the induction of HBC proliferation. A similar impairment in OSN regeneration could also be observed when JAK/STAT signaling was inhibited. Tissue analysis of JAK/STAT activation pointed to an injury-responsive population that is distinct from HBCs. These results suggest that both EGFR and JAK/STAT signaling are necessary for repair neurogenesis but that they are active in distinct populations of the OSN lineage.

ÖZET

EGFR VE JAK/STAT YOLAĞININ ZEBRABALIĞI OLFAKTÖR EPİTELİNDEKİ REJENERATİF NÖROJENEZDEKİ ROLÜ

Zebrabalığı olfaktör epiteli (OE), olfaktör duyu nöronlarının (OSN'ler) sürekli üretimini sağlayan ve hasardan sonra verimli rejenerasyonu destekleyen, olağanüstü nörojenik kapasiteye sahiptir. Bu süreçler, sırasıyla sağlam OE'nin bakımına ve hasarlı OE'nin onarımına seçici olarak katkıda bulunan küresel (GBC'ler) ve yatay bazal hücrelerden (HBC'ler) oluşan ikili bir kök hücre sistemine ağıldır. Bunların aktivitesi, farklı doku koşullarını yansıtan farklı moleküler tetikleyicilere bağı görünmektedir. Transkriptom profillemesi, HB-EGF'nin güçlü bir yükseliş gösterdiğini ortaya çıkardı. HB-EGF yolağının uyarımı ve farmakolojik inhibisyonu, HBC'lere seçici olarak etki gösterir, bu da HB-EGF'nin OE rejenerasyonu için önemine işaret eder. HB-EGF'nin hücre yüzeyi reseptörleri arasında, hasarda, yalnızca ErbB1/ EGFR' nin transkript seviyeleri yükseliş gösterir. EGFR'nin mRNA ekspresyonu, HBC' lerde lokalize olur ve bu, HB-EGF'nin, hasara duyarlı HBC' lerde aktiviteyi yaymak için EGFR'yi kullanabileceğini öne sürer. EGFR ve JAK/STAT yolaklarının OSN nörojenezi üzerindeki rollerini araştırmak için yolakların farmakolojik inhibisyonunun, OSN bakım ve onarım nörojenezine olan etkisi değerlendirildi. EGFR sinyalinin inhibisyonu, bazal proliferatif aktivitenin baskılanmasıyla sonuçlandı, ancak bu, bozulmamış OE'de yeni oluşturulan OSN'lerin sayısını sadece biraz azalttı. Öte yandan, yaralı dokuda EGFR inhibisyonu, HBC proliferasyonunun indüklenmesini önleyerek rejenerasyonunun dramatik bir şekilde bozulmasına neden oldu. Rejenerasyonda benzer bir bozulma JAK/STAT sinyali inhibe edildiğinde de gözlemlendi. JAK/ STAT aktivasyonunun doku analizi, HBC'lerden farklı, yaralanmaya duyarlı bir popülasyona işaret etti. Bu sonuçlar, hem EGFR hem de JAK/STAT sinyalinin onarım nörojenezi için gerekli olduğunu, ancak bunların OSN neslinin farklı hücre popülasyonlarında aktif olduklarını göstermektedir.

TABLE OF CONTENTS

ACKNOWLEDGEMENTS	iii
ABSTRACT	iv
ÖZET	v
LIST OF FIGURES	ix
LIST OF TABLES	xi
LIST OF SYMBOLS	xii
LIST OF ACRONYMS/ABBREVIATIONS	xiii
1. INTRODUCTION	1
1.1. Adult Neurogenesis and Regeneration	1
1.2. Neurogenesis in Tissue Maintenance and Regeneration	4
1.3. The Olfactory Epithelium as a Model of Adult	6
1.3.1. The Structure and Cellular Constituents of the Mammalian OE	7
1.3.2. Structural Differences of the Zebrafish OE	9
1.3.3. Maintenance Neurogenesis in The OE	12
1.3.4. Regeneration of The OE	14
1.4. Molecular Regulators of OE Neurogenesis	16
1.5. EGFR, Its Ligands and Downstream Targets in Regulating Neurogenesis	19
2. PURPOSE	24
3. MATERIALS AND METHODS	26
3.1. Materials	26
3.1.1. Fish	26
3.1.2. Equipment and Supplies	26
3.1.3. Buffers and Solutions	26
3.2. Methods	27
3.2.1. Fish Maintenance	27
3.2.2. BrdU Incorporation Assay	28
3.2.3. Induction of OE Degeneration	28
3.2.4. Stimulation of the OE with human-recombinant HB-EGF	29
3.2.5. Intraperitoneal Injection of Pharmacological Agents	29

3.2.6. OE Dissection	30
3.2.7. OE Cryosectioning and Sample Preparation	30
3.2.8. Immunohistochemistry on OE Cryosections	30
3.2.9. Heat-induced Antigen-Retrieval for pSTAT3 Immunostaining	31
3.2.10. Confocal Microscopy	32
3.2.11. Image Processing, Cell Quantification and Statistics	33
4. RESULTS	35
4.1. The Effect of EGFR Inhibition on Cell Proliferation and OE Regeneration	36
4.1.1. The Effect of EGFR Inhibition on Cell Proliferation	37
4.1.2. The Effect of EGFR Inhibition on the OE Regeneration	43
4.1.2.1. Evaluation of the Efficiency of OSN Neurogenesis.	45
4.1.2.2. Contribution of Newly Generated Cells to OSN Neuro- genesis	47
4.2. The Effect of JAK/STAT Inhibition on Cell Proliferation and OSN Neu- rogenesis	53
4.2.1. The Effect of JAK/STAT Signaling Inhibition on Cell Proliferation	54
4.2.2. The Effect of JAK/STAT Signaling Inhibition on the Efficiency of OSN Regeneration	62
4.3. Activation Pattern of JAK/STAT Signaling in the Intact and Injured OE	65
4.4. Activation Pattern of JAK/STAT Signaling Upon Stimulation with hu- man recombinant HB-EGF	72
5. DISCUSSION	78
5.1. EGFR and JAK/STAT in Tissue Maintenance and Regeneration	79
5.2. EGFR Expression in The OE	81
5.3. pSTAT3 Expression in The OE	82
5.4. Maintenance vs Repair	85
5.4.1. Source of EGFR Ligands and Stimulation	94
5.4.2. Effect of EGFR Signaling Inhibition on OSN Neurogenesis	95
5.4.3. Effect of JAK/STAT Signaling Inhibition on OSN Neurogenesis	97
5.5. Are EGFR and STAT3 Active in the Same Cell Types?	98
5.6. Relationship with Other Niche Factors and Signaling Events	99
5.7. Proposed Model	100

REFERENCES 102
APPENDIX A: Chemicals and Reagents 118
APPENDIX B: Disposable And Non-disposable Equipment 123

LIST OF FIGURES

Figure 1.1.	Schematic representation of the zebrafish OE.	10
Figure 1.2.	Cellular composition of the sensory OE.	11
Figure 1.3.	EGFR signaling.	21
Figure 4.1.	Effect of PD153035 on proliferation rate in the intact and 1 dpl OE.	39
Figure 4.2.	Analysis of the proliferative activity in the intact and 1 dpl OE of DMSO- and PD153035-treated fish.	41
Figure 4.3.	Effect of PD153035 on proliferation and neurogenesis rate in the intact and 5 dpl OE.	44
Figure 4.4.	Analysis of proliferative and neurogenic activity in the intact and 5 dpl OE after PD153035 treatment.	46
Figure 4.5.	Analysis of the cell fates of the newly generated cell populations in the intact and 5 dpl OE after PD153035 treatment.	50
Figure 4.6.	Distribution of single BrdU and HuC/D/BrdU double positive cells in the DMSO- and PD153035-treated OEs.	52
Figure 4.7.	Effect of JSI-124 on proliferation rate in the intact and 1 dpl OE.	55
Figure 4.8.	Analysis of the proliferative activity in the intact and 1 dpl OE of DMSO- and JSI-124-treated fish.	58
Figure 4.9.	Effect of JSI-124 on regeneration.	63

Figure 4.10. JAK/STAT signaling is active in the intact OE.	68
Figure 4.11. JAK/STAT signaling is active in the 2 dpl OE.	71
Figure 4.12. HB-EGF stimulation activates JAK/STAT signaling.	74
Figure 4.13. JAK/STAT signaling is not active in cells activated by HB-EGF. . .	77
Figure 5.1. Proposed model of maintenance and repair neurogenesis.	101

LIST OF TABLES

Table A.1.	List of chemicals and reagents	118
Table A.2.	List of chemicals and reagents (cont.)	119
Table A.3.	Solutions and Buffers	119
Table A.4.	Solutions and buffers (cont.)	120
Table A.5.	Solutions and buffers (cont.)	121
Table A.6.	Solutions and buffers (cont.)	122
Table B.1.	List of disposable and non-disposable equipment	123
Table B.2.	List of disposable and non-disposable equipment (cont.)	124

LIST OF SYMBOLS

dpl	Days post lesion
g	Gram
G	Gauge
L	Liter
M	Molar
mL	Mililiter
ng	Nanogram
μ L	Microliter
μ m	Micrometer
$^{\circ}$ C	Degree Celcius

LIST OF ACRONYMS/ABBREVIATIONS

ANOVA	Analysis of Variance
Ascl1	Achaete-Scute Family BHLH Transcription Factor 1
BrdU	5-Bromo-2'-deoxyuridine
BSA	Bovine Serum Albumin
EGF	Epidermal Growth Factor
EGFR	Epidermal Growth Factor Receptor
GBC	Globose Basal Cell
HBC	Horizontal Basal Cell
EGF	Epidermal Growth Factor
EGFR	Epidermal Growth Factor Receptor
GBC	Globose Basal Cell
HBC	Horizontal Basal Cell
HB-EGF	Heparin-Binding EGF-like Growth Factor
HuC/D	Hu Protein C / D
ILC	Inter Lamellar Curve
JAK	Janus Kinase
Krt5	Keratin 5
MS222	Tricaine Methanesulfonate
MMP	Matrix Metalloprotease
p63	Tumor Protein 63
PBS	Phosphate Buffered Saline
PBST	Phosphate Buffered Saline with Tween 20
PFA	Paraformaldehyde
pH	Potential / Power of Hydrogen
RNA	Ribonucleic Acid
SC	Sustentacular Cell
SEM	Standard Error of Means
SNS	Sensory / Non-sensory Border
Sox2	Sex Determining Region Y-box 2

Tr-X	Triton X-100
Tris	Trisaminomethane
TBS	Tris-Buffered Saline with Tween 20

1. INTRODUCTION

1.1. Adult Neurogenesis and Regeneration

Adult neurogenesis describes the generation and differentiation of nerve cells from neuronal stem/progenitor cells that are active in the postnatal nervous system. The process also includes the migration and functional integration of adult-born neurons into existing circuitries. Despite being a widely studied topic in the 21st century, the phenomenon of adult neurogenesis was subject to a long and controversial debate following its first appearance in the scientific literature. In addition to his detailed observations concerning the structure of and connectivity within the central nervous system (CNS), Santiago Ramon y Cajal described the nervous system to be “fixed” and “immutable”, and as a structure which lacks the postnatal generation of neurons (Cajal, 1913). This view, which became a central dogma of neurobiology, resulted in the widespread neglect and scientific doubt of pioneering work that was performed in the field of adult neurogenesis until the late 1990s.

In addition to arguments originating from the belief that newly born neurons would disturb the stability and function of existing neural circuitries, early studies of adult neurogenesis were also hampered by methodological limitations. A technique that dominated early studies of neurogenesis was the labelling of mitotically active cells by the incorporation of radioactive ^3H -thymidine and was first used to study the dentate gyrus of rats (Altman and Das 1965; Kaplan and Hinds 1977), the amygdala (Bayer, 1980), and the olfactory bulb (Kaplan and Hinds 1977). Yet, skepticism rooting from the lack of proper neuronal markers and the delicacy of performing the ^3H -thymidine labelling technique resulted in a heated controversy and strong disbelief within the scientific community (Owji and Shoja, 2019). Even though the resolving power of electron microscopy allowed for the visualization of detailed neuronal structures that were associated with the labeled cells in the rat (Kaplan and Hinds, 1977; Kaplan, 1981) and primate brain (Kaplan, 1983), the first demonstration of the true neuronal identity of adult-born brain cells dates back to 1988 (Alvarez-Buylla and Nottebohm, 1988).

In these studies, the fluorogold retrograde tracing technique was used on canary brains to visualize neural connections from the synapse to the cell body. The co-staining of tracer-positive cells in combination with 3H-thymidine labelling strongly suggested that the newborn cells in the canary brain were indeed neurons. The invention of a related but simpler birthdating technique, the incorporation of 5-bromo-2'-deoxyuridine (BrdU) into newly synthesized DNA during cell divisions, also allowed for the simultaneous immunohistochemical detection of neuronal markers. This approach enabled the easy and indisputable identification of neurogenic activity in the mammalian and non-mammalian brain (Eriksson *et al.*, 1998; Gould *et al.*, 1999; Kaslin *et al.*, 2008).

Despite the fact that life-long neurogenesis has now been demonstrated in a large number of vertebrate species, the neurogenic rate and the number of active brain regions appears to correlate inversely with the degree of evolutionary complexity (Kaslin *et al.*, 2008; Augusto-Oliveira *et al.*, 2019). While a generally high neurogenesis rate is observed in birds, reptiles, amphibians, and teleost fish, a much lower incidence typically occurs in mammalian species (Kaslin *et al.*, 2008). The difference may partially be explained by the observation that adult neurogenesis in lower vertebrates contributes considerably to postnatal brain growth (Bottjer *et al.*, 1985; Lopez-Garcia *et al.*, 1984; Gaze and Keating, 1972; Johns and Easter, 1977), whereas the process predominantly supports neuronal turnover and replacement of dying cells in mammals (Kaslin *et al.*, 2008). However, the demand for neural plasticity may also contribute to selective neurogenesis in the brains of higher vertebrates. In the mammalian brain, steady but low-rate adult neurogenesis is restricted to two dominant brain regions, the ventricular-subventricular zone (V-SVZ) of the lateral ventricles and the subgranular zone (SGZ) of the dentate gyrus of the hippocampus (Kempermann, 2015). The neuronal precursors generated in the V-SVZ migrate a long distance through the rostral migratory stream and eventually differentiate into inhibitory GABA-ergic interneurons that integrate into olfactory bulb circuitries (Luskin, 1993; Lois and Alvarez-Buyulla 1994; Betarbet *et al.* 1996; Carleton *et al.* 2003). From the SGZ, neuronal precursors only travel a short distance to the overlying layers of the dentate gyrus where they become functional granule cells (Cameron *et al.* 1993; Eriksson *et al.* 1998; Seri *et al.* 2001; Kempermann *et al.* 2004; Seri *et al.* 2004).

In contrast, in the non-mammalian vertebrate brain, neurogenesis occurs in numerous mitotically active regions and the newborn neurons integrate into a larger variety of diverse brain structures (Doetsch and Scharff 2001; Zupanc 2001; Garcia-Verdugo *et al.* 2002). For instance, neurogenic regions in the songbird brain largely distribute along the ventral and dorsal reaches of the lateral wall of the lateral ventricles (Alvarez-Buylla *et al.* 1990). Different from mammalian species, neuronal precursors originating from the V-SVZ also migrate to the basal ganglia (Alvarez-Buylla *et al.*, 1994) and several other telencephalic structures (Alvarez-Buylla and Kirn 1997). The best studied among these regions is the higher vocal center (HVC) in which seasonal incorporation of newly born neurons occurs throughout adulthood (Nottbohm, 1985; Alvarez-Buylla *et al.*, 1990; Kirn *et al.*, 1991; Scharff *et al.*, 2000). The seasonal growth of specific brain structures in songbirds has been associated with specific brain functions, such as song learning, spatial navigation and acoustic pattern separation, which occur repeatedly during defined annual phases (Beecher and Brenowitz, 2005; Bingham *et al.*, 2003). Neurogenesis studies have also been conducted on lizards, snakes and turtles within the reptile taxon. From these studies, the olfactory bulb, striatum, anterior dorsal ventricular ridge, nucleus sphericus, and the cerebellum have all been demonstrated to generate new neurons in adult organisms (Lopez-Garcia and Martinez-Guijarro, 1988; Garcia-Verdugo *et al.*, 1989; Perez-Sanchez *et al.*, 1989; Marchioro *et al.*, 2005). The neurogenic rate and the number of sites of adult neurogenesis are even higher in amphibians and fish, which, in addition to constitutive neurogenesis, also show efficient recovery from brain injury in contrast to mammalian species (Kaslin *et al.*, 2008; Kizil *et al.*, 2012; Alunni and Bally-Cuif, 2016; Labusch *et al.*, 2020).

1.2. Neurogenesis in Tissue Maintenance and Regeneration

Proliferative activity in the non-mammalian brain either supports the growth of the entire brain or selectively of mitotically active brain regions, which often include sensory centers (Kaslin *et al.*, 2007). The life-long addition of new neurons into these systems, therefore, suggests an important contribution of the constitutive neurogenesis process to the continued postnatal development of sensory structures. In other instances, constitutive neurogenesis contributes to the maintenance of the tissue homeostasis by promoting cell turnover and replacement of dying neurons (Rakic, 2002). In addition, acute episodes of accelerated neurogenesis may also occur in response to disturbances in tissue integrity by acute injury or damage. Often regenerative neurogenic activity is transient and subsides with the re-establishment of tissue homeostasis (Alunni and Bally-Cuif, 2016). Hence, both the active repression of the regenerative processes in the intact brain and the propagation of the regenerative neurogenesis in response to injury must be tightly controlled by spatial and temporal cues within the cellular and molecular niche that surrounds neuronal stem cells (NSCs), which enable nervous system regeneration (Diotel *et al.*, 2020).

Often, regenerative neurogenesis involves the activation of NSCs that are quiescent or dormant under physiological conditions (Becker and Becker, 2008; Kaslin *et al.*, 2008; Reimer *et al.*, 2008; Fleisch *et al.*, 2011). Radial glial cells and cells with neuroepithelial-like characteristics function as NSCs in the neural tube of the developing vertebrate CNS (Alvarez-Buylla *et al.*, 2001; Ever and Gaiano 2005; Götz and Barder 2005). During late embryogenesis, the radial glial cells either disappear or transform into persistent astrocyte-like stem cells and oligodendrocyte progenitors in mammals, which maintain their capacity to participate in constitutive and regenerative neurogenesis during adulthood (Miyata *et al.*, 2004; Levison and Golman; 1993). In contrast, radial glia cells remain the major neural stem cell type in the adult brain of non-mammalian species (Garcia-Verdugo *et al.*, 2002; Kalman, 2002). Additional neuroepithelial-like cell populations which express both neural and glial progenitor characteristics, have also been identified in zebrafish brain (Raymond and Easter, 1983; Kaslin *et al.*, 2008; Ganz *et al.*, 2010; Ito *et al.*, 2010).

The composition of intermediate filaments of glia has been shown to be altered in several processes and instances, such as development, across phylogeny, and during regeneration (Margotta and Morelli, 1997; Götz *et al.*, 2002; Pekny and Pekna, 2004). In addition to their usefulness as cell-type specific markers, these observations also suggest a complex functional relationship between intermediate filament composition, neurogenic capacity, and activation of quiescent NSCs during regeneration.

Unlike constitutive neurogenesis, which mainly produces nerve cells, unfolding of a successful regenerative response also requires the generation of other nervous tissue constituents, such as glial, structural, and supportive cells (Goldman, 2005; Zhang *et al.*, 2005). Even though the generation of these cell types is a necessary component of the response, the generation of glial cells and the activation of intermediated filaments following CNS injury often results in glial scar formation and astrogliosis (Fitch and Silver, 2009). The formation of glial scars by reactive astrocytes, the activation of microglia, and the release of inhibitory molecular signals and membrane components from injured oligodendrocytes, have all been shown to impede axon outgrowth, regeneration, and remyelination (Fawcett and Asher, 1999; Fitch and Silver, 2009). The process is often accompanied by the development of chronic inflammation around the injury site (Yang *et al.*, 2020; Qui *et al.*, 2000). Scar-free wound healing, on the other hand, occurs in the teleost brain and provides a permissive environment for efficient regeneration, which includes the generation of new neurons, the unimpeded outgrowth of dendrites and axons, and the reestablishment of long-distance neuronal connections (Diotel *et al.*, 2020). In addition to these favorable properties, other properties of the teleost brain stem cell niche have been extensively studied in the pursuit of identifying important processes and molecular players that support or enhance regeneration (Zupanc and Sîrbulescu, 2012; Cosacak *et al.*, 2015).

1.3. The Olfactory Epithelium as a Model of Adult

Olfaction, the conscious and subconscious detection of chemical molecules from the environment, is an integral part of animal life and is the basis for many important behaviors, such as foraging, avoidance of predators, and mate choice (Nielsen *et al.*, 2015). The detection of odorants is mediated by olfactory receptor proteins, which are expressed by olfactory sensory neurons (OSNs) that are located in the peripheral olfactory epithelium (OE; Ottoson and Shepard, 1966; Mombaerts, 2004). To detect odorants, the OSNs must be in direct contact with the environment (Farbman, 1990). This prerequisite property makes them vulnerable to environmental insults, such as infectious agents and cytotoxic substances (Moulton, 1974). As a potential defense mechanism, the OSNs have a short life-span that ranges between 30 to 90 days in mammals (Graziadei and Graziadei, 1979; Wilson and Raisman, 1980; Mackay-Sim and Kittel, 1991) and are continuously replaced in all vertebrates, including humans, to maintain sensory function throughout life (Calvo-Ochoa *et al.*, 2020). In addition to maintaining the life-long turnover of OSNs by constitutive neurogenic activity, the OE has also been shown to be resilient to acute injury and is able to regenerate both neuronal and non-neuronal cell types to regain functional integrity of the tissue (Constanzo, 1985). Thus, the OE is an insightful model that allows the simultaneous study of maintenance and repair neurogenesis under different tissue conditions and the elucidation of differences and similarities in the cellular and molecular signals that contribute to each process (Calvo-Ochoa *et al.*, 2020).

1.3.1. The Structure and Cellular Constituents of the Mammalian OE

Among mammals, the anatomical structure and cellular organization of the rodent OE has been studied most extensively (Dorman, 2010). The tissue inside of the nasal cavity of rodents is highly convoluted, forming protrusions into the nasal lumen that give rise to the turbinates. The OE lines the surface of the turbinate structures, which increases the surface area that is available for the detection of odorants (Green *et al.*, 2012). In addition to OSNs, the OE includes two major non-neuronal cell types, the sustentacular glial cells (SCs) and basal progenitor cells, which support OSN neurogenesis. The nuclei or cell bodies of OSNs, SCs, and progenitor cells form discernable layers in the pseudostratified epithelium, with progenitors, immature neurons, mature neurons, and SCs occurring in basal to apical order (Graziadei and Graziadei, 1979; Nomura *et al.*, 2004).

The apical-most layer of the OE is tightly packed with cell bodies of SCs in the rodent OE (Vogalis *et al.*, 2005). These cells have a columnar morphology and are capped with microvilli (Farbman, 1992). The SCs constitute the tissue specific glial cells, which provide structural and functional support to the OE and are involved in several processes, including maintenance of a defined ionic milieu, detoxification, phagocytosis of dead cells, and buffering of extracellular K⁺ (Getchell and Getchell, 1982; Ding and Coon, 1988; Getchell and Mellert, 1991; Chen *et al.*, 1992). In line with their integral role in supporting sensory function, their selective loss has been found to be a major trigger for repair neurogenesis in the OE (Herrick *et al.*, 2017).

The layers just below the SC cell bodies are occupied by mature OSNs, which are bipolar neurons that protrude their ciliated single dendrites above the SC layer at the apical surface. They send a single unmyelinated axon to basal layers which exits the OE through the cribriform plate and conveys sensory information to OB glomeruli. Odorant detection occurs on receptors that are located on the cilia that contact the lumen of the nasal cavity (Farbman, 1992). Every OSN expresses only a single member of the olfactory receptor gene family (Song *et al.*, 2008) and OSNs expressing the same receptor converge onto a pair of specific glomeruli in the OB (Mombaerts, 2006).

Immature OSNs are found to be located between the layers formed by mature OSNs and progenitor cells and migrate vertically to more apical layers as they mature into functional cells (Schwob *et al.*, 2017).

The basal-most layers are occupied by two morphologically and functionally distinct stem cell populations, which form two discernable layers (Andres, 1965; Graziadei and Graziadei, 1979). Globose basal cells (GBCs) represent a heterogeneous population of stem, committed progenitor, and immediate precursor cells, which are round-shaped and mitotically active in the intact OE (Schwartz Levey *et al.*, 1991; Huard and Schwob, 1995). The continuous mitotic activity of paired box protein 6 (Pax6)- and sex determining region Y-box2 (Sox2)-expressing GBCs supplies the constant replacement of dying OSNs as well as other cell types (Goldstein *et al.*, 1998; Chen *et al.*, 2004). GBCs, therefore represent a multipotent stem cell population that contributes to maintenance neurogenesis in the intact OE (Cau *et al.*, 1997; Manglapus *et al.*, 2004; Guo *et al.*, 2010). As they progress through the lineage, Pax6- and Sox2-expressing GBCs give rise to transit amplifying GBCs, which are committed to a neuronal fate by expressing the basic helix-loop-helix transcription factor *Ascl1* (Krolewski *et al.*, 2012). Committed progenitor cells in turn give rise to the neuronal differentiation marker-1- (*NeuroD1*-) and *Neurogenin-1*-expressing immediate neuronal precursor subpopulations of GBCs, which are capable of developing into OSNs (Cau *et al.*, 1997).

HBCs on the other hand, represent a homogenous population of stem cells, which are found to be mitotically quiescent under physiological conditions and occupy the basal-most layer just above the basal lamina (Leung *et al.*, 2007). They show a flattened morphology and express Keratin 5 and 14 (Schwartz Levey *et al.*, 1992), intercellular adhesion molecule-1 (Carter *et al.*, 2004), and the transcription factor *tp63* (Packard *et al.*, 2011). HBCs form the reserve stem cell population of the OE, which only become activated when the tissue integrity is severely compromised (Herrick *et al.*, 2017). Activated HBCs proliferate and differentiate into GBCs, which, in turn, generate neuronal and non-neuronal lineages to reconstitute the damaged tissue (Leung *et al.*, 2007).

1.3.2. Structural Differences of the Zebrafish OE

The structure and cellular organization of the zebrafish OE shows a high degree of structural and cellular similarity to the mammalian OE (Calvo-Ochoa *et al.*, 2020). However, some profound differences also exist. In addition to the main OE, a distinct sensory structure for the detection of pheromones and kairomones, the vomeronasal organ, can be recognized in rodents (Firestein *et al.*, 2001) but is absent in zebrafish. In zebrafish, the single OE acquires the function of vomeronasal organ and facilitate the detection of both odorants and pheromones as a common olfactory organ (Wang *et al.*, 2020).

The zebrafish OE consists of several bilaterally symmetrical lamellae, which converge onto a central midline structure, the median raphe. The overall structure of the lamellar pattern gives the olfactory organ a rosette-shaped appearance (Byrd and Brunjes, 1995; Hansen and Zeiske, 1998). The neuroepithelial tissue, harboring both the neuronal and non-neuronal cell types, forms U-shaped sheets between neighboring lamellae. Similar to the turbinate structure, the lamella organization increase the area that is available for odorant detection (Calvo-Ochoa *et al.*, 2020). As can be demonstrated by different general neuronal and OSN-specific markers, the occurrence of OSNs within the epithelial folds is restricted to the inner zones and is surrounded by a ring of cells with motile cilia (Celik *et al.*, 2002; Sato *et al.*, 2005; Iqbal and Byrd-Jacobs 2010; Bayramli et al. 2017). The sensory region, which is occupied by OSNs, extends approximately over two-thirds of each epithelial fold and covers the area between the interlamellar curves (ILCs) at the inner edge and the peripheral tissue, which is solely occupied by nonsensory cells (Bayramli *et al.*, 2017). The sharp transition between the sensory region and the nonsensory peripheral tissue is referred to as the sensory/nonsensory border (SNS; Bayramli *et al.*, 2017).

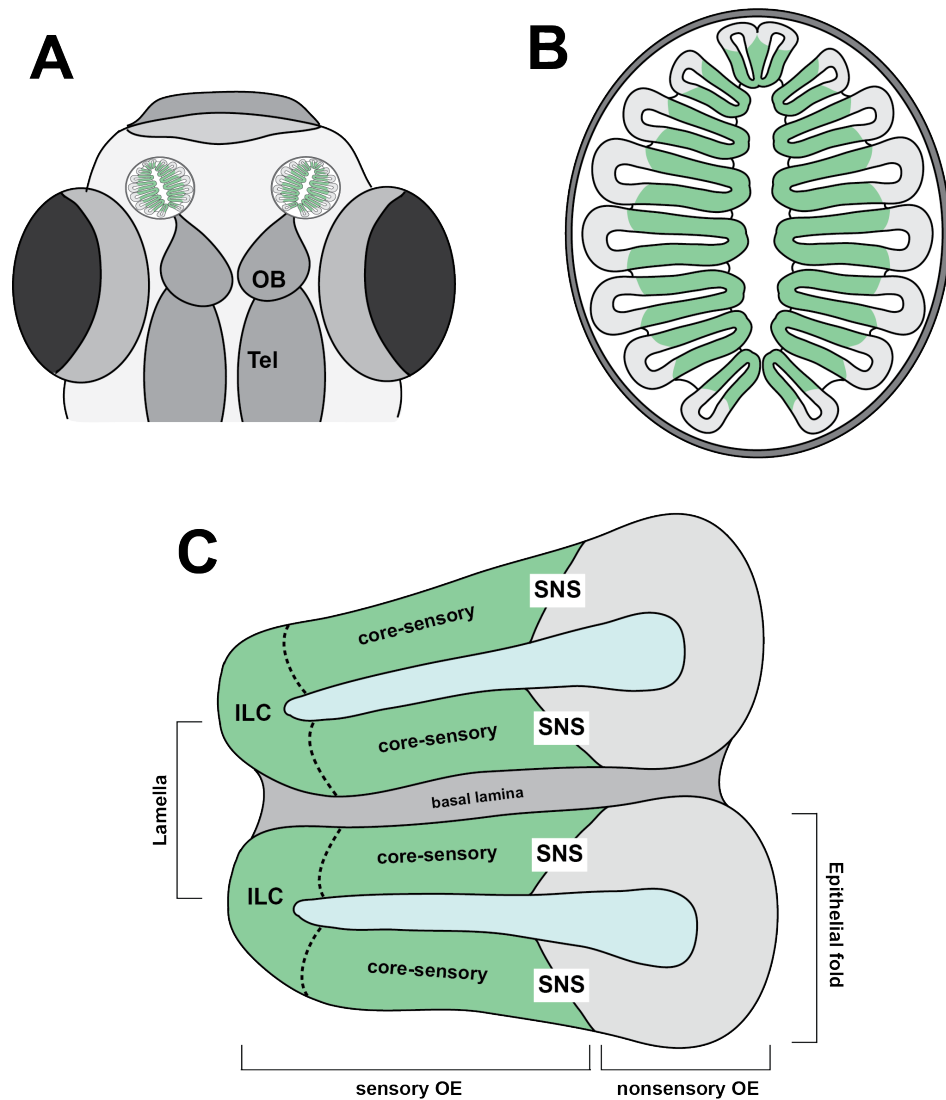


Figure 1.1. Schematic representation of the zebrafish OE. A. Position of the OE in the head and its connectivity to the brain. Tel: Telencephalon. B. Horizontal view of the OE. C. Organization of the lamellae.

The nuclei and cell bodies of the different cells within the zebrafish OE show a pseudostratified organization (Hansen and Zeiske, 1998). However, in contrast to the rodent OE, the apical regions of the zebrafish OE is almost solely occupied by OSN cell bodies and not by SCs. Resulting from their inverted morphology in zebrafish, SC cell bodies that can be labelled by staining against cytokeratin type-II and/or Sox2 occupy suprabasal layers in the zebrafish OE (Demirler *et al.*, 2020, Demirler, 2021).

In rodents, GBCs are located in basal layers just above HBCs throughout the entire OE (Schwob *et al.*, 2016). However, in zebrafish, they found restricted to specialized zones of maintenance neurogenesis at the ILC and SNS as can be detected by in-situ hybridization against *ascl1* (Bayramli *et al.*, 2017) and immunostaining against Sox2 (Kocagöz, 2021). Their localized distribution also restricts mitotic activity in the intact zebrafish OE to the ILC and SNS (Byrd and Brunjes, 2001; Oehlmann *et al.*, 2004), in contrast to the homogenous distribution of proliferating GBCs in the rodent OE (Schwob *et al.*, 1992). Hence, in the intact OE, immature neurons are born exclusively at the ILC and SNS. As a consequence, in addition to the vertical migration of immature neurons from the suprabasal to apical layers, newborn OSNs of the zebrafish OE migrate radially towards the center of the sensory region (Bayramli *et al.*, 2017). HBC-like cells in the zebrafish OE show a high degree of functional and morphological similarity to rodent HBCs. They are located basally, have flattened cellular profiles, and exhibit no, or very little, neurogenic mitotic activity in the intact OE (Kocagöz, 2021, Demirler, 2021).

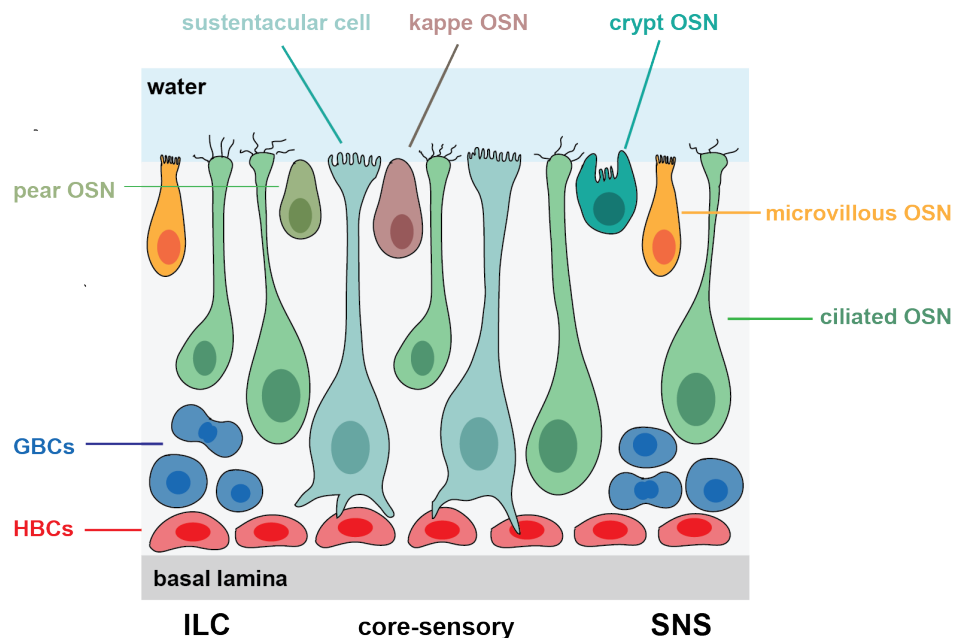


Figure 1.2. Cellular composition of the sensory OE.

1.3.3. Maintenance Neurogenesis in The OE

The unprotected nature of OSNs against environmental stressors and toxicants results in the constant loss of cells (Moulton, 1974). To overcome this loss and to maintain the functional integrity of the tissue, OSNs in the rodent OE have a high turnover rate and are continuously replaced throughout life (Schwob, 2002; Ferretti, 2011). One important aspect contributing to the high OSNs turnover rate is related to their inherently limited lifespan. The observation of dying cells in the absence of environmental stressors (Hinds *et al.*, 1984) and the detection of apoptotic neurons in the intact OE (Cowan and Roskams, 2002) support the existence of intrinsic programs that regulate OSN lifespan. However, studies aiming to determine the exact lifespan of individual OSNs in the rodent OE demonstrated conflicting results. In one study, using thymidine labelling, 10 % of the labelled OSNs have been shown to persist in the OE beyond 6 to 12 months (Hinds *et al.*, 1984). In a second study, using a retrograde tracing technique, labelled OSNs have been shown to survive for only 90 days after injection (Mackay-Sim and Kittel, 1991). A mean OSN lifetime of 37.5 days has been reported in a recent study using a genetic labelling strategy (Holl, 2018). The same study, however, also reports a small population of OSNs which survived for more much longer and cells persisted for up to 12 months. This emphasizes heterogeneity within OSN population, which should be considered in experimental setups using the bulk labelling of different OSN subpopulations. Yet, the lack of selectivity of the techniques for labelling OSNs of the same age could also explain the observation of different lifetimes in the same experimental setup (Calvo-Ochoa *et al.*, 2020).

By using BrdU pulse labelling, the mean life span of OSNs has been measured to be 28.5 days in zebrafish (Bayramli *et al.*, 2017), demonstrating their conserved intrinsic high turnover rate. An evidence supporting this control mechanism found. Even though caspase-3 labelling could not identify apoptotic OSNs (Bayramli *et al.*, 2017), deoxynucleotidyl transferase dUTP nick end labelling- (TUNEL) assay highlighted a large number dying cells, suggesting the existence of an alternative cell death mechanism for senescent OSNs in the zebrafish OE (Calvo-Ochoa *et al.*, 2020). These observations emphasize a possible intrinsic control of OSN lifespan in the zebrafish OE.

Radioactive ^3H -thymidine-labelling of the intact rodent OE shows a homogenous distribution of mitotic activity along suprabasal layers throughout the entire tissue (Schwob *et al.*, 1992). Immature OSNs, which show the expression of growth-associated protein 43 (GAP-43) but lack expression of the mature marker olfactory marker protein (OMP) have been shown to be born basally. As they mature, they migrate vertically towards more apical layers where cell bodies of functional OSNs are located (Iwema and Schwob, 2003).

In contrast to rodents, mitotic activity in the intact zebrafish OE is found to be restricted to specific neurogenic zones. Multiple studies using different techniques for the labelling of mitotic activity showed that proliferative cells in the zebrafish OE almost exclusively occur within basal layers at the ILC and SNS (Byrd and Brunjes 2001; Oehlmann *et al.*, 2004; Iqbal and Byrd-Jacobs 2010; Bayramli *et al.* 2017), while the rest of the sensory region is largely devoid of mitotic activity. Immature OSNs are generated close to the sites of mitotic activity as shown by in situ-hybridization against the neuronal commitment markers *ascl1a* and *delta-like a (dla)* or the neuronal differentiation markers *neurod4* and *gap43* in combination with BrdU birthdating (Bayramli *et al.*, 2017). Newborn OSNs generated at the ILC and SNS migrate radially along the lamellae as demonstrated by analyzing the tissue distribution of cells expressing sequential cell markers for different phases of neuronal differentiation or by successive labelling of newborn cells with different thymidine analogs. These cells successively invade the inner zones of the sensory region as they mature and are eliminated in the center of the sensory region as they age (Bayramli *et al.*, 2017).

1.3.4. Regeneration of The OE

In contrast to the overall poor recovery of CNS structures and regeneration of neurons in mammals, the peripheral OE has been shown to reconstitute successfully even after severe injury (Schwob *et al.*, 2018). Starting with pioneering studies in rodents that employed an experimental nerve injury method (Nagahara, 1940), the successful regeneration of the OE has been demonstrated multiple times using different experimental paradigms (Schwob, 2002) and species (Calvo-Ochoa *et al.*, 2020). Perturbations in tissue integrity, either by direct physical and chemical injury or by genetic ablation of defined cell types, not only allow for a close examination of the cellular events that take place during OE regeneration but also the identification of the molecular players that contribute to repair and maintenance neurogenesis. The time that is necessary for full functional recovery to occur largely depends on the type and the extent of the injury but may also be influenced by organismal age and species-specific differences (Brann and Firestein, 2014).

The use of cytotoxic agents generally results in the nonselective damage of all resident cells, which may be analogous to the naturally occurring injury that results from exposure to pathogens and environmental toxins (Schwob, 2002). Irrigation of the OE with zinc sulfate (ZnSO₄) solution causes the death of all OE cell types and disruption of tissue integrity in rodents, which are reconstituted within only 30 days (Matulionis, 1975). Similarly, exposure to the toxic gas methyl bromide (MeBr) results in a nonselective, global loss of cells in the OE (Hallier *et al.*, 1994; Yang *et al.*, 1995) and the duration required for recovery ranges between 4 to 6 weeks (Schwob *et al.*, 1995).

In zebrafish, irrigation with the non-ionic detergent Triton X-100 can be used to apply direct injury to the OE (Iqbal and Byrd-Jacobs, 2010). Concentration, duration of the exposure, and the number of repetitive pulses have been shown to result in injuries of different degree and severity (Paskin *et al.*, 2011). Two minutes exposure to 0.7 % Triton X-100 results in the destruction of more than half of the OSNs within 1 day. Complete reconstitution of the OE is quite fast (Iqbal and Byrd-Jacobs, 2010).

Occurs within only 2 to 5 days following the manipulation (Iqbal and Byrd-Jacobs, 2010). Multiple pulses of application, on the other hand, extends the duration of the recovery to 21 days (Paskin *et al.*, 2011). Insertion of wax plug into the naris in an attempt to induce sensory deafferentation of the OB results in an almost complete loss of the entire OE structure. Surprisingly, the OE regains a rosette-like appearance within only one week and the system reaches full functional capacity within 3 weeks (Scheib *et al.*, 2019).

Lineage tracing analysis from HBCs in the intact rodent OE and after MeBr exposure shows that, even though they are largely quiescent under physiological conditions, injury selectively activates HBC proliferation and their differentiation into GBCs, which contribute to both neuronal and nonneuronal lineages (Leung *et al.*, 2007).

As described above, the proliferative and neurogenic activity in the intact zebrafish OE is restricted to ILC and SNS while the remainder of the sensory region is largely devoid of proliferative and neurogenic activity (Iqbal and Byrd-Jacobs 2010; Bayramli *et al.*, 2017). Following nasal irrigation with Triton X-100, an almost uniform pattern of proliferative activity is observed that includes the region between the ILC and SNS (Iqbal and Byrd-Jacobs, 2010; Demirler *et al.*, 2020). Co-immunostaining with BrdU and the HBC marker keratin 5 (Krt5) shows that HBCs are activated in response to tissue injury (Demirler *et al.*, 2020). The occurrence of *Ascl1*+ GBCs in the sensory OE following injury suggests that, similar to the rodent OE, HBCs proliferation gives rise to a transient population of GBCs in the zebrafish OE, which ultimately reconstitutes the OE (Kocagöz, 2021).

Regeneration studies that utilize selective ablation methods bear interpretations, which are equally related to both maintenance and repair neurogenesis. Selective loss of OSNs can be induced by removal of the OBs or transection of the olfactory nerve. While the rodent OE never fully recovers from this intervention (Carr and Farbman, 1992, 1993; Schwob *et al.*, 1992), proliferative activity is increased exclusively in GBCs, while no effect on the HBC activation could be observed (Schwartz Levey *et al.*, 1991). The activity of GBCs are influenced by neuronal cell death (Schwartz Levey *et al.*, 1991).

Which is in line with their role in the constant generation of new OSNs. In contrast, HBC activation appears to depend on the selective loss of SCs, which has been shown to be the major trigger for regenerative neurogenesis (Herrick *et al.*, 2017). Interestingly, selective ablation of OSNs by axotomy results in an increase in proliferative but not neurogenic activity of HBCs in the zebrafish OE (Kocagöz, 2021), suggesting the existence of a distinct control mechanism of HBC activity through OSN death that is different from the rodent OE.

1.4. Molecular Regulators of OE Neurogenesis

To preserve tissue function, new OSNs must be generated at appropriate rates in the intact OE and also at remarkable speed after injury (Demirler *et al.*, 2020; Calvo-Ochoa *et al.*, 2021). An important aspect of both maintenance and repair neurogenesis is that exactly the right number of OSNs needs to be generated. Preventing excessive proliferation and OSN generation is important for the avoidance of neuroblastoma-like cancers (Bailey and Barton 1975; Yamate *et al.* 2006; Parker *et al.* 2010), but also stem cell depletion (Post and Clevers, 2019), and dysfunctions in odor discrimination (Fleischmann *et al.*, 2008). Therefore, the accuracy of constitutive neurogenesis and regenerative responses is very important and must be tightly regulated by molecular signals that convey information between the tissue and GBC/HBC progenitor cells.

As previously mentioned, selective loss of OSNs exclusively activates GBCs but has no noticeable effect on HBC proliferation in rodents (Leung *et al.*, 2007). It has been shown that leukemia inhibitory factor (LIF) is upregulated in the OE following bulbectomy (Nan *et al.*, 2001; Getchell *et al.*, 2002) and that LIF expression localizes to dying OSNs (Bauer *et al.*, 2003). Exclusive expression of the LIFR receptor in GBCs and the reduction in proliferation rate in response to LIF knock-out demonstrates that LIF signaling is an important stimulator of GBCs activity that correlates with the loss of OSNs following axotomy (Kim *et al.*, 2005).

The activity of GBCs is also negatively regulated by the density of OSNs in the rodent OE. The transforming growth factor- ($TGF\beta$) superfamily could be an example.

The TGF β is generally known for their negative effects on cell proliferation (Shou *et al.*, 1999). Growth and differentiation factor 11 (GDF11; aka bone morphogenic protein 11), a member of the TGF β superfamily, is expressed in immature and mature OSNs and has been shown to cause temporary cell cycle arrest in neuronal progenitor subpopulation of GBCs (Wu *et al.*, 2003). Thus, increasing levels of GDF11 may restrain GBC activity when a sufficiently large number of OSNs is reached in the intact tissue or after injury.

Interestingly, not the loss or density of OSNs but damage to SCs triggers the propagation of repair neurogenesis in rodent OE (Herrick *et al.*, 2017), emphasizes the integral role of SCs in maintaining tissue homeostasis. The maintenance of a self-renewing quiescent HBC state in the intact OE is controlled by the expression of the transcription factor tp63 (Fletcher *et al.* 2011; Schnittke *et al.* 2015). It has been shown that expression of tp63 is driven by active Notch signaling in HBCs and that knockout of Notch1 results in HBC differentiation. Among Notch ligands, Jagged1 is exclusively expressed in SCs. Thus, it was suggested that the loss of SCs disrupts Jagged1/Notch signaling and triggers a decline in tp63 in HBCs after injury. In turn, HBCs respond with mitotic activity, which results in increased OSN neurogenesis (Herrick *et al.*, 2017). The fact that activation of HBCs depends on loss of SCs rather than OSNs suggest the existence of an internal control mechanism, which aims to keep HBCs in a reserve stem cell state, which becomes active only when the tissue integrity is severely compromised but is unresponsive to the daily loss of OSNs that are eliminated by age.

Damage-associated molecular patterns (DAMPs) are a heterogeneous group of molecules which have physiological functions inside cells but are recognized as alerting motifs that stimulate immune and regenerative responses when they are released from dying or damaged cells (Venereau *et al.*, 2015). Extracellular adenosine triphosphate (ATP) is recognized as a DAMP in various tissues and has been shown to be involved in modulating mitotic activity in adult neurogenic niches (Suyama *et al.*, 2012, Cao *et al.*, 2013). Thus, extracellular ATP, which could be released from dying or damaged OSNs, might also have a role in the positive regulation of OE neurogenesis. In the mouse OE, ATP stimulation triggers the activation of basal cell populations (Hayoz *et al.*, 2012).

By both evoking Ca^{2+} transients in basal cells through SCs (Hegg *et al.*, 2009) and by upregulating the expression of proliferation-promoting molecules in OSNs and SCs (Jia and Hegg, 2010). Our group has also shown that ATP stimulation triggers Ca^{2+} transients in the zebrafish OE, predominantly in GBCs, HBCs, and SCs through P2-type purinergic receptors and that exogenous application of ATP stimulates selective proliferation of GBCs but not of HBCs (Demirler *et al.*, 2020).

Different from tissue maintenance, an immune response almost always accompanies injury and tissue repair (Karin *et al.*, 2016). Therefore, interactions between tissue-resident cells and immune cells may also be an integral part of regulating tissue repair (Gurtner *et al.*, 2008). In fact, tissue repair in mammals has been shown to occur in three successive stages: inflammation starting with the recruitment of immune cells by pro-inflammatory cytokines that are released from tissue-resident cells, new tissue formation, and remodeling (Karin and Clevers, 2016). Increased inflammatory cell infiltration and expression of the pro-inflammatory cytokine tumor necrosis factor- α (TNF) occur in the mouse OE following injury, which suggests a similar interaction between the immune system and OE regeneration. Loss of TNF- receptor (TNFR1) which cause significantly lower expression of cytokine and chemokines in HBCs and failed recruitment of immune cells, results in impeded proliferation of HBCs (Chen *et al.*, 2017).

1.5. EGFR, Its Ligands and Downstream Targets in Regulating Neurogenesis

The Epidermal Growth Factor Receptor (EGFR) belongs to the ErbB family of Receptor Tyrosine Kinases (RTKs; Schlessinger, 2002; Ayati *et al.*, 2020). The ErbB family include four members, EGFR (ErbB1), ErbB2, ErbB3, and ErbB4 (Wieduwilt and Moasser, 2008). These receptors are single pass transmembrane glycoproteins that contain an extracellular ligand binding domain, a transmembrane domain, and an intracellular tyrosine kinase domain (Wieduwilt and Moasser, 2008). Ligand binding stimulates homo- or heterodimerization of ErbB subunits, which results in the activation of their tyrosine kinase activity (Linggi and Carpenter, 2006). Autophosphorylation of the receptor leads to receptor activation (Linggi and Carpenter, 2006). EGFR consists of an ErbB1 homodimer and functions as a cell surface receptor for seven known ligands, epidermal growth factor (EGF), heparin-binding EGF-like growth factor (HB-EGF), tumor necrosis factor alpha (TNF), Epigen, Epiregulin, Betacellulin and Amphiregulin (Knudsen *et al.*, 2014). Upon activation, EGFR can stimulate a variety of downstream signaling pathways, including PI3K-Akt, MAPK, PLC-1-PKC, SRC kinases, and JAK/STAT signaling (Wee and Wang, 1999). The cellular outcome of the activation of EGFR signaling often is context-dependent and varies greatly between different tissues and physiological states and is influenced both by the ligand and the downstream transduction pathway that is activated by EGFR signaling. The interconnected nature of these pathways allows EGFR activation to stimulate a complex signaling network, which propagate a wide variety of diverse cellular responses, including cell proliferation, differentiation, migration, and survival (Wells, 1999, Wee and Wang, 2017). These responses have been found to contribute to the development, homeostasis, and repair of various tissues, including the nervous system (Peus *et al.*, 2000; Repertinger *et al.*, 2001; Chen *et al.*, 2016; Romano and Bucci, 2020).

Neurogenesis in rat brain begins around E9, and reaches a peak by E13, which coincides with strong EGFR expression rising around the same time. The expression of EGFR can be detected in the V-SVZ progenitor cells, as well as in the astrocytes, oligodendrocytes, and specific populations of neurons (Mazzoni and Kenigsberg, 1994).

Mice lacking EGFR expression show defects in the formation of cortical layers caused by the combinatorial effects of reduced differentiation of neural progenitors, decreased proliferation of astrocytes, as well as impairment of the migration of neurons. In addition, loss of EGFR expression results in postnatal neurodegeneration resulting from massive neuronal cell death, which is promoted both cell autonomously by increased apoptosis of neurons and non-cell autonomously by the lack of a sufficient number of supporting astrocytes (Sibilia *et al.*, 1998). Conversely, increasing the level of EGFR signaling or stimulation with EGFR ligands appears to increase differentiation of progenitor cells and proliferation of astrocytes, respectively (Burrows, 1997, Simpson *et al.*, 1982). While stimulation with EGF has been shown to induce the migration of neurons from the lateral ventricles to adjacent areas (Craig *et al.*, 1996), EGF and TNF were also found to regulate the survival of midbrain and cortical neurons (Kornblum *et al.*, 1990; Casper *et al.*, 1991; Alexi and Hefti, 1993). Therefore, EGFR signaling may be critically involved in CNS development by regulating cell proliferation, differentiation, and survival as well as guiding the migration of neurons and glial cells towards destined cortical layers (Tucker *et al.*, 1993, Sibilia *et al.*, 1998, Puehringer *et al.*, 2013).

Many cellular processes, which are required for the proper development of an organ, are also utilized during the maintenance of tissue homeostasis and in tissue repair. Hence, not surprisingly, EGFR signaling is also expressed in various adult tissues, including the nervous system, and is involved in the preservation of tissue integrity as well as recovery from tissue injury in adulthood (O'Loughlin *et al.*, 1985; Poulsen *et al.*, 1986; Beauchamp *et al.*, 1990; Stoll *et al.*, 2001; Carver *et al.*, 2002; Abe *et al.*, 2009). EGFR has been shown to be expressed in the neurogenic niches of the adult CNS to regulate both the maintenance of NSC/NPC pools (Robsen *et al.*, 2018) and the generation of neural cell diversity (Miyata *et al.*, 2001; Noctor *et al.*, 2001). Notch signaling typically maintains the identity and self-renewing state of NSCs (Hitoshi *et al.*, 2002) and interactions between EGFR and Notch signaling control the size of their pool by regulating proliferation and differentiation (Aguirre *et al.*, 2010). Self-renewal capacity of the NPCs on the other hand, is controlled mainly by the persistence of the Sox2 expression (Kondo and Raff, 2004; Brazel *et al.*, 2005).

Positive feedback loop between Sox2 and EGFR signaling appears to be involved in the regulation of their self-renewal (Hu *et al.*, 2001). EGFR signaling also contributes to the neural cell diversity by regulating cell fate choices in NPCs (Sun *et al.*, 2005).

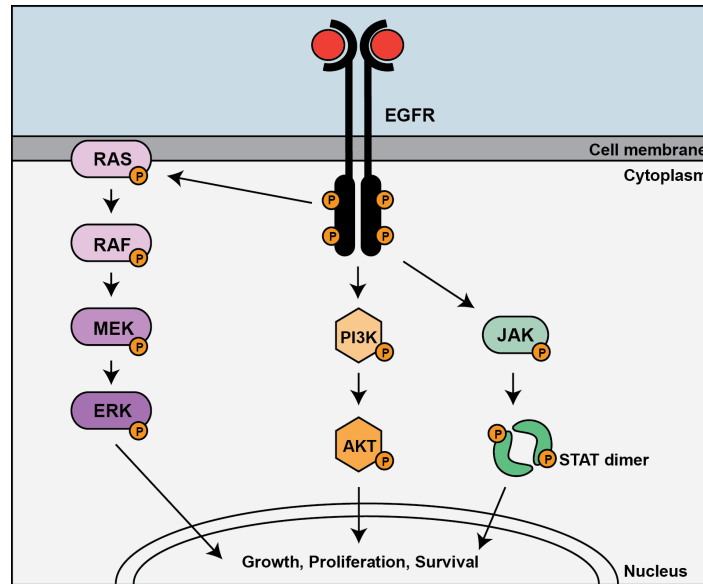


Figure 1.3. EGFR signaling.

Among the downstream targets of EGFR, PI3K-Akt, MAPK and JAK/STAT signaling was previously implicated in regulating embryonic and adult neurogenesis and regeneration (Chen *et al.*, 2016). Through activation of RTKs, PI3K becomes phosphorylated and it stimulates the activation of Akt via a multistep process. Activation of the Akt in turn regulates cellular processes like growth, proliferation and survival (Hemmings and Restuccia, 2012). The activity of the PI3K-Akt signaling was shown to be critical for the regulation of proliferation and maintenance of the progenitor state of the NPCs during hippocampal neurogenesis (Peltier *et al.*, 2006). MAPK signaling is initiated via the activation of a common phosphorylation cascade via ligand binding to RTKs, GPCRs or cytokine receptors, which ends up with the activation of different MAPKs (Guo *et al.*, 2020). The MAPK family includes three major protein kinases, the extracellular signal-regulated kinase (ERK), c-Jun N-terminal kinase (JNK), and p38 MAPK, which become activated in response to different stimuli and result in different cellular consequences (Owens and Keyse, 2007; Kyriakis and Avruch, 2012).

Different isoforms of JNKs show differential distribution in distinct early progenitor cells in the adult hippocampus and were shown to have a common role in controlling their pool size (Castro-Torres *et al.*, 2018). While ERK and PI3K-Akt signaling were shown to be involved in controlling the size of NPC pool by negatively regulating the self-renewal in the embryonic CNS (Rhim *et al.*, 2015), their crosstalk is necessary for injury-induced neurogenesis in adult CNS NPCs *in vitro* (Sung *et al.*, 2007). Members of the Janus kinase (JAK) and Signal Transducer and Activator of Transcription (STAT) protein families together comprise the JAK/STAT intracellular signaling pathway (Aaronson and Horvath, 2002). Activation of JAK/STAT signaling occurs through the activation of different growth factor, cytokine, and hormone receptors (Bousoik and Montazeri Aliabadi, 2018). Essentially, the activated receptor activates JAK, which then phosphorylate STAT proteins. Phosphorylation of STATs leads to their dimerization and subsequent translocation into the nucleus, where they regulate gene expression by acting as transcription factors (Nicolas *et al.*, 2013). Synergistic action of ERK and JAK/STAT signaling was also shown to be necessary for NSC and NPC proliferation and differentiation in the adult SVZ under physiological conditions (Gomez-Nicola *et al.*, 2011; Pereira *et al.*, 2015). Role of JAK/STAT signaling in regeneration has been characterized the best in spinal cord within the CNS, where it was suggested to attain both protective and regenerative functions with the time-dependent action of different members of its signaling components (Wang *et al.*, 2014).

Much less is known about the role of EGFR signaling in regulating OSN neurogenesis under physiological and injury conditions. EGFR is expressed by HBCs in the rodent OE (Krishna *et al.*, 1996; Gilbert *et al.*, 2015; Chen *et al.*, 2020). A recent study showed that activation of EGFR signaling by the non-canonical activator neural glial-related cell adhesion molecule (NrCAM) promotes the HBC activity and that inhibition of the EGFR prevents OE regeneration after methyl bromide lesions (Chen *et al.*, 2020). Transcriptome analysis of the intact and injured zebrafish OE shows that among the various EGFR ligands, HB-EGF is selectively and transiently upregulated during the first 24 h following Triton X-100 lesions (Kocagöz, 2021). Exogenous stimulation with recombinant HB-EGF promotes HBC proliferation and the OSN neurogenesis. In contrast, inhibition of the HB-EGF signaling suppresses the OSN regeneration. Inhi-

bition of matrix metalloproteases, which cleave and activate HB-EGF (Higashiyama and Nanba, 2005) or direct sequestration of HB-EGF by CRM197 (Dateoka *et al.*, 2012) diminishes the number of OSNs that have been regenerated by 5 d following OE damage (Şireci, unpublished). Thus, EGFR signaling may be an important regulator of the injury response in the zebrafish OE. In the framework of this thesis, the contribution of EGFR activity and the candidate downstream target JAK/STAT have been investigated in detail.

2. PURPOSE

Transcriptome analysis of intact and injured zebrafish OE samples revealed a strong injury-induced upregulation in the expression levels of HB-EGF and related signaling components (Kocagöz, 2021). Intranasal administration of human recombinant HB-EGF stimulates an increase in neurogenic cell proliferation, which resembles repair neurogenesis from HBCs (Kocagöz, 2021). Inhibition of HB-EGF signaling by direct sequestration or inhibition of matrix metalloproteases, which prevents the release of the active extracellular signaling domain of HB-EGF, results in an impairment of OSN neurogenesis and OE regeneration in response to injury (Kocagöz, 2021; Sireci, unpublished). These findings show that HB-EGF is both necessary and sufficient to induce repair neurogenesis in the zebrafish OE and suggest that HB-EGF is a key molecular signal during OE regeneration. Among the known cell surface receptors of HB-EGF, only the expression levels of EGFR are upregulated in response to injury (Kocagoz, Demirler, and Fuss, unpublished). EGFR expression can be detected in HBCs in the intact OE (Güler, 2021), suggesting that HB-EGF might signal through EGFR to stimulate the activation of HBCs during repair neurogenesis. However, the significance of EGFR signaling and its candidate downstream signaling components to OE regeneration remain elusive. In the work presented in this thesis, the contribution of EGFR and JAK/STAT, as one candidate intracellular effector of EGFR signaling, to maintenance and repair neurogenesis were examined.

For the functional characterization of EGFR signaling in the context of maintenance and repair neurogenesis, two set of experiments were performed. Firstly, proliferative activity in the intact and injured OEs were evaluated in a quantitative and spatial analysis of mitotic cell divisions in control animals and under pharmacological inhibition of EGFR signaling by PD153035. In a second experiment, the contribution of EGFR signaling to OSN neurogenesis and OE regeneration were evaluated by a quantitative analysis of the efficiency of OSN generation in response to injury.

Similar experiments were performed to investigate the functional contribution of JAK/STAT signaling to maintenance and repair neurogenesis in the zebrafish OE. The rate and tissue distribution of cell proliferation was examined in the intact and injured OEs under pharmacological inhibition of JAK/STAT signaling by JSI-124 and were compared to control animals that did not receive the inhibitor. In a second series of experiments, the contribution of JAK/STAT signaling to OSN neurogenesis and OE regeneration were quantified by assessing the presence of OSNs at defined time points following tissue injury.

In order to determine whether JAK/STAT signaling is active under different tissue conditions, the activity of JAK/STAT signaling was analyzed in intact and injured OEs samples using immunoreactivity against the activated effector pSTAT3. The identities of cell populations which JAK/STAT signaling is active during maintenance and repair neurogenesis were further determined by examining pSTAT3-positive cells for the expression of the general stem cell marker Sox2, colocalization with the proliferation marker BrdU, and spatial analysis of their apicobasal and radial position.

Lastly, to determine a candidate relationship between HB-EGF and JAK/STAT signaling, the spatial activation pattern of JAK/STAT signaling upon human recombinant HB-EGF stimulation was determined using anti-pSTAT3 immunoreactivity and compared to control and injured OE samples. The identity of the cell populations that were activated in response to HB-EGF stimulation was further determined by colocalization with Sox2 expression and BrdU labeling, and analysis of their spatial tissue distribution.

3. MATERIALS AND METHODS

3.1. Materials

3.1.1. Fish

Adult zebrafish (*Danio rerio*, > 6 months of age) of the AB/AB strain (ZFIN ID: ZDB-GENO-960809-7) and animals bred from founders that were obtained from a local pet store were used in all experiments. Fish were maintained in the Animal Facility (Vivarium) of Boğaziçi University Center for Life Sciences and Technologies.

3.1.2. Equipment and Supplies

All equipment and disposable and non-disposable supplies are listed with their manufacturer in the Appendix B.

3.1.3. Buffers and Solutions

A complete list of all chemicals, buffers, reagents, solutions, and antibodies that were used in this study are provided with their manufacturer in the Appendix A.

3.2. Methods

3.2.1. Fish Maintenance

Adult zebrafish (*Danio rerio*, > 6 months of age) of the AB/AB strain (ZFIN ID: ZDB-GENO-960809-7) and animals bred from founders that were obtained from a local pet store were used in all experiments. Animals were kept at a constant temperature of 28°C and a 14/10 hours light-dark cycle and maintained at the AAALAC-accredited Vivarium of the Center for Life Sciences and Technologies at Boğaziçi University. Fish were kept at a maximum density of 5 fish/l in either 1, 3, or 10 l tanks. The circulating tank water was controlled by an automated fish maintenance system (Aquatic Habitats), which is equipped with concomitant filtration, heating, ventilation, and UV sterilization units. Water quality was maintained by regular supply of artificial freshwater to balance ion homeostasis and to dilute accumulating metabolic waste products. Artificial freshwater was prepared by dissolving 2 g sea salt, 7.5 g sodium bicarbonate, and 0.84 g calcium sulfate in 100 liters of reverse osmosis water. Flake food, live and/or frozen brine shrimp (*Artemia* sp.) larvae were used to feed fish twice daily.

The use of experimental zebrafish for this study was approved by the Institutional Ethics Board for Animal Experiments at Boğaziçi University (BÜHADYEK) under title 2020-17 (“The role of heparin-binding epidermal growth factor (HB-EGF) signaling during regenerative neurogenesis in the zebrafish olfactory epithelium”). All relevant international, national, and institutional guidelines for the care and use of animals were followed, including the National Animal Protection Act (Turkish national law number 5199, “Hayvanları Koruma Konunu”, published 24.06.2004), the directive 2010/63/EU of the “European Parliament and the Council of 22. September 2010 on the Protection of Animals Used for Scientific Purposes” and the “Guide for the Care and Use of Laboratory Animals” (NRC2011) of the Association for Assessment and Accreditation of Laboratory Animal Care (AAALAC).

3.2.2. BrdU Incorporation Assay

To label mitotically active cells, the thymidine analog 5-Bromo-2'-deoxyuridine (BrdU; AppliChem) was dissolved freshly in aerated freshwater at a concentration of 30 mg/l. Fish were transferred to and incubated in the BrdU solution in a dark container at 28°C for up to 24h in the same solution. If longer incubation times were required, the BrdU water was exchanged for freshly prepared solution at 24h intervals. BrdU incorporation was visualized using anti-BrdU immunohistochemistry on OE tissue sections.

3.2.3. Induction of OE Degeneration

To induce degenerative lesions to the OE, fish were treated by nasal irrigation with the non-ionic detergent Triton X-100 (AppliChem) according to Iqbal and Byrd (2010). Briefly, fish were anesthetized in tank water containing 160 mg/mL MS222 (Sigma) until opercular movements slowed down and fish became unresponsive to tactile stimuli. Anesthetized fish were placed into the groove of a wet sponge to keep them stationary during the procedure. Under a stereomicroscope, the olfactory cavity was filled with about 1 μ l of a solution containing 1% Triton X-100 and 0.1% phenol red (AppliChem) dissolved in 0.1 M PBS that was applied to the left naris with a pulled-out glass capillary using an Eppendorf FemtoJet Express microinjector. The Triton solution was applied twice at 45 sec intervals over a total time course of 90 sec. The detergent was washed out from the olfactory cavity immediately at the end of the lesion period with a stream of freshwater delivered from a Pasteur pipette. Following the procedure, fish were put back into tank water and observed until the initiation of ordinary movement.

3.2.4. Stimulation of the OE with human-recombinant HB-EGF

A total of 1 μg human recombinant HB-EGF (RD Systems) were given to fish weighing approximately 1 g. Fish were anesthetized in tank water containing 160 mg/mL MS222 (Sigma) until the opercular movements slowed down. Anesthetized fish were placed into the groove of a wet sponge with the dorsal side facing up. Afterwards, a 200 μl micropipette tip connected to a container containing an 80 mg/L MS222 solution through a plastic hose was placed into the mouth of fish for continuous perfusion. After the flow rate of the anesthetic was adjusted using an attached plastic switch, fish received 80 mg/L MS222 solution orally until the end of the procedure. Approximately 2.5 μl of a solution containing 200 ng/ μl HB-EGF dissolved in 0.1% BSA (New England Biolabs)/PBS solution were given over 30 min in pulses repeating in every 30 seconds. Fish were given an additional 2-3 min for the complete absorption of the solution before being placed back to their tanks. The same procedure was followed for a second round of HB-EGF stimulation on the next day. Following the stimulation, fish were placed into BrdU-containing tank water for a 24 h incubation period.

3.2.5. Intraperitoneal Injection of Pharmacological Agents

For systemic inhibition of EGFR and JAK/STAT signaling, fish weighing approximately 1 g received 80 μg of PD153035 (Sigma) and 1 μg of JSI-124 (Tocris), respectively. Fish were anesthetized in tank water containing 160 mg/mL MS222 until the opercular movements slowed down. Afterwards, the fish were placed into the groove of a wet sponge with their abdomen facing upwards. The signaling pathway inhibitors were injected intraperitoneally into the midline of the abdomen, just anterior to the anal fin, by using a 0.5 ml U100 insulin syringe (Beckon Dickinson) with a 30G sized needle. For the pharmacological inhibition of EGFR, fish received, a maximum volume of 30 μl of 2.7 $\mu\text{g}/\mu\text{l}$ PD153035 dissolved in 33.3 % DMSO (Sigma)/PBS solution in every dose. For the establishment of identical control conditions for the PD153035 treatment, fish received a maximum volume of 30 μl of the 33.3 % DMSO/ PBS solution in every dose. For the pharmacological inhibition of the JAK/STAT signaling, fish received, a maximum of 30 μl of the 33.3 ng/ μl JSI-124 dissolved in 6.7 % DMSO/PBS.

For the establishment of identical control condition of the JSI-124 treatment, fish received a maximum volume of 30 μ l of 6.7 % DMSO/PBS solution.

3.2.6. OE Dissection

In order to dissect the OE, fish were euthanized by prolonged incubation in MS-222, decapitated, and the heads were transferred to a dissection pad filled with ice-cold 1 x PBS. Using fine forceps (Drummond No 5; Fine Science Tools), first the cranial bones were removed, then the OEs were gently detached from remaining bones that form the nasal cavity and residual skin.

3.2.7. OE Cryosectioning and Sample Preparation

Dissected OEs were mounted in rubber molds filled with optimum cutting temperature O.C.T. medium (Sakura Finetek) and stored at -20°C until completely frozen. Frozen samples were then transferred to a LEICA CM3050S cryostat, pre-cooled at -22°C object and -20°C chamber temperatures. The frozen O.C.T. bricks were removed from the rubber molds and positioned onto the cryostat stage and cut into sections of 12 μm thickness. Sections were carefully collected onto positively charged glass slides (Superfrost® Plus; Thermo Scientific). Specimen which were used in standard immunohistochemistry experiments were heat dried for 1 hour and 15 minutes at 60°C in a hybridization oven. To be used in immunohistochemistry experiments which require antigen-retrieval, the specimen were air dried at room temperature (RT) overnight. Both specimens were either used immediately or stored at -80°C before immunohistochemistry.

3.2.8. Immunohistochemistry on OE Cryosections

OE cryosections were allowed to obtain room temperature for 10 minutes and the edges of the glass slides were sealed with a PAP-pen (Liquid Blocker) in order to prevent leakage of liquid. Samples were then rehydrated in 1x PBS for 5 minutes before the tissue was fixed with 4% paraformaldehyde (PFA) in 1x PBS (pH 7.4) for 15 min.

Slides were transferred to the Coplin jars and washed with 1x PBST for 10 min for three times. Nuclei were permeabilized by a 15 min incubation in 4 N HCl in Coplin jars (VWR) for BrdU-immunostaining. Afterwards, slides were washed again with 1x PBST for 10 min each for 3 times. Slides were blocked with 3% (w/v) bovine serum albumin BSA in 0.1% PBST for 1 h in a moist chamber at room temperature. At the end of the blocking period, the blocking solution was discarded and slides were covered with primary antibody solution prepared in 3% BSA. Slides were incubated overnight at 4°C in a moisturized chamber. Dilutions of antibodies were as follows: mouse anti-human neuronal protein (HuC/D; Life Technologies, 16A11, 1661237) 1:500, rat anti-BrdU (Abcam, BU1/75 (ICR1), ab6326) 1:500. Following incubation, the samples were washed with 1x PBST for 10 min each for three times at room temperature. Afterwards slides were covered with secondary antibody solution dissolved in 3% BSA and incubated for 2 hours at room temperature. Secondary antibody dilutions were as follows: anti-mouse Cyanine®5 (CY5-647; Jackson Immuno Research, polyclonal, 715-175-151) 1:250, anti-rat Cyanine®2 (CY2-488; Jackson Immuno Research, polyclonal, 712-225-153) 1:250. At the end of the incubation, samples were washed in 1x PBS for 10 min each for three times. Immunoreactivity against HuC/D and BrdU was analyzed on a confocal microscope.

3.2.9. Heat-induced Antigen-Retrieval for pSTAT3 Immunostaining

OEs were dissected in ice-cold 1x TBS and transferred to 1.5 μ l Eppendorf tubes containing 4% PFA for overnight fixation at 4°C on a nutator (Polymax 2040; Heidolph). On the following day, OEs were washed in 1.5 μ l Eppendorf tubes placed on a nutator at 4°C for 15 min each for three times. Then, the OEs were embedded in O.C.T. medium and stored at -20°C until completely frozen. Afterwards, OEs were cut to 12 μ m thick sections on the cryostat and collected onto positively charged slides and air dried overnight at RT.

The slides were then rehydrated in 1x TBS for 10 minutes before the antigen retrieval procedure. For antigen retrieval, 200 ml of Sodium Citrate Buffer (10 mM Na₃C₆H₅O₇, 0.05% Tween 20, pH 6) per slide was heated in a glass beaker to 100°C.

Meanwhile, a water bath was heated to 95°C. The Sodium Citrate Buffer solution was poured into plastic boxes and slides were placed into the solution and transferred immediately onto the water bath and incubated for 40 min. After the antigen retrieval step, slides were transferred to 1x TBS immediately and cooled for 10 min at RT. The edges of the slides were covered with PAP-pen (Liquid Blocker) in order to prevent leakage. Afterwards, slides were transferred to Coplin jars containing 4 N HCl for BrdU immunostaining for 15 min. Samples were then washed with 1x TBST for 15 min each for four times. Afterwards, slides were blocked with 5% goat serum dissolved in 0.1% TBST for 1 h. After blocking, slides were covered with primary antibody solution dissolved in 5% goat serum in 0.1% TBST and incubated for 2 d at 4°C. Antibody concentrations for this experiment were as follows: mouse anti-pSTAT3 (MBL Life Science, PS3/1, D128-3) 1:200, rabbit anti-Sox2 (Genetex, polyclonal, GTX124477) 1:1000, rat anti-BrdU 1:500. Following the primary antibody incubation, slides were washed with 1x TBST for 15 min each for four times. Afterwards, slides were covered with secondary antibody solution dissolved in 5% goat serum in 0.1% TBST and incubated for 1 day at 4°C. Secondary antibody concentrations used in this experiment were as follows: anti-mouse CY5-647 1:250, anti-rabbit Alexa-555 (Thermo Fisher Scientific, polyclonal, A32732) 1:800, anti-rat CY2-488 1:250. On the following day, slides were washed with 1x TBS for 15 minutes for four times and visualized using confocal microscopy.

3.2.10. Confocal Microscopy

Tissue samples that were stained by immunohistochemistry were visualized on Leica SP5-AOB or SP8 confocal microscopes (Leica Microsystems). Digital images with 1024x1024 and 2048x2048 pixel resolution were taken using 20X and 40X lenses, respectively.

3.2.11. Image Processing, Cell Quantification and Statistics

Acquired digital images were stored and transferred in the Leica image file (lif) format. The FIJI image processing software was used for image processing (Schindelin *et al.*, 2012). Proper brightness and contrast adjustments were made depending on the staining quality of the samples. For the positional profiling of labelled and co-labelled cells, first, the center of the vertical midline of the OE sections were determined using the line drawing tool. A horizontal line stretching between the center of the vertical midline and either right or left peripheral edge of the OE was drawn and the length was measured. By defining this line as the horizontal midline, a rectangular region of interest (ROI) with the vertical height of two-thirds of the horizontal length was generated and cropped. The same procedure was then applied to the hemi OE on the opposite side of the section. A total of 10 cropped images representing hemi OEs of five tissue sections were generated for each of four experimental group for each experiment saved in the tagged image file format (tiff). Using a custom macro (Demirler, 2021), the positions of labelled and co-labelled cells in the cropped images were marked separately in their designated color channels and saved as separate ROIs. Afterwards, the number and positions of cells within each ROI were counted into ten equidistant bins using a custom FIJI macro and corrected using R software scripts (R Core Team).

The Fiji image processing software was further used for the quantification of the normalized area covered by HuC/D⁺ cells. First, the channels of the acquired digital images were split. The channel corresponding to HuC/D-immunostaining was selected and saved in the tiff format for all five OE sections for each of the four experimental groups for every experiment. Afterwards, all single channel images were converted into binary representations and saved in tiff format. Binary images were then manually thresholded using signal thresholding tool and the area covered by signal was measured using build-in FIJI functions. Using the polygon drawing tool the circumference of the OE section was outlined and the selected ROI corresponding to total OE area was measured as a reference. The fractional area covered by HuC/D⁺ cells in the OE was calculated and normalized to control group in Microsoft Excel (2018).

For the statistical analysis of the data, one-way analysis of variance (ANOVA) with post-hoc Tukey honestly significant difference (HSD) test was performed using Prism Software v7 (Graph Pad, USA). Graphs were drawn in Prism Software v7 and edited using Illustrator CS6 (Adobe, USA).

4. RESULTS

HB-EGF is a membrane bound glycoprotein and a member of the EGF family which signals through EGFRs (Nakamura *et al.*, 1995). Signaling through EGFRs has been known for its effects on cell proliferation, migration, adhesion and differentiation (Wee and Wang, 2017). A positive effect of soluble HB-EGF on wound healing has also been demonstrated in different animal models including zebrafish (Wan *et al.*, 2012; Dao *et al.*, 2018). Gene expression analysis of injured OE samples showed a rapid and transient upregulation in the levels of one of the zebrafish paralogs of HB-EGF, *hbegfa* and its related extracellular signaling components in zebrafish as early as 4 h post injury (Kocagöz, 2021). Exogenous activation and deactivation of HB-EGF shedding by metalloproteases or direct inhibition of soluble HB-EGF showed that HB-EGF is necessary and sufficient to induce OE regeneration (Kocagöz, 2021; Sireci, unpublished). HB-EGF predominantly binds to ErbB1 homodimers (EGFR) or ErbB1/ErbB4 heterodimers with high affinity (Higashiyama *et al.*, 2008). Among the ErbB family, only the transcript levels of ErbB1 zebrafish paralog, *egfra* is selectively upregulated during injury (Kocagoz, Demirler, and Fuss, unpublished). Furthermore, *egfra* is expressed in the basal-most layer by tp63⁺ HBCs (Güler 2021), suggesting that EGFR might be the target receptor for HB-EGF during OE regeneration. However, the importance of EGFR and candidate downstream signal transduction components and their individual contribution to regenerative OE neurogenesis have not been studied.

In the light of these findings, the main aim of this study was to further examine EGFR signaling and the JAK/STAT pathway as one of the candidate intracellular components of HB-EGF signaling and to characterize their function in OE regeneration. PD153035 is a small molecule inhibitor of EGFR, that competes with ATP for the phosphorylation of the Tyrosine kinase domain of the receptor, hence, it inhibits the activation of EGFR by preventing autophosphorylation (Fry *et al.*, 1994). To characterize the role of EGFR signaling during OE neurogenesis, cell proliferation and neurogenesis assays were performed on intact and Triton X-100 (TrX)-treated tissue samples in the presence of the inhibitor and compared to untreated control samples.

Candidate signal transduction pathways downstream of EGFRs include PI3K-Akt, MAPK and JAK/STAT signaling (Wee and Wang, 2017). The functional contribution of JAK/STAT signaling during constitutive and regenerative OSN neurogenesis was examined by using JSI-124, a small molecule inhibitor of JAK2 and STAT3 (Blaskovich *et al.*, 2003). In addition, the activation of JAK/STAT signaling in response to stimulation of the OE with recombinant HB-EGF was further investigated by using a specific antibody against the STAT3 protein phosphorylated at Tyr708 (pSTAT3). The antibody was also utilized to examine the spatial pattern of activated cells under physiological conditions and following tissue damage.

4.1. The Effect of EGFR Inhibition on Cell Proliferation and OE Regeneration

EGFR is a target receptor for the signaling molecules EGF, TGF α , Amphiregulin, Epigen, and Betacellulin in addition to HB-EGF (Singh *et al.*, 2016). Activation of EGFR via different signal molecules has been shown to have different cellular consequences, in part, because different downstream signaling transduction pathways are favored in response to these ligands (Wee and Wang, 2017).

In order to investigate the effect of EGFR inhibition on OE neurogenesis two set of experiments were performed, by evaluating the effect of EGFR inhibition on the early proliferative and the late neurogenic responses. While the early analysis evaluates the effect of EGFR inhibition on the rate and spatial pattern of mitotic activity that can be observed during maintenance and repair neurogenesis, the late analysis aims to uncover the effect of EGFR inhibition on OE regeneration and restoration of the OSN population. The late analysis includes an evaluation of the efficiency of OSN neurogenesis and the analysis of cell fate determination of the newly generated cells.

4.1.1. The Effect of EGFR Inhibition on Cell Proliferation

To characterize the role of EGFR inhibition on cell proliferation that occurs during maintenance and repair neurogenesis, adult fish ($n=3$) were treated with 80 μg of the EGFR inhibitor PD153035 via intraperitoneal injection, 4 h before, 4 h after, and at the time of the nasal irrigation with TrX. To establish comparable control conditions, the vehicle DMSO was used in an identical experimental setup. For each experimental group, fish were continuously incubated in 30 mg/l BrdU containing tank water for 24 h immediately following the lesion. At the end of the incubation period, OEs were dissected immediately and analyzed for BrdU-immunoreactivity along with immunohistochemistry against the pan-neuronal marker HuC/D which labels mature OSNs, to visualize the success and extent of the tissue lesion (Figure 4.1).

For each experimental condition, namely PD153035-intact, PD153035-injured, DMSO-intact, DMSO-injured, five 12 μm sections were selected from each fish for quantitative analysis. Rectangular regions of interest (ROIs; indicated as dashed boxes in the top row of Figure 4.1) with the horizontal width of one hemi-OE stretching between the ILC and the peripheral edge of the tissue section, and a vertical height of two-thirds of this dimension were selected. The selections comprise about three full epithelial folds of one side of the intact OE. The selected folds project perpendicular from the midline raphe and are roughly of equal length, which simplifies accurate measurements of the positions of labeled cells by projecting the position of labeled cells onto the radial dimension of the OE. This quantification method was preferred over measurements of individual lamellae or epithelial folds because their structure becomes severely compromised and difficult to identify in TrX-lesioned tissue, especially at early time points after the lesion when OSNs are largely absent. The method, thus, allows for an accurate comparison of identical OE regions from intact and injured OEs that is largely independent of tissue conditions and integrity. Independent ROIs were generated from the left and right side of each OE section and the number and position of BrdU⁺ cells within each ROI were counted into ten equidistant bins along the radial dimensions between the ILC and peripheral circumference of the tissue sections using a custom macro in Fiji (Demirler, 2021).

Figure 4.1 depicts representative images of HuC/D (cyan) and BrdU (red) double immunostaining on horizontal sections of intact and TrX-injured OEs of DMSO- (left) and PD153035-treated (right) fish. In intact OEs, immunohistochemistry against HuC/D labels OSNs that are restricted to the sensory region within the center of the OE. The labeled area extends roughly over two-thirds of the tissue dimension and is characterized by a sharp transition in the occurrence of HuC/D-positive and HuC/D-negative cells at the sensory/non-sensory border (SNS). In contrast, treatment with 1% TrX results in a dramatic loss of HuC/D immunoreactivity as a consequence of OSN injury. However, occasional patches of labeled cells can be observed. Remaining HuC/D-positive cells often occupy the ILCs, probably, because the detergent did not enter these narrow spaces effectively. BrdU⁺ cells, which are indicative of mitotic activity can be observed at the ILC and within the nonsensory region of the intact OE, as previously described (Bayramli *et al.*, 2017), regardless whether the fish were treated with DMSO or PD153035. However, PD153035 treatment appears to slightly reduce the number of BrdU⁺ cells, predominantly around the SNS and within the non-sensory region. As can be seen in the representative image of the DMSO-control group (Figure 4.1, left), chemical insult to the OE results in a randomized distribution of BrdU⁺ cells along the radial dimensions of the OE. Labelled cells become evenly distributed and can be observed in regions that correspond to the sensory OE, which is largely devoid of BrdU⁺ cells in the intact tissue. Importantly, treatment with PD153035 severely reduced the overall number of BrdU⁺ cells in the injured tissue, including the occurrence of injury-induced mitotic cells in the sensory OE. The bottom panel of Figure 4.1 depicts higher power views of the BrdU staining pattern for selected ROIs for which the respective epithelial regions have been indicated below. PD153035 treatment appears to reduce the number of BrdU⁺ cells across all regions (ILC, core sensory, SNS, non-sensory) of the injured OE in comparison to DMSO-treated control animals.

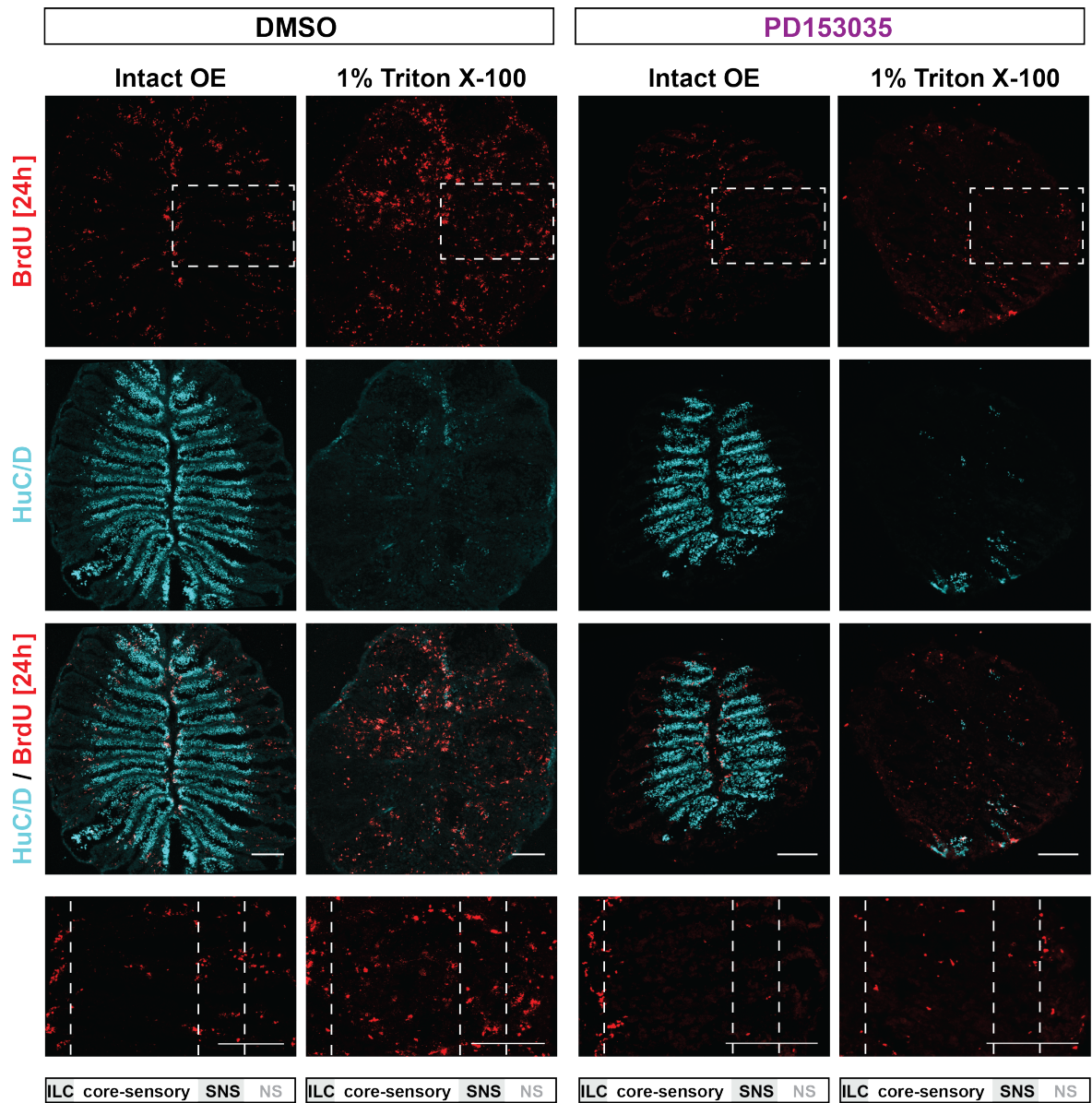


Figure 4.1. Effect of PD153035 on proliferation rate in the intact and 1 dpl OE. Immunohistochemistry against BrdU (red) and HuC/D (cyan) in DMSO- and PD153035-treated fish. Scale bars: 100 μ m.

To better describe the effect of EGFR inhibition by PD153035 treatment quantitatively, positional counts of BrdU⁺ cells were performed on selected rectangular areas. Figure 4.2.A depicts the average number of proliferating cells that can be observed across the whole OE regions (top), within the combined ILC/SNS (radial index 0.05 and 0.65-0.75, middle)), and the core-sensory region ((radial index 0.25-0.45; bottom)). An average number of 79.4 ± 0.4 (mean \pm SEM) BrdU⁺ cells can be observed per hemi-OE within the intact tissue of DMSO-treated fish (10 hemi-OEs from 5 tissue sections of 3 fish). Injury with TrX resulted in a 1.5-fold increase in the number of BrdU⁺ cells. In which, 118.9 ± 0.4 cells could be observed. Treatment with PD153035 resulted in a decrease in the basal proliferation rate in the intact OE compared to DMSO-treated control animals (PD153035: 42.2 ± 0.3 cells/hemi OE; DMSO: 79.4 ± 0.4 cells/hemi OE). More importantly, however, PD153035 treatment also prevented the typical increase in the number of mitotically active cells in the injured OE. In fish injected with the PD153035 inhibitor, the number of BrdU⁺ cells only reached up to 49.6 ± 0.3 cells, which represents a modest 1.2-fold difference between the injured and intact OE but was 2.4-fold lower compared to the DMSO control condition. To test the significance of the observed differences, a one-way ANOVA, followed by a post hoc Tukey HSD test ($F_{(3,12)} = 62.6$) has been performed on BrdU⁺ cell counts for all experimental groups. As indicated in the graph, injury stimulated a statistically significant increase in the number of BrdU⁺ cells between the intact and injured OEs of DMSO-treated fish ($p = 8.2 \times 10^{-9}$). In contrast, no significant difference among the intact and injured OEs of PD153035-treated fish could be observed ($p = 0.6652$). PD153035-treatment also significantly reduced the rate of cell proliferation observed in the intact and injured OEs compared to DMSO treatment (intact, DMSO vs PD153035: $p = 4.6 \times 10^{-7}$); injured, DMSO vs PD153035: $p = 2.0 \times 10^{-14}$).

To further pinpoint which regions of the OE were affected from the inhibition of EGFR signaling by PD153035 treatment, the regions of maintenance neurogenesis at the ILC and SNS region and the injury-responsive core sensory OE were evaluated independently (Figure 4.2.A, middle and bottom, respectively). While, 43.8 ± 2.8 BrdU⁺ cells can be counted in the ILC/SNS of DMSO-treated intact OEs, only 24.5 ± 2.1 cells found PD153035-treated animals. Similarly, PD153035-treatment caused

a decrease in the number of BrdU⁺ cells in the injured ILC/SNS (15.1 ± 1.7 cells), compared to DMSO-treated fish (38.6 ± 2.2 cells; $p = 2.0 \times 10^{-10}$, one-way ANOVA, post hoc Tukey HSD ($F_{(3,12)} = 33.5$)).

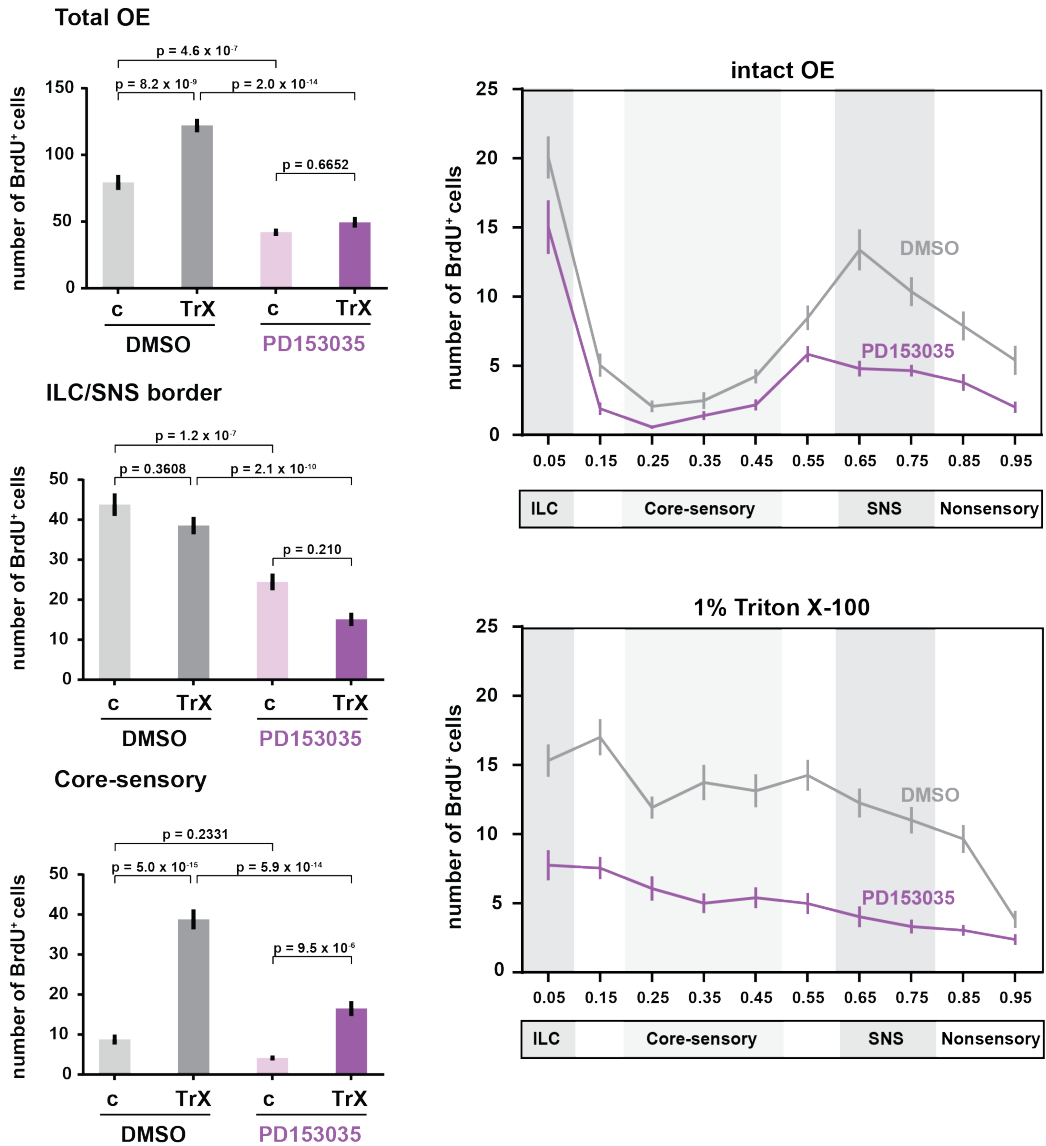


Figure 4.2. Analysis of the proliferative activity in the intact and 1 dpl OE of DMSO- and PD153035-treated fish. A. Positional profiling of BrdU-positive cells. B. Distribution of BrdU-positive cells in the intact and injured OE.

The injury-stimulated increase in the number of BrdU⁺ cells was more pronounced in the core-sensory region in which a 4-fold increase in the number of labeled cells could be observed in DMSO-treated fish (ctrl: 8.8 ± 1.3 cells; TrX: 38.8 ± 2.5 cells; one-way ANOVA, post-hoc Tukey HSD ($F_{(3,12)} = 78.9$), $p = 5.0 \times 10^{-15}$). In the core-sensory region of the PD153035-treated intact and injured OEs, only 4.1 ± 0.6 and 16.5 ± 1.9 BrdU⁺ cells could be detected, respectively ($p = 9.5 \times 10^{-6}$). Even though this difference still amounts to a 4-fold increase between the intact and injured OEs, the strength of this injury-induced increase was found to be dramatically impaired in the PD153035-treated experimental groups compared to DMSO-treated experimental groups ($p = 9.5 \times 10^{-6}$ and $p = 5.0 \times 10^{-15}$, respectively). Thus, PD153035 treatment appears to both reduce the base proliferation rate in all regions of the intact OE and prevented the development of a robust response to injury.

The positional distribution of proliferating cells for each group is depicted in Figure 4.2.B. In the DMSO-treated intact OE, BrdU⁺ cells exhibit a bimodal distribution that peaks around the ILC and SNS. In the case of the PD153035-treated intact OE, an overall mild decrease in the number of BrdU⁺ cells can be observed in all OE regions compared to DMSO-treated samples. However, a more pronounced decrease is observed in the SNS, which distorts the originally bimodal distribution. Among these inhibitor effects, only the decrease in the SNS region was found to be significant (ILC: 0.0793, one-way ANOVA, post-hoc Tukey HSD ($F_{(3,12)} = 11.9$); core-sensory: 0.2332, ($F_{(3,12)} = 78.9$), SNS: 4.3×10^{-9} , ($F_{(3,12)} = 33.9$). In DMSO-treated injured OEs, an increased number and almost homogenous distribution of BrdU⁺ cells can be observed in the core-sensory region (38.8 ± 2.5 cells) compared to DMSO-intact control fish (8.8 ± 1.3 cells). While the even distribution of proliferating cells is conserved in PD153035-treated animals, the number of BrdU⁺ cells appears to be dramatically decreased (16.5 ± 1.9 cells) along the entire radial dimension compared to the DMSO-treated injured OE, including the core-sensory OE.

Taking together, inhibition of EGFR by PD153035 resulted in a decrease in the rate of cell proliferation that occur during both maintenance and the repair neurogenesis. The inhibitory effect of PD153035 was selective for the SNS region in the intact.

In contrast, the inhibitory effect did not disrupt the random distribution of proliferating cells that occurs during repair neurogenesis but resulted in a decreased rate of cell proliferation along all radial dimensions of the OE.

4.1.2. The Effect of EGFR Inhibition on the OE Regeneration

As shown above, PD153035 has a strong inhibitory effect on cell proliferation both during maintenance and repair neurogenesis. In order to further characterize the role of EGFR signaling in OE regeneration, the efficiency of OSN neurogenesis in PD153035-treated animals was analyzed and compared to DMSO-treated animals (n=3). Two critical measures, the number of BrdU⁺ cells that can be labeled at the peak of mitotic activity in the injured OEs between 48 and 72 h post lesion (hpl) and the contribution of newly generated cells to the pool of HuC/D⁺ OSNs were evaluated.

For both of analyses, PD153035 was injected 4 h before, 4 h after, and during the nasal irrigation with TrX and fish were incubated in BrdU-containing tank water between 48 and 72 hpl. All samples were analyzed for BrdU and HuC/D immunoreactivity at 5 d post lesion (5dpi).

Representative images of HuC/D (cyan) and BrdU (red) double immunostaining on horizontal sections of intact and TrX-injured OEs of DMSO- (left) and PD153035-treated fish (right) are depicted in Figure 4.3. In the intact OE of both the DMSO- and PD153035-treated fish, HuC/D immunostaining labels the characteristic restricted pattern of HuC/D⁺ OSNs in sensory OE region. As previously indicated in Figure 4.1, chemical lesion to the OE results in an almost complete degeneration of HuC/D⁺ OSNs at 24 hpl. Thus, HuC/D immunostaining in the injured OEs at 5 d post lesion (dpl) largely represents regenerated OSNs. While an almost complete regeneration can be observed after injury in DMSO-treated animals, HuC/D⁺ OSNs only occupy small tissue patches around the ILC and the surrounding inner regions in PD153035-treated injured OEs. In addition to the visualization of mitotic activity zones, BrdU/HuC/D co-immunostaining also marks the progeny of cells that were labelled during the two-day incubation period between 72 and 120 hpl in this experimental setup.

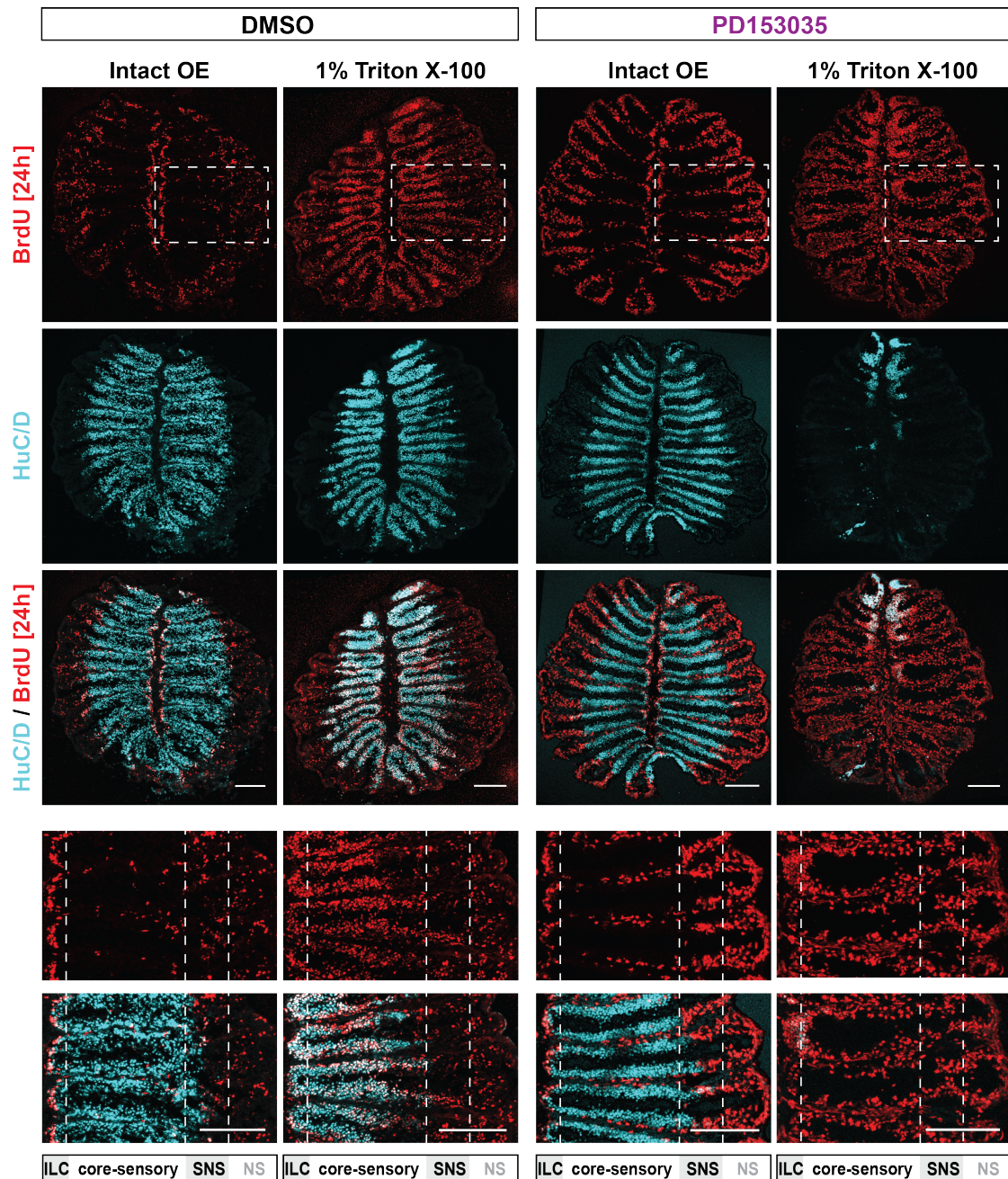


Figure 4.3. Effect of PD153035 on proliferation and neurogenesis rate in the intact and 5 dpl OE. Immunohistochemistry against BrdU (red) and HuC/D (cyan) in DMSO- and PD153035-treated fish. Scale bars: 100 μm .

In intact OEs of DMSO- and PD153035-treated animals, BrdU⁺ cells largely occupy the ILC and SNS/nonsensory region. However, a slightly increased number mitotic activity in the core-sensory region of PD153035-treated animals can be observed.

The injured OE of the both experimental groups show the expected increase and characteristic random distribution. However, in PD153035-treated fish, these cells often appear to form clusters in the sensory region compared to their uniformly dispersed appearance in control group.

Moreover, BrdU⁺ cells in PD153035-treated injured OEs are largely restricted to basal layers, whereas they also occupy more apical layers in DMSO control animals. The two bottom panels of Figure 4.3 depict higher power views of the BrdU and HuC/D/BrdU staining pattern for selected ROIs, which have been indicated in the images at the top. The slightly increased mitotic activity in the core-sensory region of PD153035-treated intact OEs is observed to be not neurogenic as indicated by the absence of HuC/D co-immunostaining and appears to originate largely from within the lamina propria. The dispersed pattern of HuC/D⁺/BrdU⁺ cells in the sensory region of injured OEs from the DMSO control group seems to be largely related to neurogenic mitotic activity, which is absent in PD153035-treated animals. Thus, in the presence of PD153035, injury results in increased mitotic activity within the basal layers of the sensory OE, which, however, remains largely non-neurogenic as late 5 dpl. Newborn OSNs can also be observed in some, but not all, ILCs of PD153035-treated injured OEs, the only region where HuC/D⁺ OSNs are present, most likely as a result of ongoing maintenance neurogenesis at these sites.

4.1.2.1. Evaluation of the Efficiency of OSN Neurogenesis.. To obtain a quantitative descriptor for the efficiency of OSN neurogenesis in response to injury, the area covered by HuC/D⁺ OSNs relative to the total OE area of was measured using signal thresholding and pixel counting in Fiji. For the measurement of area covered by HuC/D⁺ OSNs, the channel corresponding to the HuC/D staining was selected, manually thresholded, and the images converted into binary representations. For the measurement of total OE area, the polygon drawing tool was used to outline the circumference of OE section and then the area of the selected ROI was measured. The area covered by HuC/D⁺ OSNs relative to the total OEs was calculated and normalized to DMSO-treated intact OEs at 5dpl and compared across different experimental groups.

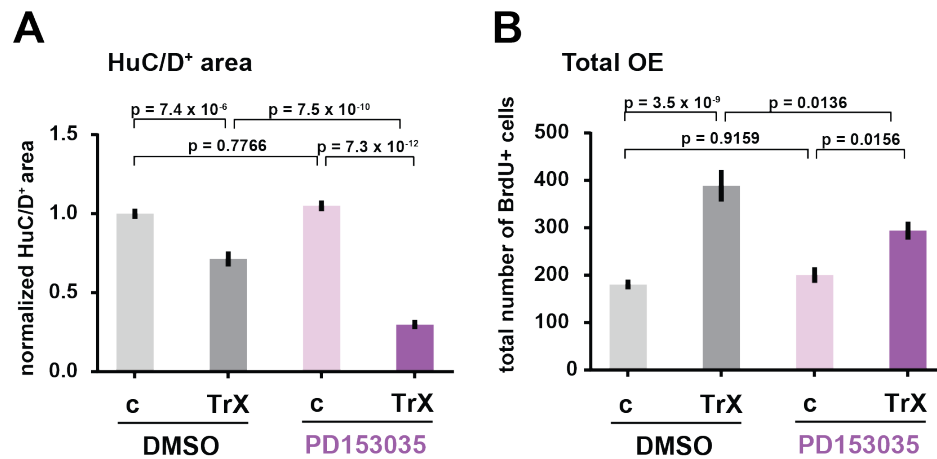


Figure 4.4. Analysis of proliferative and neurogenic activity in the intact and 5 dpl OE after PD153035 treatment. A. The efficiency of OSN neurogenesis. B. Total number of newly generated cells.

Figure 4.4.A represents the normalized HuC/D⁺ areas of the experimental groups. In DMSO-treat injured OEs, area covered by HuC/D⁺ OSNs reaches 71.4 ± 4.7 % of intact OE values, a regeneration rate which is accepted to be successful (Kocagöz, 2021). Also, similar to previously described values for this time point (Kocagöz, 2021). However, the area covered by HuC/D⁺ cells is reduced to 29.9 ± 2.9 % in PD153035-treated injured OEs. Thus, PD153035 significantly reduced the area covered by regenerated OSNs in response to injury (one-way ANOVA post-hoc Tukey HSD ($F_{(3,56)} = 85.6$); $p = 7.5 \times 10^{-10}$), while it had no effect on intact OEs ($p = 0.7766$). Thus, inhibition of EGFR signaling by PD153035, significantly reduces the rate of OSN regeneration compared to vehicle-treated control animals. Surprisingly, however, the number of BrdU⁺ cells, which represent mitotically active cells that did not generate or develop into mature OSNs over the course of the experiment was also increased in PD153035-treated animals at 5 dpl (Figure 4.4.A, right).

4.1.2.2. Contribution of Newly Generated Cells to OSN Neurogenesis. For evaluating the effect of PD153035 on OSN neurogenesis, the mitotic activity observed between 48 and 72 hpl and the resulting cell-fates of newborn cells was analyzed. For each condition, rectangular ROIs (indicated as dashed boxes in the top row of Figure 4.3) were selected from five sections per fish for quantitative analysis as previously described. Independent ROIs were generated from the left and right side of each OE section and the number and position of single BrdU⁺ and BrdU⁺/HuC/D⁺ double positive cells within the ROIs were counted into ten equidistant bins along the radial dimensions using a custom macro in Fiji.

Figure 4.4.B shows the total cell counts of BrdU⁺ cell for each experimental group. Injury causes the total number of BrdU⁺ cells to increase 2.2-fold from 180.8 ± 10.3 to 389.0 ± 33.2 in DMSO-treated animals. This increase accounts for a highly significant difference between the intact and injured OEs of the DMSO-treated fish ($p = 3.5 \times 10^{-9}$; one-way ANOVA, post-hoc Tukey HSD, $F_{(3,12)} = 19.3$). In PD153035-treated animals a milder 1.5-fold increase was observed, in which 200.8 ± 16.3 and 294.2 ± 18.9 cells could be detected in the intact and injured OEs, respectively. Although not as pronounced as the increase observed in controls, the difference between intact and injured OEs of the PD153035-treated animals was also found to be significant ($p = 0.0156$). PD153035 treatment results in a 2.4-fold decrease in the efficiency of OSN regeneration at 5 dpl (Figure 4.4.A), which might be the consequence of the reduced number of BrdU⁺ cells in the injured OEs of PD153035-treated animals compared to DMSO controls ($p = 0.0136$). However, PD153035 treatment seems to only slightly alter the total number of newly generated cells. Therefore, the strong reduction in the number of regenerated OSNs cannot be solely explained by the change in the captured mitotic activity of 3 dpl. Examining the cell fates of newly generated cells by counting single BrdU- and BrdU/HuC/D-double-positive cells in different epithelial positions appears to be helpful to gain further insight into the nature of the inhibitory effect.

Figure 4.5.A represents the average number of single BrdU⁺ cells that can be observed in the total (left), the combined ILC/SNS region (middle), and the core-sensory region (right) of the intact and injured OEs of the each experimental group.

While an average number of 134.6 ± 5.6 cells can be observed per hemi-OE across the intact OE (10 hemi-OEs from 5 tissue sections of 3 fish), injury caused a slight increase in the number of labelled cells in DMSO-treated animals (156.1 ± 10.9). A similar number of 169.7 ± 11.4 single BrdU⁺ cells could be observed in PD153035-treated intact OEs. Surprisingly, injury caused a more pronounced 1.5-fold increase in the average number of single BrdU⁺ cells in the PD153035-treated fish (252.6 ± 18.2 cells). The increased number of single BrdU⁺ cells observed in the DMSO-treated injured OEs and PD153035-treated intact OEs relative to DMSO-treated intact OEs was not found to be significant in both cases (DMSO-injured: $p = 0.6208$; PD153035-intact: $p = 0.2046$; one-way ANOVA, post-hoc Tukey HSD, $F_{(3,12)} = 16.8$). In contrast, PD153035-treatment resulted in a highly significant increase in the average number of single BrdU⁺ cells in the total OE after injury relative to unlesioned inhibitor-treated control OEs ($p = 5.0 \times 10^{-5}$).

To further determine the origin of these difference, the ILC/SNS and core sensory OE were scored separately. The average number of single BrdU⁺ cells observed in the ILC/SNS region of the different experimental groups is shown in Figure 4.5.A (middle). An average number of 63.7 ± 3.3 and 62.9 ± 4.9 single BrdU⁺ cells can be counted in DMSO-treated intact and injured OEs, respectively ($p = 0.9994$; one-way ANOVA, post-hoc Tukey HSD, $F_{(3,12)} = 3.7$). Thus, injury does not induce increased mitotic activity in the regions of maintenance neurogenesis. In PD153035-treated intact and injured OEs, an average number of 70.7 ± 4.9 and 83.3 ± 5.8 single BrdU⁺ cells could be detected, respectively. None of the statistical comparisons between experimental groups reached significance, suggesting that base mitotic activity at the ILC/SNS resumes normally in the lesioned OE at this experimental time point, although a small increase in the number of labeled cells could be detected in the presence of the inhibitor.

Figure 4.5.A (right) represents the average number of single BrdU⁺ cells in the core-sensory region of all experimental groups. While an expectedly low number of 10.1 ± 1.4 single BrdU⁺ cells can be observed in this region in DMSO-treated intact OEs, injury induces a 3-fold increase in the number of labelled cells (37.5 ± 2.7 cells).

Similar to ILC/SNS, the basal proliferation rate seems to be modestly increased in the core sensory region in response to PD153035 in the intact tissue (25.1 ± 2.1 cells). Interestingly, a similar 3-fold increase occurs after injury (83.7 ± 6.0 cells). It should be noted, however, that this elevated number of cells in the core-sensory OE corresponds to an 8-fold higher rate compared to intact OEs of the DMSO-treated animals (DMSO-intact: 10.1 ± 1.4 ; PD153035-injured: 83.7 ± 6.0 cells). The differences among the intact and injured OEs of DMSO- and PD153035-treated fish were both significant. However, the injury-induced increase in the average number of single BrdU⁺ cells observed in the core-sensory region is found to be more pronounced under the effect of PD153035-treatment (DMSO: $p = 1.9 \times 10^{-6}$; PD153035: $p = 1.6 \times 10^{-14}$). Therefore, the overall increase in the average number of single BrdU⁺ cells observed across the total OE after injury in PD153035-treated fish seems to be almost completely attributable to the increase that occurs in the core-sensory region (Figure 4.4.B, right).

Figure 4.5.B represents the average number of HuC/D⁺/BrdU⁺ double positive cells that can be observed in the total (left), the combined ILC/SNS (middle), and the core-sensory (right) region of the OE. A 5-fold increase, which causes the average number of double positive cells to change from 46.2 ± 8.7 to 232.0 ± 26.4 , could be noticed in the OE of DMSO-treated fish after injury. In PD153035-treated fish however, this injury-induced induction is found to be much lower, and only 31.1 ± 10.0 and 37.0 ± 5.3 double positive cells could be detected in intact and injured total hemi-OEs, respectively. While the injury-induced difference among PD153035-treated fish was not significant (one-way ANOVA, post-hoc Tukey HSD, $F_{(3,12)} = 40.6$, $p = 0.9928$), the difference was found to be highly significant among DMSO-treated intact and injured hemi-OEs ($p = 2.8 \times 10^{-12}$). Thus, PD153035 appears to selectively block OSN neurogenesis in response to injury.

Similar to the analysis for single BrdU⁺ cells, ILC/SNS and core sensory region were scored independently to gain further insight into their differential behavior. The average number of double-positive cells observed in the ILC/SNS regions of the hemi-OEs is depicted in Figure 4.5.B (middle). An average number of 30.6 ± 5.3 and 37.7 ± 4.8 double-positive cells could be counted in DMSO-treated intact and injured OEs.

PD153035 treatment resulted in a reduction in both the base rate of mitotic activity and the response to injury at the sites of maintenance neurogenesis at the ILC and SNS. While an average number of 17.3 ± 4.5 double-positive cells can be seen in PD153035-treated intact OEs, only 5.2 ± 1.1 cells were found after injury. However, none of these changes were found to be significant (DMSO: $p = 0.7245$ and PD153035: $p > 0.9999$; one-way ANOVA, post-hoc Tukey HSD, $F_{(3,12)} = 4.4$).

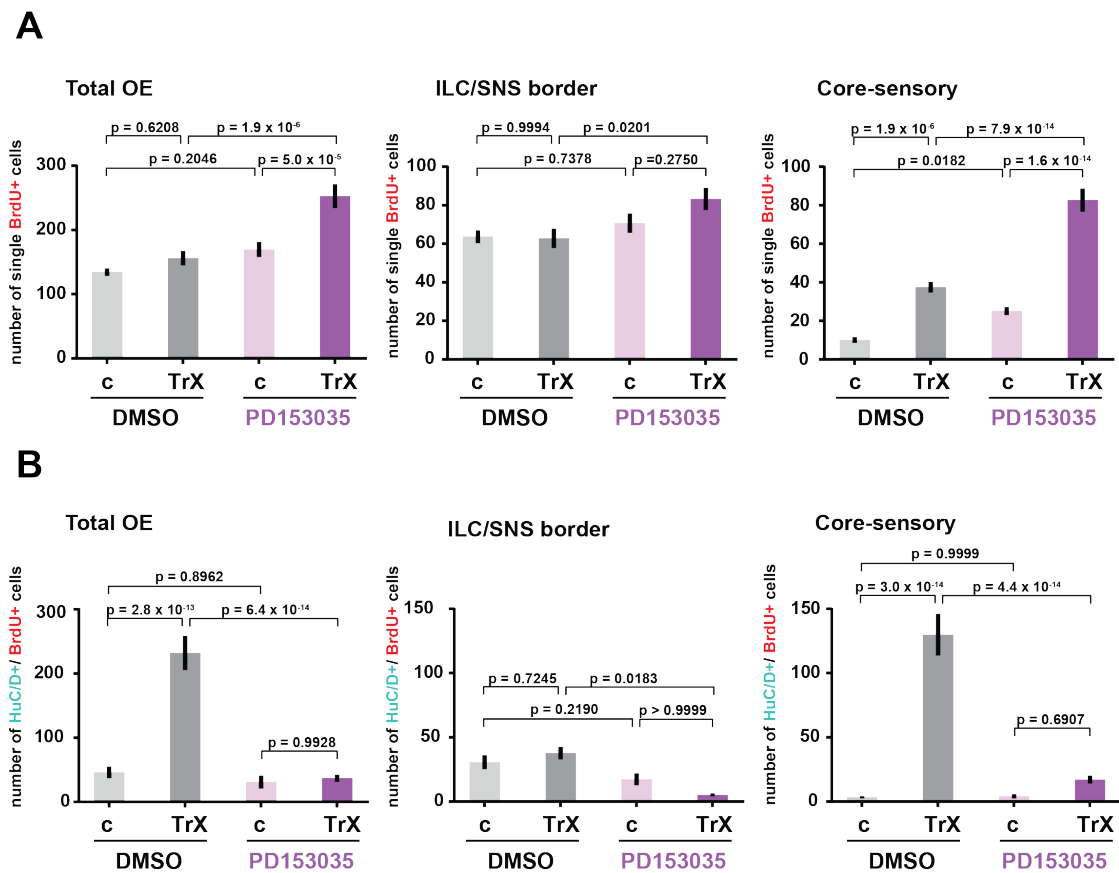


Figure 4.5. Analysis of the cell fates of the newly generated cell populations in the intact and 5 dpl OE after PD153035 treatment. A. Positional profiling of single BrdU-positive cells. B. Positional profiling of HuC/D/BrdU-double positive cells.

More importantly, the OSN neurogenesis, as indicated by the presence of the BrdU/ HuC/D-double positive cells, was severely reduced in core-sensory region, which shows the largest change number in response to injury. Figure 4.5.B (right) represents the average number of double-positive cells in the core-sensory region of hemi-OEs.

While an expectedly low number of 3.3 ± 0.7 BrdU⁺/HuC/D⁺ cells can be found in the intact OEs of DMSO-treated fish, a dramatic 40-fold increase to 130.0 ± 16.1 double-positive cells can be detected after injury. In contrast, a similar injury-induced increase did not occur in PD153035-treated fish. An average number of 4.1 ± 1.6 and 17.1 ± 3.0 cells can be counted in PD153035-treated intact and injured OEs, respectively. While the injury-induced increase observed in the DMSO-treated fish is found to be highly significant ($p = 3.0 \times 10^{-14}$; one-way ANOVA, post-hoc Tukey HSD, $F_{(3,12)} = 53.3$), the increase observed in the PD153035-treated fish did not reach significance ($p = 0.6907$). The residual increase that occurs in the core-sensory OE appears to be responsible for the small increase in newly generated OSNs that can be observed across the total OEs after injury.

Although injury induced an increase in the number of single BrdU⁺ cells in the core-sensory region of the DMSO-treated fish ($p = 1.9 \times 10^{-4}$), the increase was more pronounced in PD153035-treated fish, where the pattern assumes an almost homogeneous distribution of cells across the hemi-OE (Figure 4.6.B., left). The increase that results from the PD153035 treatment was found to be highly significant in the core-sensory OE ($p = 7.9 \times 10^{-14}$). As expected, injury induces a substantial increase in the average number of double-positive cells across the sensory region of DMSO-treated fish (Figure 4.6.B, right). This increase resulted in the formation of a highly significant difference among the intact and injured OEs of the DMSO-treated fish along the core-sensory region ($p = 3.0 \times 10^{-14}$). PD153035-treated and injured OEs have a similar distribution of double-positive cells which peaks around the central margin of the core-sensory but gradually approaches zero towards the SNS. Despite having a similarly shaped distribution, the average number of double-positive cells observed in the sensory region of the PD153035-treated injured OEs was dramatically decreased. No significant difference could be detected in the number of double positive cells observed in the core-sensory region of the PD153035-treated intact and injured OEs ($p = 0.6907$).

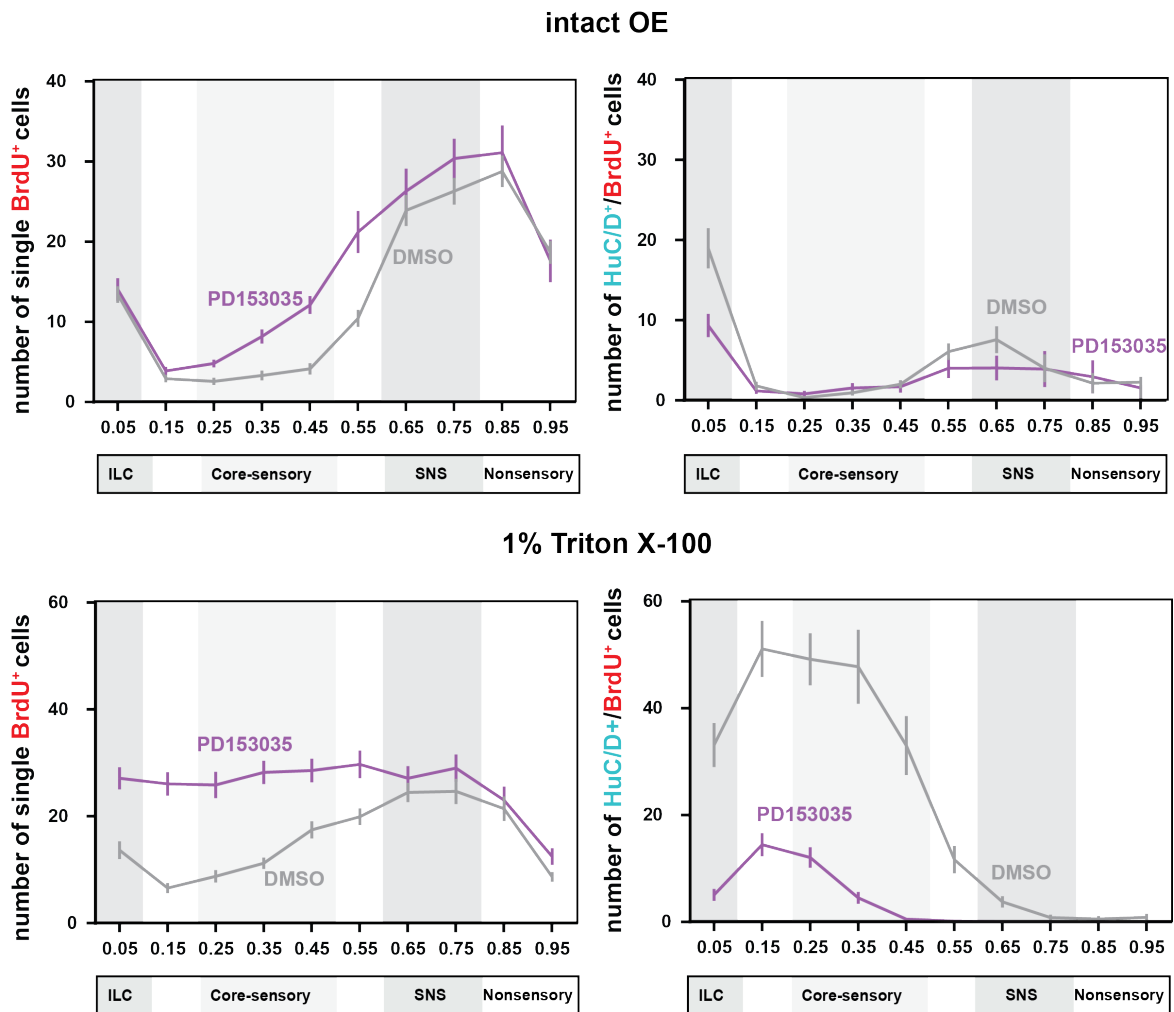


Figure 4.6. Distribution of single BrdU and HuC/D/BrdU double positive cells in the DMSO- and PD153035-treated OEs. A. Intact OE. B. 5dpl OE.

In summary, PD153035 caused an impairment in OSN regeneration. This effect can be partly explained by a decrease in the overall number of cells that are newly generated in response to injury at 5 dpl in the presence of inhibitor. However, the results showed that in contrast to newly generated OSNs, the number of newly generated non-neuronal cells did not show a decrease, but, in fact, a highly significant increase. Therefore, a selective decrease in the contribution of the 3 dpl proliferative activity to OSN lineages seems to be the actual cause of the dramatic impairment in OSN regeneration. The non-neuronal cells that occur in the injured OEs could indicate either stem cells or differentiated non-neuronal cells. Due to lack of additional cell identity markers in zebrafish, it is not possible to discriminate between these two cell types.

The effect might be explained by a delay in regenerative response caused by PD153035 treatment by postponing the initial generation of GBCs from HBCs that occurs during the early phase after injury to a later time point.

Therefore, the increased number of non-neuronal single BrdU⁺ cells might indicate proliferative stem cells, which show late activity due to the inhibition of their proliferative activity between 1 and 3 dpl after PD153035 treatment. The resemblance of the multiple BrdU⁺ basal layers observed at 5 dpl after PD153035 treatment to multiple layers formed by Sox2-expressing cells at 2dpl (Kocagöz, 2021; Kocagoz *et al.*, 2022) further supports this interpretation.

4.2. The Effect of JAK/STAT Inhibition on Cell Proliferation and OSN Neurogenesis

The common signaling routes that convey intracellular activity downstream of EGFRs include the PI3K-Akt, MAPK and JAK/STAT pathways (Wee and Wang, 2017). The negative effect of EGFR inhibition on cell proliferation and OE neurogenesis has been demonstrated previously in the framework of this thesis. In order to investigate the possible contribution of JAK/STAT signaling on OE neurogenesis two set of experiments were performed by evaluating the early and late neurogenic responses under JAK/STAT inhibition similar to the analysis described for EGFR. While the early analysis examines the early effect of JAK/STAT signaling inhibition on cell proliferation observed during maintenance and repair neurogenesis, the late analysis aims to evaluate the efficiency of OSN regeneration in terms of newly generated OSNs.

4.2.1. The Effect of JAK/STAT Signaling Inhibition on Cell Proliferation

In order to functionally characterize the effect of JAK/STAT signaling on cell proliferation, the small molecule inhibitor JSI-124 was utilized. JSI-124 selectively inhibits the phosphorylation of JAK2 and STAT3 and therefore prevents the activation of JAK/STAT signaling (Blaskovich *et al.*, 2003). Fish (n=3) received 1 μ g of the inhibitor JSI-124 dissolved in DMSO intraperitoneally, 6 h before, at the time of the nasal irrigation with 1 % TrX, and 6 h after. To establish comparable control conditions, the vehicle DMSO was used in an identical experimental setup. For the examination of the effect of JAK/STAT signaling on cell proliferation, fish were incubated in 30 mg/l BrdU-containing tank water for 24 h. Afterwards, the OEs were dissected immediately and analyzed for BrdU-immunoreactivity along with immunohistochemistry against HuC/D. For each condition (JSI-124-intact, JSI-124-injured, DMSO-intact, DMSO-injured), five 12 μ m sections were selected from each of three fish for quantitative analysis on selected rectangular ROIs as described previously.

Figure 4.7 shows representative images of immunohistochemistry against HuC/D (cyan) and BrdU (red) on OE horizontal sections of intact and TrX-injured OEs of DMSO- and JSI-124-treated fish. Similar to the previous results, HuC/D labels OSNs that are restricted to the sensory region in intact OEs, while in the TrX-injured OEs, HuC/D-immunostaining is reduced to occasional patches of cells appear in several lamellae. Both the DMSO- and JSI-124-treated intact OEs shows BrdU⁺ cells at the ILC and in the SNS/nonsensory region, which is characteristic in the intact tissue (Bayramli *et al.*, 2017, Demirler *et al.*, 2020). However, the number of BrdU⁺ cells appear to be increased in the JSI-124-treated OE.

Injured control OEs show an almost homogenous distribution of BrdU⁺ cells across the OE as observed in experiments described in the previous part. Interestingly, the pattern of BrdU⁺ cells in the JSI-124-treated injured OE largely resembles that of intact control. The higher power views of the BrdU staining pattern for selected ROIs (indicated as dashed boxes in the images at the top) are depicted in the bottom panel.

JSI-124 treatment seems to increase the occurrence of BrdU⁺ cells mainly in the ILC and core-sensory region of the intact OE compared to DMSO-treated fish. The DMSO-treated injured OE shows an increased number of BrdU⁺ cells within the core-sensory region, characteristic of the injury condition (Kocagöz, 2021). This injury-induced increase in the core-sensory region seems to be suppressed in JSI-124-treated fish and the overall distribution pattern of BrdU⁺ cells loosely resembles the intact OEs.

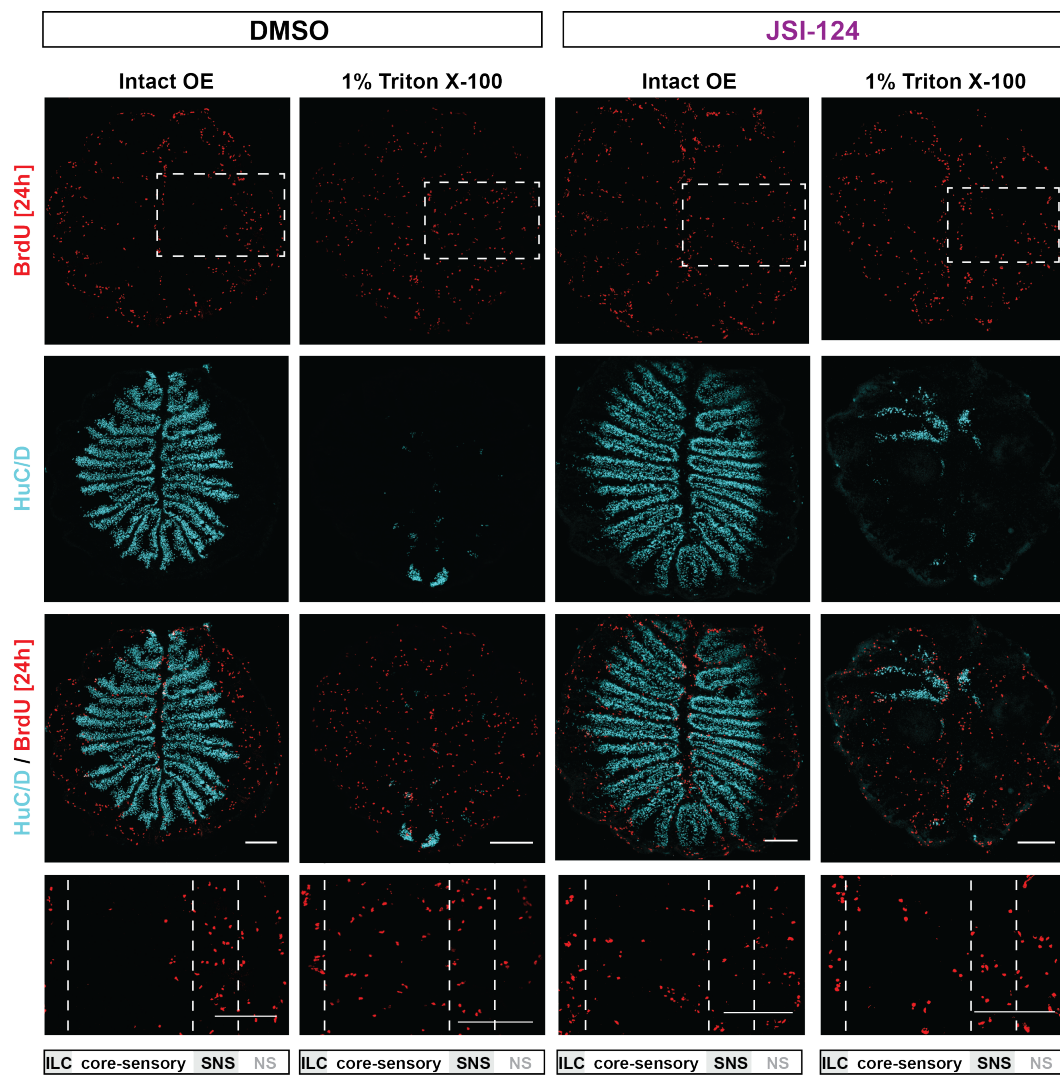


Figure 4.7. Effect of JSI-124 on proliferation rate in the intact and 1 dpl OE. Immunohistochemistry against BrdU (red) and HuC/D (cyan) in DMSO- and JSI-124-treated fish. Scale bars: 100 μm .

To describe the changes that occur in tissue homeostasis and in response to tissue injury following JSI-124 treatment with more detail, the full radial profiles of mitotically active cells were plotted. Figure 4.6 represents the radial distribution profiles of single BrdU⁺ (left) and HuC/D⁺/BrdU⁺ (right) that can be observed in intact (top) and injured (bottom) OEs of DMSO- and JSI-124-treated fish. DMSO-treated intact OEs show the expected bimodal distribution, which is characterized by a low number of single BrdU⁺ cells in the core-sensory OE and increased activity at the ILC and SNS/nonsensory region. Although, JSI-124 treatment resulted in an increased number of single BrdU⁺ cells within the core-sensory region and the SNS in the intact OEs compared to DMSO-treated fish, only the difference in the core-sensory region reached significance (core-sensory: $p = 0.0182$; SNS: 0.6713 ; one-way ANOVA, post-hoc Tukey HSD, $F_{(3,12)} = 0.9390$). In contrast, PD153035 treatment causes a decrease in the average number of HuC/D⁺/BrdU⁺ double-positive cells around the ILC and SNS in intact OEs and slightly suppresses the bimodal distribution pattern of double-positive cells that peaks around the ILC and SNS (Figure 4.6.A, right). However, only the decrease observed at the ILC reached significance (ILC: $p = 0.0467$; one-way ANOVA, post-hoc Tukey HSD, $F_{(3,12)} = 23.2$; SNS: $p = 0.7384$; one-way ANOVA, post-hoc Tukey HSD, $F_{(3,12)} = 3.7$).

To describe the effect of JAK/STAT signaling inhibition by JSI-124 quantitatively, the number of BrdU⁺ cells in the whole OE, at the ILC/SNS, and core-sensory region were evaluated separately. Figure 4.8.A depicts the number of proliferating cells that can be observed in total hemi-OEs (top), the combined ILC/SNS (middle), and the core-sensory region (bottom) for all experimental groups. In DMSO-treated fish, an average number of 33.7 ± 2.7 BrdU⁺ cells can be observed per hemi-OE within the intact tissue (10 hemi-OEs from 5 tissue sections of 3 fish). JSI-124-treatment results in an increase in the basal proliferative activity in the intact OE, compared to DMSO-treated fish, in which a 1.7-fold higher number of BrdU⁺ cells (57.8 ± 3.7 cells/hemi-OE) could be counted. A more pronounced 2.2-fold increase however, was observed within the DMSO-treated control animals after TrX treatment. The number of BrdU⁺ cells increased to 73.3 ± 5.3 in the injured OE of these animals.

In JSI-124-treated fish on the other hand, the number of BrdU⁺ cells shows no additional increase in response to TrX treatment (intact: 57.8 ± 3.7 cells/hemi-OE; injured: 58.3 ± 3.9 cells/hemi-OE). Thus, treatment with JSI-124 resulted in 1.3-fold lower number of BrdU⁺ cells in the injured OE compared to DMSO-treated animals (DMSO: 73.3 ± 5.3 cells/hemi-OE; JSI-124: 58.3 ± 3.9 cells/hemi-OE). As indicated in the graph (Figure 4.8.A, top), JSI-124 treatment results in a significant increase in the basal proliferative activity in the intact OE when compared to DMSO-treatment ($p = 0.0001$; one-way ANOVA post hoc Tukey HSD ($F_{(3,12)} = 16.2$)). Injury with TrX treatment also results in a highly significant increase in the total number of BrdU⁺ cells in the DMSO-treated fish ($p = 1.9 \times 10^{-9}$). In JSI-124-treated fish, however, no statistically significant difference could be detected between the intact and injured OE ($p = 0.9998$). Thus, JSI-124 treatment results in a significant decrease in the number of BrdU⁺ cells observed in the injured OE compared to DMSO treatment ($p = 0.0500$).

To pinpoint the effect of JSI-124 treatment in the neurogenic regions of the intact tissue, the ILC and SNS were evaluated together (Figure 4.8.A, middle). All experimental groups showed similar numbers of BrdU⁺ cells in this region. While an average number of 19.0 ± 2.0 BrdU⁺ cells could be found in the DMSO-treated intact OE, this number increases slightly to 22.0 ± 2.3 with injury. A slight increase in the number of BrdU⁺ cells (25.7 ± 2.3 cells) could also be observed in the JSI-124-treated intact OEs compared to DMSO controls. However, injury by TrX treatment, resulted in a decreased number of 19.1 ± 1.7 BrdU⁺ cells in JSI-124-treated fish. None of the differences between experimental groups were significant (DMSO-intact/injured: $p = 0.7108$; DMSO-intact/JSI-124-intact: $p = 0.00961$; JSI-124-intact/injured: $p = 0.1094$; one-way ANOVA post-hoc Tukey HSD $F_{(3,12)} = 2.4$). Thus, JSI-124 treatment did not show evidence for any effect on cell proliferation at the neurogenic regions for tissue maintenance.

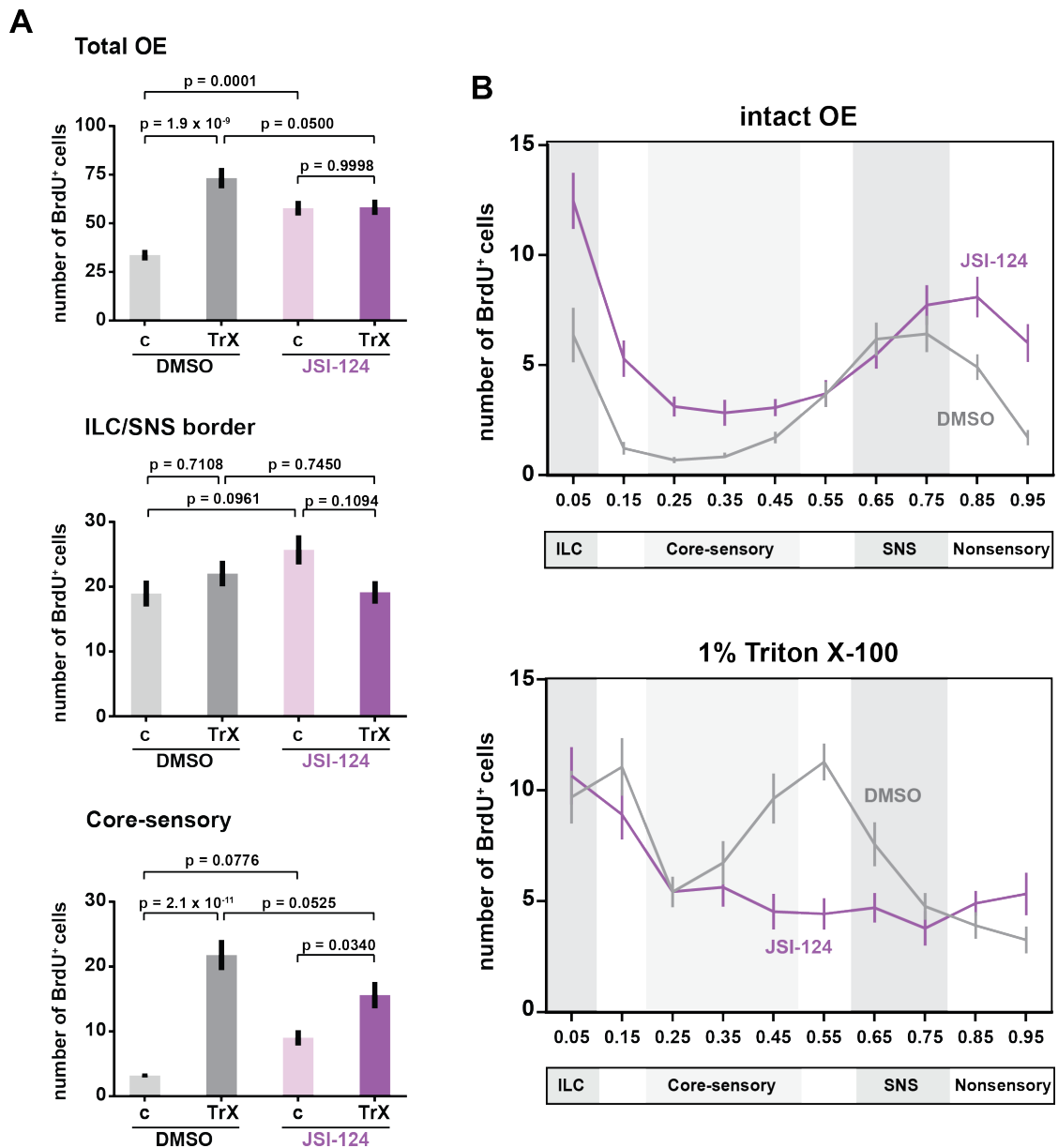


Figure 4.8. Analysis of the proliferative activity in the intact and 1 dpl OE of DMSO- and JSI-124-treated fish. A. Positional profiling of BrdU-positive cells. B. Distribution of BrdU-positive cells in the intact and injured OE.

Next, proliferative activity of the injury-responsive core-sensory region was examined (Figure 4.8.A, bottom). A small average number of 3.2 ± 0.3 BrdU⁺ cells could be observed in DMSO-treated control fish, characteristic of the previously established uninjured OE conditions. Injury with 1% Triton X-100 treatment caused the number of BrdU⁺ cells to increase 6.8-fold to 21.8 ± 2.3 cells in DMSO-treated animals.

An injury-induced increase was also observed in JSI-124-treated fish, in which an average number of 9.0 ± 1.2 and 15.6 ± 2.0 BrdU⁺ cells can be seen in intact and injured OEs, respectively. This difference only accounts for a small, 1.7-fold increase in the average number of BrdU⁺ cells in response to injury. The average number of BrdU⁺ cells in the core-sensory region of the JSI-124-treated injured OE was found to be 1.4-fold lower than in DMSO controls. The difference between DMSO-treated fish in response to injury was found to be highly significant ($p = 2.1 \times 10^{-11}$; one-way ANOVA, post hoc Tukey HSD, $F_{(3,12)} = 22.7$). In contrast, after TrX-injury in JSI-124-treated fish, the increase in the number of BrdU cells was significantly impaired ($p = 0.0340$). Although JSI-124-treatment increases the average number of BrdU⁺ cells observed in the intact OE, the difference did not reach significance ($p = 0.0776$).

The radial distribution profiles of proliferating cells in intact OEs of each group are depicted in the top graph of Figure 4.8.B. In DMSO-treated intact OEs, the characteristic bimodal distribution of BrdU⁺ cells that peaks around the ILC and SNS/nonsensory region can be observed. JSI-124 treatment caused the proliferative activity to increase in nearly all regions of the intact OE without disrupting the bimodal distribution pattern of BrdU⁺ cells. Among the regions within the sensory OE, the ILC and the core-sensory region seems to be most affected by the JSI-124 treatment and only a small increase could be observed in the SNS region. Only the individual increase observed in the ILC of the intact OE in response to JSI-124 treatment reached significance (ILC: $p = 0.0043$; one-way ANOVA post-hoc Tukey HSD, $F_{(3,12)} = 4.2$; core-sensory: $p = 0.0776$, $F_{(3,12)} = 22.7$; SNS: $p = 0.9861$, $F_{(3,12)} = 2.9$).

Distribution profiles in injured OEs depicted in the bottom Figure 4.8.B. Interestingly, the distribution of BrdU⁺ cells in the DMSO-treated injured OE do not resemble the previously established pattern at 1 dpl (Kocagöz, 2021), which could also be observed in PD153035 (Figure 4.2.B). The distribution curve starts with 9.7 ± 1.2 BrdU⁺ cells at the ILC and shows one of the highest number of BrdU⁺ cells in the next radial position (11.1 ± 1.3 cells, radial index: 0.15). In the next position, which corresponds to the first segment of the core-sensory, a large decrease follows peak of activity, in which only an average number of 5.4 ± 0.7 could be seen (radial index: 0.25).

In the subsequent segments, average number of BrdU⁺ cells starts to increase again and a second peak of mitotic activity emerges between the core-sensory region and the SNS region (11.3 ± 0.8 cells;; radial index: 0.55). Following this second peak of mitotic activity, the average number of BrdU⁺ cells starts to decrease again and shows the lowest number of 4.8 ± 0.6 cells in the peripheral-most segment of the SNS region (radial index: 0.75). Therefore, in this experiment the DMSO-treated injured OE shows a bimodal distribution of proliferative activity, rather than the homogenous distribution which was regularly observed at 1 dpl (Kocagöz, 2021). The reason for this deviation is unclear but most likely reflects a difference between animals rather than a specific effect of DMSO treatment.

In JSI-124 treated injured OE, BrdU⁺ cells peak around the ILC and shows an almost homogenous distribution in the rest of the OE regions. Because of the second peak of mitotic activity in DMSO-treated fish, a large difference can be observed between DMSO- and JSI-124-treated animals from the beginning of core-sensory region until the peripheral edge of SNS. In the position at which the second peak of mitotic activity emerges in the DMSO-treated OE (radial index: 0.55), the difference between the DMSO- and JSI-124-treated OE is maximal. While 11.3 ± 0.8 cells observed in the DMSO-treated OE, only 4.4 ± 0.7 cells observed in the JSI-124-treated OE. This difference corresponds to a 2.6-fold decrease in the number of BrdU⁺ cells after JSI-124 treatment and was found to be highly significant (radial index: 0.55: $p = 1.3 \times 10^{-9}$; one-way ANOVA post-hoc Tukey HSD, $F_{(3,12)} = 28.1$). However, neither the difference observed in the core-sensory region nor in the SNS could reach significance (core sensory: $p = 0.0525$; one-way ANOVA post-hoc Tukey HSD, $F_{(3,12)} = 22.7$; SNS: $p = 0.1473$; $F(3, 12) = 2.9$).

The BrdU⁺ cell profiles of the DMSO-treated injured OEs did not resemble that of injured OEs established for this time point (Kocagöz, 2021). However, when compared to established control conditions in lesioned OEs, the mitotic activity in JSI-124-treated animals appears to be reduced in the sensory OE, suggesting inhibition of JAK/STAT signaling reduces injury-induced cell proliferation. Nevertheless, an experimental error can be suspected in the DMSO group was used in this experiment.

Although no difference was detected in the BrdU⁺ cell profiles of the intact OE compared to established control conditions (Kocagöz, 2021), the possibility remains that a similar experimental error could also affect the intact OE. Which, however, was not detectable from the BrdU⁺ cell distribution profiles. Therefore, in order to understand if the observed discrepancy in the proliferative activity pattern was due to an experimental error, and if so, to which extent, a second set of DMSO-control fish was prepared (n = 3; data not represented here). In these samples, injured OE also showed the characteristic distribution profiles of BrdU⁺ cells observed regularly in other control samples, further supporting the idea that an experimental error occurred in the preparation of first control group. In order to understand the extent of this experimental error, the intact OE samples of the second control group was compared to first control and the JSI-124-treated group. The proliferative activity in the second control group was found to be much higher than in the first control group. Also, when compared to the second control group, the effect of JSI-124 treatment was found to be different from the results presented in this chapter. While JSI-124 treatment was found to be significantly increase the proliferative activity observed in the ILC compared to first control group, it was found to be significantly decreased the proliferative activity observed across all positions of the sensory region compared to second control group.

In conclusion, considering the discrepancies observed between the control groups and the conflicting results obtained from the evaluation of the effect of JSI-124 treatment, the results presented in this chapter appear to be unreliable. Therefore, the effect of JAK/STAT signaling inhibition by JSI-124 treatment on cell proliferation remains inconclusive and needs to be evaluated by a repetition of this experiment.

4.2.2. The Effect of JAK/STAT Signaling Inhibition on the Efficiency of OSN Regeneration

In order to understand the role of JAK/STAT signaling in regeneration, the efficiency of OSN neurogenesis was analyzed in JSI-124-treated fish and compared to DMSO controls (n=3). Fish received 1 μg of the inhibitor JSI-124 dissolved in DMSO intraperitoneally, 6 h before, at the time of the nasal irrigation with 1 % TrX, and 6 h after the TrX treatment. Afterwards, fish were incubated in regular tank water and samples were analyzed for HuC/D-immunoreactivity at 5 dpl.

To obtain a quantitative assessment of the efficiency of OSN neurogenesis in response to injury, the area covered by HuC/D⁺ OSNs relative to the total OE area was measured as previously described. The fractional areas were then normalized to the DMSO-treated intact OEs and compared across different experimental groups.

Figure 4.9.A depicts the representative images of immunohistochemistry against HuC/D (cyan) on horizontal sections of the intact (left) and injured OEs (right) of DMSO- (top) and JSI-124-treated (bottom) fish. Regardless of the treatment, in the intact OE, HuC/D immunostaining labeled a restricted area, which corresponds to the sensory region occupied by OSNs. In DMSO-treated fish, the pattern of HuC/D-immunostaining in the injured OE at 5 dpl largely resembles the pattern of the intact OEs. This appearance is consistent with previously described HuC/D immunostainings observed in control samples at 5 dpl (Kocagöz, 2021) and indicates the almost complete recovery of DMSO-treated injured OEs. The pattern and density of HuC/D⁺ cells in the JSI-124-treated injured OE on the other hand, did not resemble that of control samples at 5 dpl (Kocagöz, 2021). HuC/D-immunostaining only labeled fragmented patches of cell clusters predominantly located near to the inner edge of the sensory region, rather resembling the HuC/D⁺ cell pattern of earlier time points after injury (Kocagöz, 2021). As previously described, TrX treatment results in an almost complete loss of HuC/D⁺ OSNs in the OE at 1 dpl (Kocagöz, 2021), which was also observed in experiments described above (Figure 4.7). Hence, the HuC/D immunostaining in JSI-124-treated injured OE at 5dpl most probably labeled newly generated OSNs.

Therefore, JSI-124-treatment appears to either slow down or to prevent the efficiency of the OSN regeneration after TrX treatment.

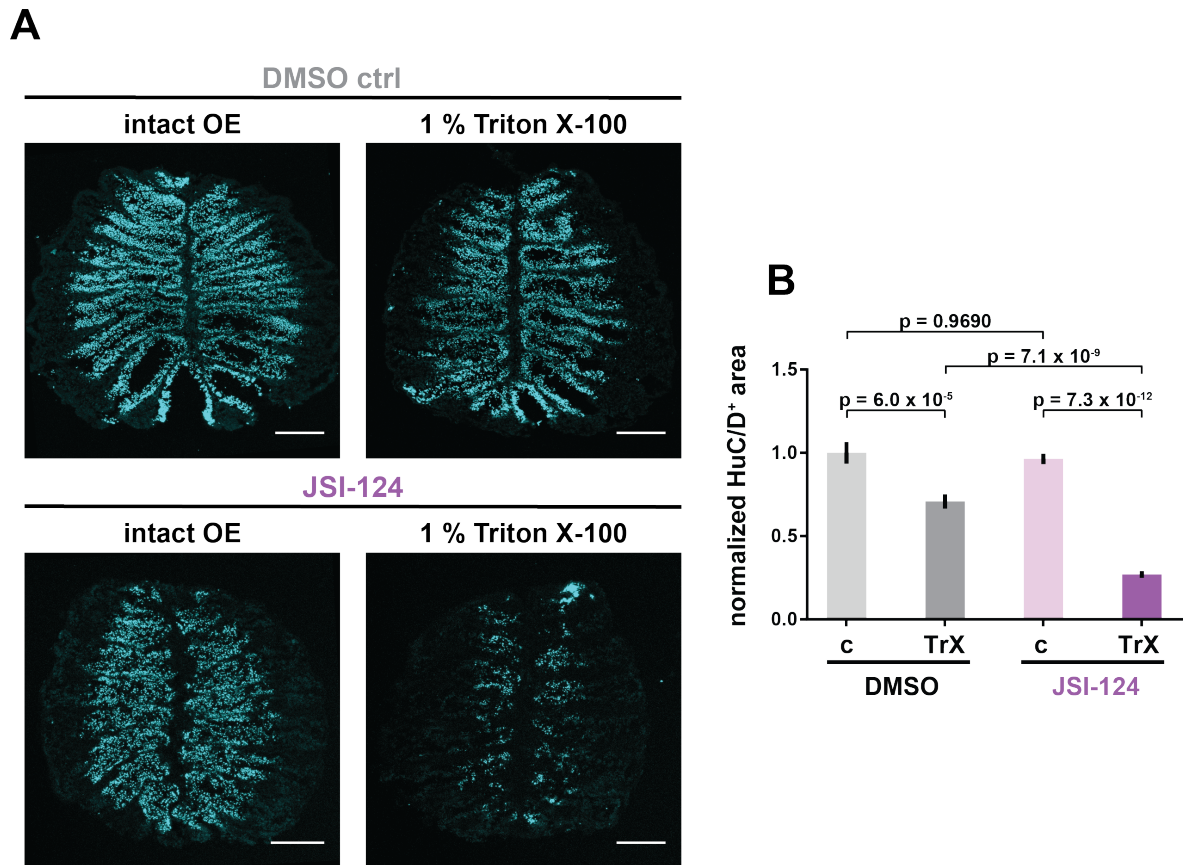


Figure 4.9. Effect of JSI-124 on regeneration. A. Immunohistochemistry against HuC/D (cyan) on the intact and 5 dpl OE. B. The efficiency of OSN neurogenesis.

The results of the analysis of the effect of JSI-124 treatment on regeneration are shown in Figure 4.9.B, which represents the normalized HuC/D⁺ areas of all groups. As already recognized in the Figure 4.9.A, the majority of the OSNs in the DMSO-treated injured OE were found to be regenerated. The area covered by HuC/D⁺ OSNs reaches 70.8 ± 4.2 % of intact OE values. As expected from the resemblance of the HuC/D-staining pattern between DMSO-treated injured OEs (Figure 4.9.A) and previously established control samples, the recovery rate appears in a range. In the range of that was previously observed at the same time point ($81.3 \pm 10.1\%$; Kocagöz, 2021).

Full recovery of the injured zebrafish OE appears at the seventh day of regeneration at which it reaches too $97.4 \pm 7.4\%$, a value that is statistically similar to the values off unlesioned controls. At 5 dpl, on the other hand, the difference between the intact and injured OEs of the DMSO group was found to be still significant ($p = 6.0 \times 10^{-5}$; one-way ANOVA, post-hoc Tukey HSD, $F_{(3,12)} = 63.26$).

In JSI-124 treated intact OEs, the area covered by HuC/D⁺ OSNs found to be not significantly different from the values of DMSO-treated fish ($96.4 \pm 3.1\%$; $p = 0.9690$; Figure 4.9.B). As expected from the observed fragmented appearance of HuC/D immunostaining pattern in injured OE (Figure 4.9.A), only a small fraction of the OSNs were found to be regenerated in JSI-124-treated animals (Figure 4.9.B). The area covered by HuC/D⁺ OSNs only amounts to $26.9 \pm 2.0\%$ of intact DMSO controls. This value corresponds to a percentage which was previously observed at 1 dpl during the degeneration of OSNs following injury (Kocagöz, 2021). Since the recovery rate was not analyzed previously between 1 dpl and 3 dpl, it was not possible to identify the exact time point to which the JSI-124-treated injured OE shows similarity. However, the area covered by HuC/D⁺ OSNs may corresponds to a recovery rate that is characteristic for a time point between 1 and 2 dpl (Kocagöz, 2021). Therefore, it can be assumed that the pattern observed in JSI-124-treated injured OE might represent a stage at which regeneration of OSNs has just started. Due to the technical problems with BrdU labelling during this experiment, the proliferative activity could not be determined in this experiment. Thus, it is not possible to discriminate between OSNs that were newly generated and OSNs that sustained the injury. Nevertheless, the recovery rate was dramatically decreased when fish were treated with JSI-124, which accounts for a highly significant difference between the injured OEs of the DMSO- and JSI-124-treated fish ($p = 7.1 \times 10^{-9}$) and between the intact and lesioned OE of the JSI-124 group ($p = 7.3 \times 10^{-12}$).

In summary, inhibition of JAK/STAT by JSI-124, significantly reduces the efficiency of OSN regeneration compared to DMSO controls. In order to further evaluate the effect of JSI-124 treatment on OE regeneration, additional experiments including the labelling of proliferative activity at early and late time points should be performed.

These additional experiments would help to properly evaluate a possible relationship between EGFR and JAK/STAT signaling. Regardless of the experimental errors and limitations of the experiments, JSI-124 treatment results in a dramatic decrease in the recovery rate to a similar extent as EGFR signaling inhibition by PD153035 (Figure 4.4.A). Considering this similarity, EGFR and JAK/STAT signaling seems to contribute to related events during OE regeneration. Therefore, an interaction between these two pathways during the progression of a regenerative response could be assumed.

4.3. Activation Pattern of JAK/STAT Signaling in the Intact and Injured OE

In order to investigate whether JAK/STAT signaling is activated in the OE under physiological conditions or during regeneration, immunoreactivity against the phosphorylated STAT3 protein (pSTAT3) was probed on intact and injured OE samples (n=1 fish). Following nasal irrigation with 1% Tr X-100, fish were incubated in BrdU-containing tank water for 24 h and transferred to regular tank water for another 24 h incubation. Afterwards, the OEs were dissected at 48 hpl and immunostained against pSTAT3, Sox2, and BrdU. The experimental time point of 48 hpl was chosen for analysis because the tissue integrity is severely compromised at 24 hpl and did not sustain the harsh antigen-retrieval treatment that was required for the pSTAT3 staining in preliminary trials.

Figure 4.10 and Figure 4.11 depict the representative images of the immunohistochemistry against pSTAT3- (green), Sox2- (red), and BrdU (blue) on the intact (Figure 4.10) and injured OE (Figure 4.11). The B panels of both figures depict the selected higher power views of the pSTAT3 immunostaining pattern for selected ROIs, which represent the sensory region of the OE as determined by the multi-layered and apically intrusive Sox2-labeling pattern at the transition between the sensory OE and the SNS as previously described (Demirler *et al.*, 2020; Demirler, 2021). In both the intact and injured OE, pSTAT3 generally labeled the cytoplasm.

Some labelled areas were identified as clusters of cells which showed a larger morphology that most likely includes multiple cells. When examined carefully, some pSTAT3⁺ profiles could be observed with multiple nuclear spaces that were elongated in both horizontal and/or vertical axes (Figure 4.10.B, asterisk). During repair, pSTAT3⁺ cell profiles presented with enlarged globular morphologies with possibly multiple nuclear spaces along the radial axis of the tissue (Figure 4.11.B, asterisks). However, the close proximity of pSTAT3⁺ profiles to each other made it difficult to identify individual cells. The structures which did not show these indications and could be identified as individual cells are indicated with arrowheads in both Figure 4.10 and 4.11.

As described above, inhibition of JAK/STAT signaling results in reduced or delayed OSN regeneration (Figure 4.9). On the other hand, the effect of JAK/STAT signaling inhibition on cell proliferation and the OE regions affected by the inhibition could not be determined. Thus, the identity of cells in which JAK/STAT signaling is active still remains elusive. The initial hypothesis was that JAK/STAT signaling may be active in HBCs. HBCs in the zebrafish OE co-express Krt5, tp63, and Sox2, of which Krt5 and tp63 are exclusively expressed by HBCs (Demirler *et al.*, 2020; Kocagöz, 2021). However, the possibility that cells in which the JAK/STAT signaling is active are different from HBCs also exists and could comprise injury-induced GBC-like cells. Although anti-Sox2 staining labels multiple non-neuronal cell populations in addition to HBCs, the various morphological and positional characteristics of Sox2-positive cells allows for the discrimination between different cell types (Demirler *et al.*, 2020; Demirler, 2021). Therefore, co-immunolabelling against Sox2 expression was performed in an attempt to identify cells in which JAK/STAT signaling is active.

The arrowheads in Figure 4.10.B and Figure 4.11.B indicate pSTAT3⁺ and , pSTAT3⁺/ Sox2⁺, pSTAT3⁺/BrdU⁺, and pSTAT3⁺ / Sox2⁺/ BrdU⁺ individual cells which are located in sensory region. Together with HuC/D⁺ OSNs, Sox2⁺ cells comprise nearly all cell types in the sensory OE, except for a few, supposedly intermediate neuronal precursors and/or immature neurons which are neither Sox2⁺ nor HuC/D⁺ and preferentially locate to the ILC and SNS in intact OE (Demirler *et al.*, 2020).

As previously shown, Sox2⁺ cells comprise Krt5⁺ HBCs with horizontally elongated nuclear morphology at the basal layer, Ascl1⁺ GBCs that are more globular and which are located in suprabasal layers at the ILC and SNS, and CKII⁺ SCs that show vertically elongated columnar nuclear morphologies in suprabasal layers throughout the sensory OE (Demirler, 2021). In this experimental setup, BrdU⁺ cells indicate both activated stem/progenitor/precursor cells in the first 24 h and also their progeny generated during the entire 48 h period. Figure 4.10.C and Figure 4.11.C shows the ROIs indicated in B parts of the figures and include the cell populations representing the majority of the pSTAT3⁺ cell profiles observed in the sensory region of the intact and injured OEs.

In the intact OE, pSTAT3⁺ cells are found largely to be located in the ILC, the SNS, and the non-sensory region. Occasional cells can also be seen in the core-sensory OE (Figure 4.10.A). Overall, the distribution of pSTAT3⁺ cells resembled the distribution of proliferative cells in the intact OE, which were previously described in the experiments detailed above. The pSTAT3⁺ cells in the sensory OE generally occupied basal portion of the epithelium as shown in the Figure 4.10.B, which are generally occupied by stem, progenitor, precursor and immature neurons (Bayramlı, 2016; Demirler *et al.*, 2020; Kocagöz, 2021; Demirler, 2021). However, a few cells with more apical orientation could also be detected in different tissue sections which are not shown here. The cells occupying the sensory OE were found to have various morphologies. The majority of the cells appeared to be globular, but some cells with horizontally elongated morphology or with irregular profiles could also be observed (Figure 4.10.C). Together with their biased distribution towards proliferative zones, their basal orientation, and their predominantly globular or horizontal morphologies strongly suggest that pSTAT3-positive have stem/progenitor and/or immature OSN cell identities in the intact OE.

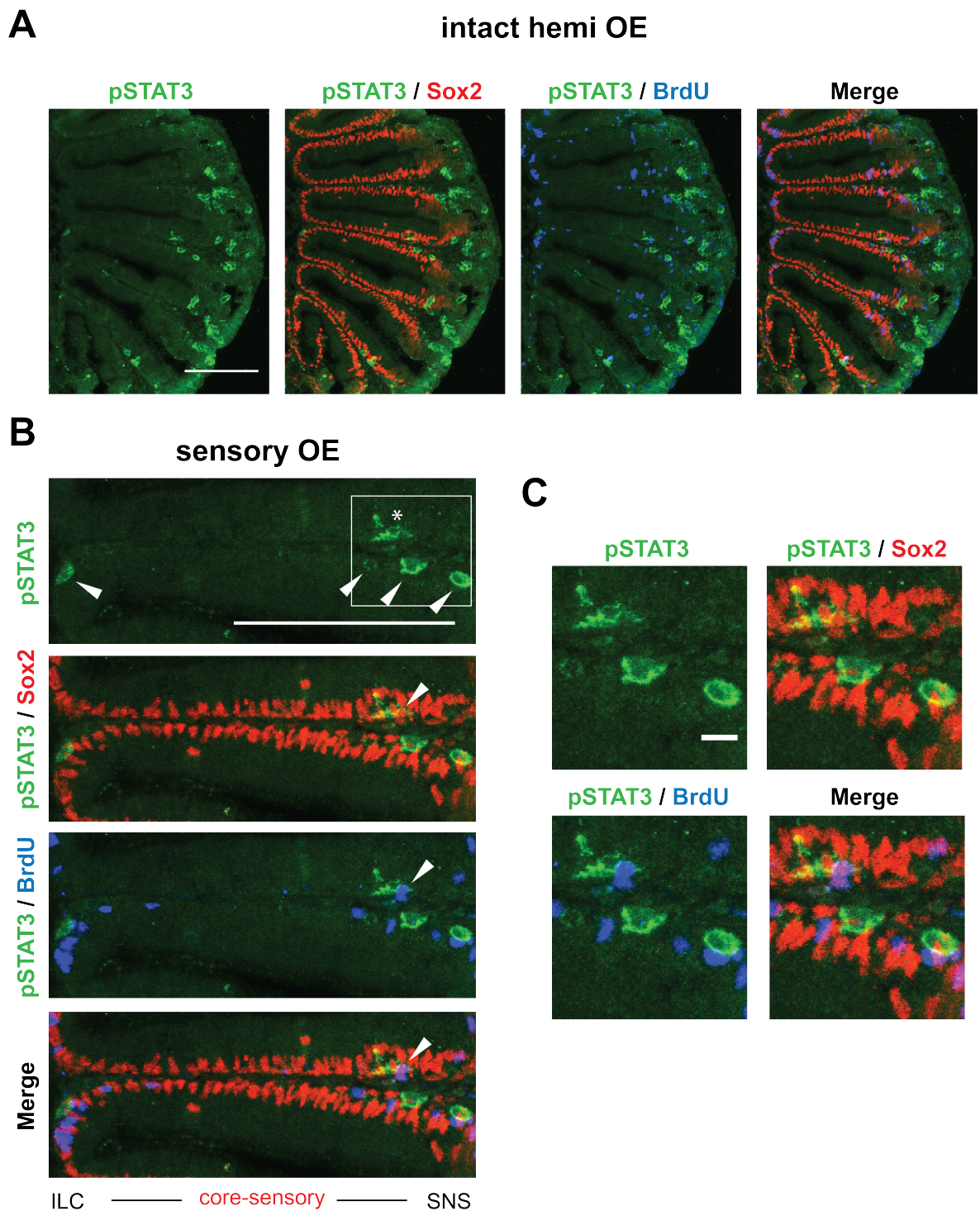


Figure 4.10. JAK/STAT signaling is active in the intact OE. A. Activity pattern. B. Co-localization of pSTAT3- (green) positive cells with Sox2- (red) and BrdU- (blue) cells. C. Images of the selected cell clusters. Scale bars: 100 μm (A, B), 10 μm (C).

Among the pSTAT3⁺ in the intact sensory OE, all the possible combinations of single-, pSTAT3⁺ /Sox2⁺ or pSTAT3⁺ /BrdU⁺ double-, and triple (pSTAT3⁺ /Sox2⁺ /BrdU⁺) cells could be identified. However, single-positive cells accounted for majority of pSTAT3⁺ cells (Figure 4.10.B). A small portion of pSTAT3⁺ cells in basal layer were also Sox2⁺, indicating HBC- and GBC-like cells as a small subpopulation of cells with active JAK/STAT signaling. These results show JAK/STAT is active mainly in neuronal progenitor, precursor and/or immature OSNs. In addition, low co-localization with BrdU indicates a higher probability of immature OSN identity, since neuronal progenitor and precursor cells have a constant base proliferative activity which would be expected to be captured during the incubation period. However, it should also be noted that, BrdU appears to label only a low number of cells compared to BrdU staining applied on equivalent intact OE samples that have not been subjected to the antigen retrieval protocol. Thus, BrdU labeling in this procedure may underrepresent the actual numbers of proliferative cells or their progeny with activated JAK/STAT signaling and leaves the possibility of these cells to have progenitor or precursor identities.

In the injured OE, the distribution of pSTAT3⁺ cells in the sensory region appears to be less defined. More cells and cell clusters also appear in the core-sensory region compared to the largely bimodal distribution of pSTAT3⁺ cells biased towards the ILC and SNS in the intact OE (Figure 4.11.B). This observation is consistent with identities of pSTAT3⁺ cells suggested above, since activated HBCs give rise to these cell types across all positions of the sensory OE upon injury (Kocagöz, 2021). Injury, by inducing an increase in the number of BrdU⁺ cells in the core-sensory region, remodels the bimodal distribution observed in the intact OE and results in a homogenous distribution of proliferative activity (Kocagöz, 2021; Kocagoz *et al.*, 2022). It is possible that distinct cell types would have active JAK/STAT signaling in the injured OE. Therefore, the increased occurrence of pSTAT3⁺ cells in the core-sensory region might also suggest a relationship between JAK/STAT signaling and injury-induced activation of proliferative activity. Thus, single pSTAT3⁺ cells, which form the majority even in damage condition, eliminates the possibility of HBC- or Sox2-expressing GBC-like cells to have active JAK/STAT pathway.

Since the same antigen retrieval protocol was applied, the relatively low BrdU labelling also occurs in the injured OE samples. Low labelling appears in all samples which were subjected to antigen retrieval protocol, however, when compared to corresponding equivalent samples, the problem was observed to be more severe in the injured OE, probably caused by the additional decomposition of the tissue resulting from the TrX treatment. In addition, as seen in Figure 4.11.C, pSTAT3⁺ cells appear to be slightly more apically located in the injured OE compared to the intact OE. This observation is consistent with an assumed neuronal progenitor or immature neuron cell identity since Ascl1⁺ cells, which represent their common parental origin, are also found in more apical layers in the injured relative to the intact OE (Kocagöz, 2021).

According to their morphology, radial position, apicobasal localization and Sox2-expression, pSTAT3⁺ cells seem to represent neuronal progenitor, precursors and/or immature neurons in the intact OE. The increased occurrence in the core-sensory region and the transition from mainly basal to more apically located cells observed with active JAK/STAT signaling pathway upon injury is consistent with these proposed identities. However, is mainly indicative of the proliferative activity in the OSN lineage in the zebrafish OE. Exact identities of these cells could only be determined with additional specific cell identity markers, which can withstand the antigen retrieval protocol. On the other hand, the general lack of Sox2-positive cells with active JAK/STAT pathway suggests that these cells are definitely not HBC or cells of the early GBCs lineage. Initial findings show that human-recombinant HB-EGF increases cell proliferation from basal cell layers in the core-sensory OE that are occupied by HBCs (Kocagöz, 2021; Sireci unpublished), that egfra expression localizes to HBCs (Guler, master's thesis). These different distributions of pSTAT3⁺ cells largely reject the hypothesis that JAK/STAT signaling directly works downstream of HB-EGF/EGFR signaling in HBCs.

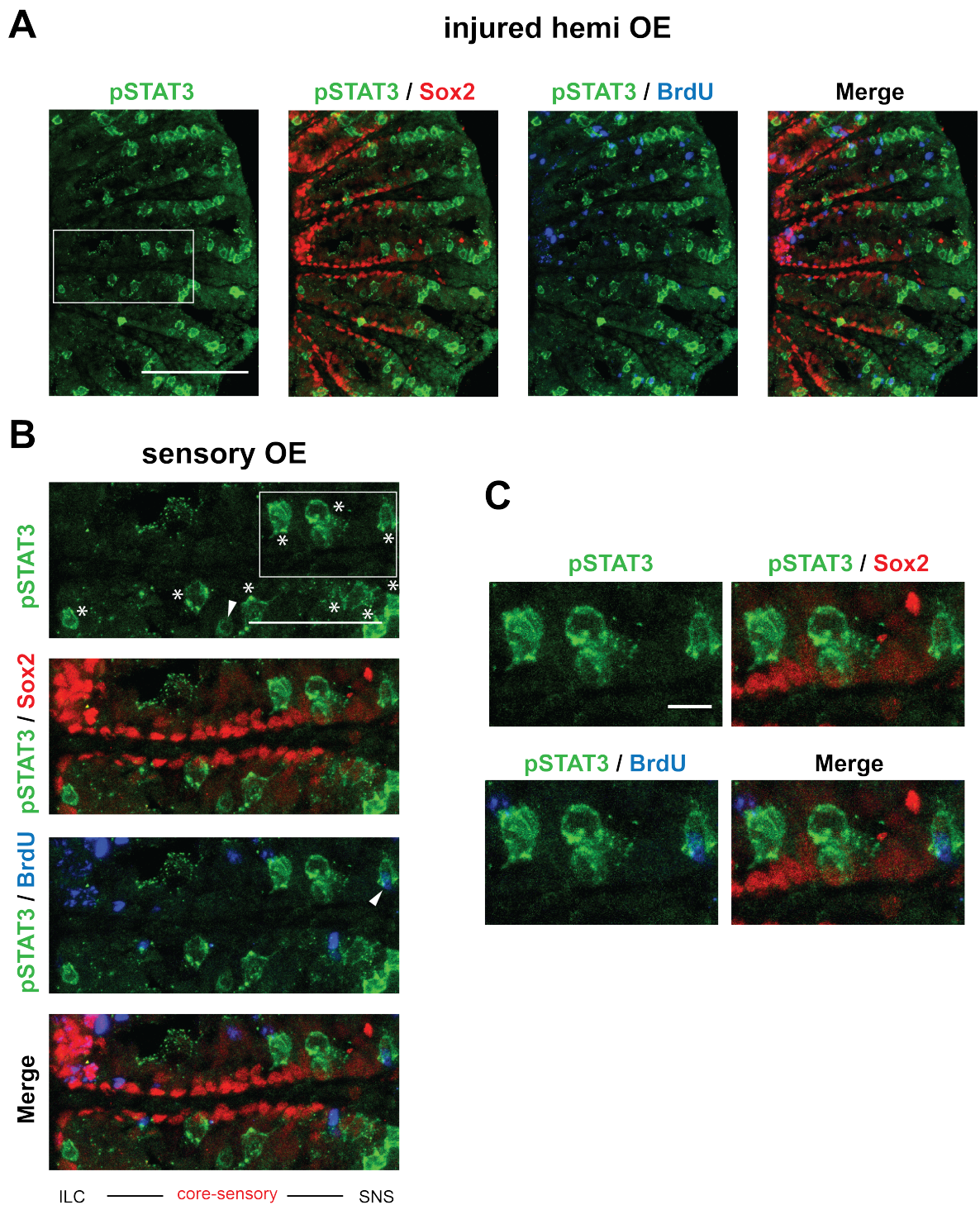


Figure 4.11. JAK/STAT signaling is active in the 2 dpl OE. A. Activity pattern. B. Co-localization of pSTAT3- (green) positive cells with Sox2- (red) and BrdU- (blue) cells. C. Images of the selected cell clusters. Scale bars: 100 μm (A, B), 10 μm (C).

4.4. Activation Pattern of JAK/STAT Signaling Upon Stimulation with human recombinant HB-EGF

HB-EGF and EGFR signaling seem to act directly on HBCs, while the majority of pSTAT3+ cells seem to represent a cell population that is distinct from HBCs. Nevertheless, activation of JAK/STAT signaling is necessary for a full regeneration response. Thus, even though the two signaling pathways may not be active in the same cell, they may be involved in the activity of cells at different stages within the same lineage. To examine whether soluble HB-EGF induces the activation of JAK/STAT signaling, an experiment was designed in which one OE (n=1) was stimulated with intranasal administration of 200 ng/ μ l human recombinant HB-EGF dissolved in 0.1% BSA/PBS for 20 minutes in two consecutive days and the other nose was kept as a control. After the second HB-EGF administration, fish were immediately incubated in BrdU-containing tank water for 24 h to label cells which are activated in response to HB-EGF stimulation. Afterwards, OEs were dissected immediately at 24 h post administration (hpa) and analyzed for pSTAT3, Sox2 and BrdU-immunoreactivity. Experimental time of analysis was chosen as 24 hpa since this was the earliest time point at which the effect of HB-EGF-stimulation has been analyzed previously (Kocagöz, 2021).

Figure 4.12.A depicts the representative images of the pSTAT3- (green), Sox-2- (red) and BrdU-immunostaining (blue) on the control (top) and HB-EGF-stimulated hemi-OEs (bottom). Surprisingly, even though the same staining protocol was applied, the quality of the pSTAT3 staining appears to be very low compared to the same staining on intact and injured OEs (Figure 4.10 and 4.11). The total of 40 minutes incubation of fish outside of water during the HB-EGF-stimulation might be probable reason of low staining quality by causing tissues to dry unintentionally. Figure 4.12.B, depicts the selected higher power view of the pSTAT3 staining pattern for selected ROI which represent the sensory region of the OE as determined by exploiting the transitioning pattern of Sox2-labelling as previously described (Demirler *et al.*, 2020; Demirler, 2021).

Arrowheads in Figure 4.12.B indicate pSTAT3⁺, pSTAT3⁺/Sox2⁺, pSTAT3⁺/BrdU⁺ and pSTAT3⁺/Sox2⁺/BrdU⁺ cells located in the sensory region of the intact OE, respectively. The signals which could not be identified as individual cells due to the low staining quality in control and HB-EGF-stimulated OE and due to the clustering of cells in the injured OE are indicated with asterisks.

In the unstimulated control OE, pSTAT3⁺ cells largely occupy basal layers and majority appear biased towards the ILC and the SNS and occasional cells can be seen in in the core-sensory region (Figure 4.12.B, left), similar to the intact OE (Figure 4.10.B). However, their morphologies could not be directly compared due to the low staining quality. Similarly, among all the existing populations of single pSTAT3⁺, pSTAT3⁺/Sox2⁺, pSTAT3⁺/BrdU⁺ and pSTAT3⁺/Sox2⁺/BrdU⁺ cells, single pSTAT3⁺ cells seem to represent the majority of cells. Since the exact antigen retrieval protocol is applied on these samples, BrdU also appears to label a low number of cells compared to equivalent samples of control and HB-EGF-stimulated OE (Kocagöz, 2021), which were not subjected to antigen retrieval protocol, as expected.

Exogenous stimulation of the OE with recombinant HB-EGF seems to increase the occurrence of pSTAT3⁺ cells across a wider segment of the core-sensory region while maintaining a bias towards the ILC and SNS region (Figure 4.12.A, bottom). The increase in the core-sensory region somewhat resembles the increase observed in the occurrence of pSTAT3⁺ cells with the injury (Figure 4.11.A) and is consistent with the pattern of activation of cell proliferative after HB-EGF-stimulation at 24 hpa as previously described (Kocagöz, 2021). The increase of pSTAT3⁺ cells in radial positions where HB-EGF-stimulation increases the proliferative activity is suggestive of a functional relationship between HB-EGF activity and JAK/STAT signaling.

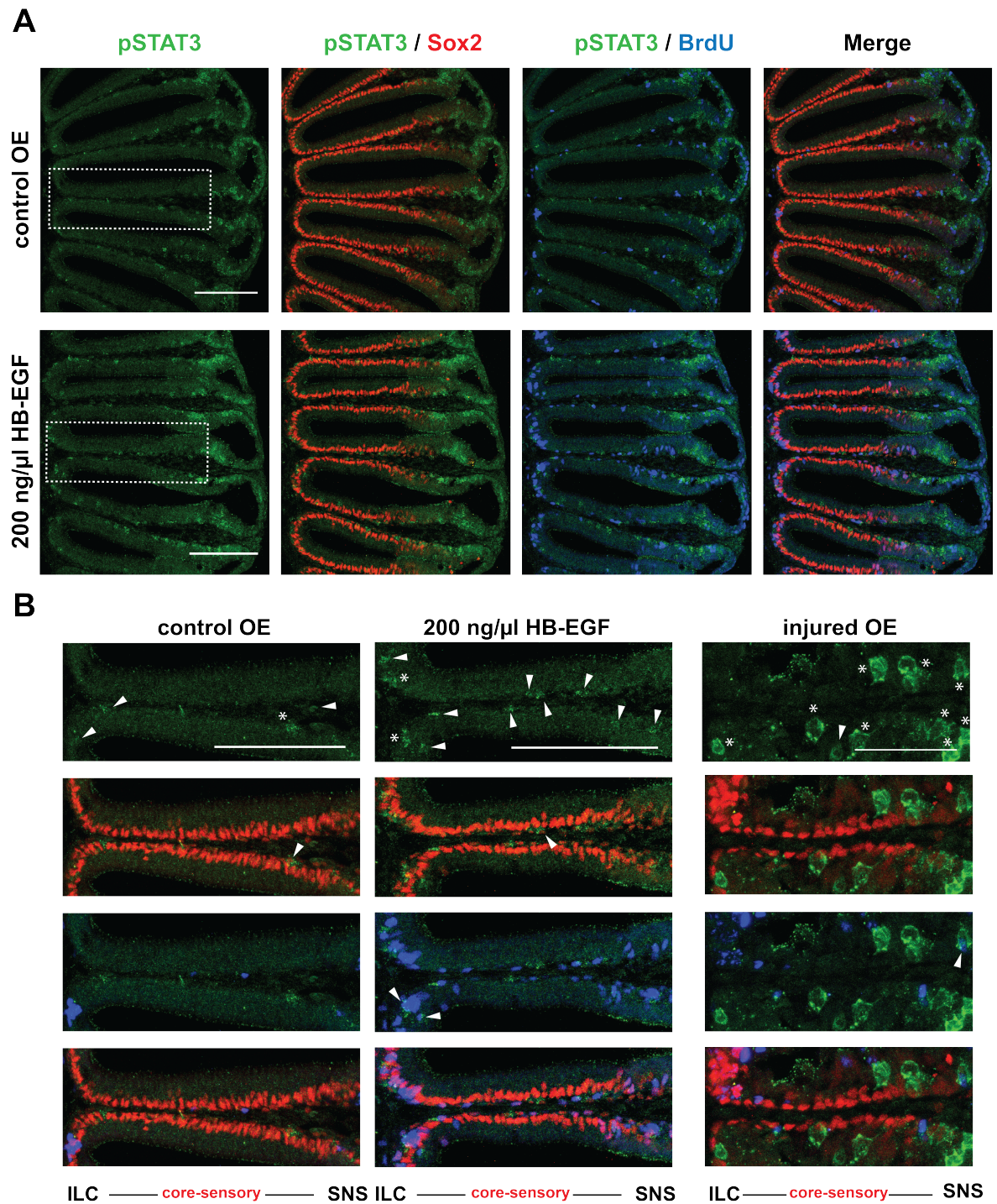


Figure 4.12. HB-EGF stimulation activates JAK/STAT signaling. A. Activation pattern. B. Co-localization of pSTAT3- (green) positive cells with Sox2- (red) and BrdU- (blue) cells. Scale bars: 100 μ m.

Figure 4.12.B depicts selected higher power view of the pSTAT3 staining pattern for selected ROIs, which represent the sensory region of the HB-EGF-stimulated OE. To accurately compare the injured and HB-EGF-stimulated OE in the means of JAK/STAT signaling activation, Figure 4.12.B also includes selected higher power view of the injured OE sample (right) which was examined in the previous experiment. Arrowheads in the Figure 4.12.B (middle) and (right) indicate single pSTAT3⁺, pSTAT3⁺/Sox2⁺, pSTAT3⁺/BrdU⁺ and pSTAT3⁺/Sox2⁺/BrdU⁺ cells located in the sensory region of the HB-EGF-stimulated and injured OE, respectively. Different from injured OE which shows slightly more apically located pSTAT3⁺ cell populations compared to control OE, all the populations seem to largely occupy basal layers in the HB-EGF-stimulated OE. With HB-EGF-stimulation, the occurrence of pSTAT3⁺ cells can be seen to be increased across all positions in the sensory region, with more pronounced increases at the ILC and in the core-sensory region. The number of pSTAT3⁺/Sox2⁺, pSTAT3⁺/BrdU⁺ and pSTAT3⁺/Sox2⁺/BrdU⁺ cells remain largely the same in the HB-EGF stimulated OE compared to control. Therefore, the increase observed in the number of pSTAT3⁺ cells with the HB-EGF-stimulation largely occur in the favor of single pSTAT3⁺ cells similar to injury conditions (Figure 4.11.B).

As previously mentioned, HB-EGF-stimulation increases proliferative activity across the OE, with a significant bias towards the core-sensory region (Kocagöz, 2021). Since this region is exclusively occupied by HBCs in the intact OE, it has previously been suggested that HB-EGF selectively regulates HBC activity (Kocagöz, 2021). However, this conclusion was not supported by simultaneous staining with markers for HBC identity. HBCs in the zebrafish OE co-express Krt5, Sox2 and tp63 (Demirler *et al.*, 2020). In the core-sensory region, Sox2-expressing cells form two discernable layers. With flattened HBC nuclei occupying the basal-most layer and vertically elongated SC nuclei occupying suprabasal layers just above HBCs (Demirler *et al.*, 2020). Therefore, by profiting from this previously established differences, the identity of cells, which are activated in response to HB-EGF stimulation, could be determined.

Figure 4.13.A depicts the selected higher power views of the BrdU and Sox2 staining pattern for selected ROIs which represent the sensory region of the intact (left) and HB-EGF-stimulated (right) OE. White arrowheads indicate BrdU⁺ and Sox2⁺/BrdU⁺ cells. Yellow arrowheads indicate single BrdU⁺ cells in the Sox2/BrdU images. The core-sensory region of the control OE shows a low number of BrdU⁺ cells, characteristic of uninjured control conditions. This low proliferative activity was previously shown to result in symmetric HBC divisions and to largely contribute to expansion of the HBC pool in the zebrafish OE (Demirler, 2021). An almost complete co-localization of BrdU with flattened Sox2⁺ cell nuclei occupying the basal-most layer validates these findings. Stimulation with HB-EGF increases the number of BrdU⁺ cells occupying the core-sensory region at 24 hpa. The increased number of BrdU cells that co-localize with Sox2 staining and occupy the basal-most layer suggests that HB-EGF activates the HBCs. A low number of single BrdU⁺ cells also can be observed in the same region, which are indicated with yellow arrowheads.

To further dissect the relationship between HB-EGF and JAK/STAT signaling, co-localization of the cells which were activated in response to HB-EGF-stimulation and cells in which the JAK/STAT signaling is active were evaluated in Figure 4.13.B. Yellow arrowheads indicate BrdU⁺ cells in the core-sensory region and which were activated in response to HB-EGF stimulation, while white arrowheads indicate pSTAT3⁺ cells. BrdU⁺ and the pSTAT3⁺ cells predominantly occupy the basal-most layer, however, almost never co-localize.

In conclusion, exogenous human recombinant HB-EGF stimulation seems to increase the occurrence of cells with activated JAK/STAT signaling in the core-sensory region, however, not in cells that are directly responsive to HB-EGF. Cells that are positive for pSTAT3 are induced in the core-sensory region with injury (Figure 4.11). Exogenous human recombinant HB-EGF stimulates a similar increase in the number of pSTAT3⁺ cells in the core-sensory region, many of which are observed to be single pSTAT3⁺ cells. Therefore, considering the similarities in the activation pattern of JAK/STAT signaling upon injury and HB-EGF-stimulation, a relationship between HB-EGF and JAK/STAT signaling during injury-induced repair might be suggested.

However, different from TrX-treatment, HB-EGF-stimulation seems increase the number of pSTAT3⁺ cells also in the ILC. One other difference appears in the apicobasal position of pSTAT3⁺ cells in the core-sensory region. While the pSTAT3⁺ cells appear to be slightly more apically oriented in the injured OE, they almost exclusively occupy basal layers in the HB-EGF-stimulated OE. The differences might be suggested to be the result of differences in the experimental time of analysis or the additional structural changes accompanying the injury. The difference in tissue distribution of HB-EGF-responsive cells and cells in which JAK/STAT signaling is activated suggests that HB-EGF does not activate HBCs by JAK/STAT signaling. However, JAK/STAT signaling appears to become activated during later stages of the HBC lineage.

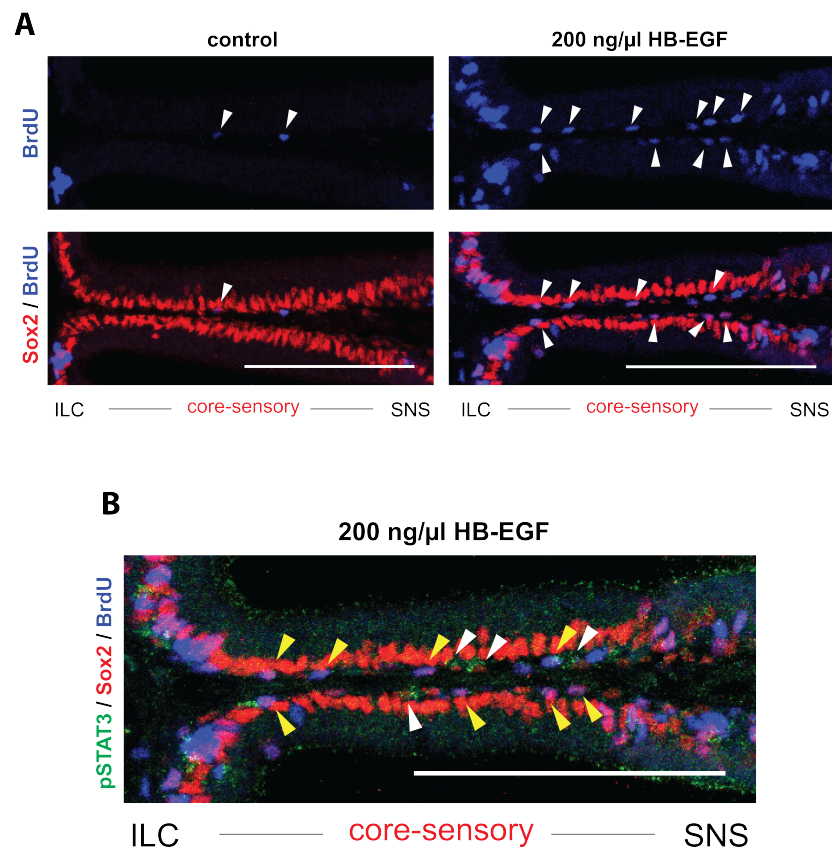


Figure 4.13. JAK/STAT signaling is not active in cells activated by HB-EGF. A. Cell populations activated by HB-EGF. B. Co-localization of pSTAT3- (green) positive cells with Sox2/BrdU- (magenta) double positive cells. Scale bars: 100 μ m.

5. DISCUSSION

In the work presented in this thesis, the individual roles of EGFR and JAK/STAT signaling were investigated during OE maintenance and regeneration. Two sets of experiments aiming at an understanding of whether signaling pathway inhibition influences injury-induced progenitor cell proliferation immediately after injury and/or the regeneration of OSNs at 5 dpl were performed using small molecule inhibitors of the EGFR and JAK/STAT signaling pathways. Inhibition of EGFR signaling with PD153035 treatment resulted in a decrease in the rate of cell proliferation both in the intact and injured OE. However, when the rate of OSN neurogenesis and the efficiency of regeneration were analyzed, PD153035 treatment was found to predominantly prevent injury-induced repair neurogenesis while only a minor decrease in the number of newly generated OSNs could be identified during maintenance neurogenesis. Due to technical problems with control animals, the effect of the JAK/STAT inhibitor JSI-124 on the rate of cell proliferation could not be determined with full certainty. Nevertheless, JSI-124 treatment significantly impaired OSN regeneration at 5 dpl and caused a similar decrease in OSN recovery rate as EGFR inhibition. Thus, the inhibition of EGFR and JAK/STAT signaling have common effects by preventing the unfolding of a successful regenerative response in the zebrafish OE. Therefore, EGFR and JAK/STAT signaling might be active in the same cell lineage and contribute to related events during repair neurogenesis. However, the exact cell types in which the two pathways are active and the detailed mechanisms which are regulated by their activity remain elusive.

5.1. EGFR and JAK/STAT in Tissue Maintenance and Regeneration

During development in mammals, EGFR signaling plays fundamental roles in embryogenesis and organogenesis of lungs, kidneys, heart, bone and epithelial tissues (Chen *et al.*, 2016). For instance, during preimplantation, EGFR signaling through EGF and TGF α has been shown to regulate protein synthesis, cell number, and blastocyte expansion (Hardy and Spanos, 2002; Richter, 2008; Zeng and Harris, 2014). In lung development, EGFR null mice show reduced branching and defects in alveolarization (Miettinen *et al.*, 1997). TGF α has also been demonstrated to be expressed during kidney development and it has been suggested that EGFR signaling contributes to the determination of the final number of nephrons and the maintenance of collecting duct morphology (Goodyer *et al.*, 1991; Rogers *et al.*, 1992; Ishibe *et al.*, 2009). In heart development, EGFR activation via HB-EGF has been implicated in the differentiation of valve mesenchymal cells (Iwamoto *et al.*, 2003). While EGFR signaling has no direct effect on the proliferation and differentiation of chondrocytes, it has been shown to affect bone formation through interactions with receptor activator of NF- κ B (RANK) and its ligand, and matrix metalloproteinases (Zhang *et al.*, 2011). In addition, it also controls the development of epithelial lining organs by directly regulating epithelial cell proliferation and differentiation (Sibilia and Wagner, 1995; Threadgill *et al.*, 1995; Hansen *et al.*, 1997).

Commonly, cellular processes, which are required for the proper development of a tissue or organ, are also utilized during the maintenance of tissue homeostasis and during repair. Hence, not surprisingly, EGFR signaling is also expressed in various adult tissues and is involved in the preservation of tissue integrity as well as the recovery from injury in adulthood (O'Loughlin *et al.*, 1985; Poulsen *et al.*, 1986; Beauchamp *et al.*, 1990; Stoll *et al.*, 2001; Carver *et al.*, 2002; Abe *et al.*, 2009). Under physiological conditions, EGFR is expressed in the adult skin, heart, gastrointestinal system, liver and pancreas (O'Loughlin *et al.*, 1985; Poulsen *et al.*, 1986; Beauchamp *et al.*, 1990; Stoll *et al.*, 2001; Carver *et al.*, 2002; Abe *et al.*, 2009). In the skin, the keratinocyte stem cells express EGFR (Mascia *et al.*, 2003) and their self-renewal and survival is regulated by EGFR ligand Amphiregulin (Peipkornn *et al.*, 1996; Noma *et al.*, 2007).

In the heart, activation of β_1 -adrenergic receptors causes EGFR transactivation, which promotes survival of cardiac myocytes (Noma *et al.*, 2007). Hepatocytes of the liver express high levels of EGFR and TGF α acts as a major regulator of their proliferation (Carver *et al.*, 2002). In the gastrointestinal system, EGFR attains proliferative and anti-apoptotic roles in the gut via multiple ligands. G protein-coupled peptide YY neuropeptide receptor Y1 subtype activation stimulates EGFR signaling and promotes proliferation of gut epithelial cells (Mannon *et al.*, 2000). In addition, it has been shown that glucagon-like peptide-2 secretion by enteroendocrine cells stimulated by nutrient ingestion also promotes EGFR activation by increasing the expression of the EGFR ligands, Epireregulin, Amphiregulin and HB-EGF, which further stimulates proliferation by suppressing apoptosis of crypt cells (Yusta *et al.*, 2009). Lastly, in the pancreas, while EGFR activation via Amphiregulin, Betacellulin, EGF and HB-EGF stimulates the proliferation of all pancreatic cell types and result in organ growth (Ohlsson *et al.*, 1997; Rescan *et al.*, 2005; Wang *et al.*, 2010), transactivation via glucagon-like peptide-1 promote β -cell proliferation (Buteau *et al.*, 2003).

Although they share many similarities, tissue maintenance and repair differ vastly in the nature of their response and the mechanism of their regulation. While tissue maintenance contributes to the continuous turnover and survival of resident cell types, tissue repair progresses as an acute response and ceases upon restoration of tissue integrity. Different from tissue maintenance, an immune response is typically found to accompany tissue repair in many cases (Fang *et al.*, 2021). Therefore, regulation of these separate processes by EGFR often requires distinct upstream and/or downstream signaling elements and regulation of tissue repair may additionally involve the cross-talk between EGFR signaling and immune responses (Chen *et al.*, 2016). It has been demonstrated that the EGFR ligands, EGF, TGF α , and HB-EGF are generally involved in tissue repair by regulating both regenerative and immune responses (Chen *et al.*, 2016).

The cellular mechanisms regulated by JAK/STAT signaling has been studied best in *Drosophila* and subsequent work in vertebrates demonstrated the conservation of JAK/STAT signaling during development, tissue maintenance and, regeneration.

(Herrera and Bach, 2019). In the fly, activation of JAK/STAT signaling regulates the survival of developing wing disc cells and stem cells of the adult testis via a common mechanism of promoting the expression of the anti-apoptotic gene *diap1* (Hasan *et al.*, 2015; Betz *et al.*, 2008; Recasens-Alvarez *et al.*, 2017). In the mouse, the survival of cells both in embryonic and adult tissues was shown to be reduced when components of JAK/STAT signaling were disrupted (Yoshida *et al.*, 1996; Onishi and Zandstra, 2015; Kleppe *et al.*, 2017). Expression of anti-apoptotic Bcl-2 family genes was also shown to be dependent on STAT in vitro (Catlett-Falcone *et al.*, 1999). In *Drosophila*, increased cytokine secretion and subsequent JAK/STAT signaling activation induces survival and proliferation of cells during wing disc regeneration (Katsuyama *et al.*, 2015; La Fortezza *et al.*, 2016). While a similar induction in the levels of IL-11 and IL-6 was observed early during *Xenopus* tail regeneration (Tsujioka *et al.*, 2017), deficiency of *il-6*, its receptor *gp130*, or *stat3* was shown to impair mouse liver regeneration (Cressman *et al.*, 1996; Taub, 2004). JAK/STAT signaling was also implicated in zebrafish, in which its involvement was shown to be crucial for the proper regeneration of multiple tissues, including heart (Fang *et al.*, 2013), retina (Zhao *et al.*, 2014) and inner ear (Liang *et al.*, 2012).

5.2. EGFR Expression in The OE

Prompted by initial in vitro studies showing stimulatory effect of the EGFR ligands TNF and EGF on dissociated OE cells and organotypic OE cultures (Mahanthappa and Schwarting, 1993; Farbman, 1994; Farbman and Buchholz, 1996), the expression of EGFR in the rodent OE was examined in multiple studies in a pursuit of identifying populations which are responsive to EGFR ligands. Utilizing in situ real-time polymerase chain reaction, EGFR mRNA was found to be localized to basal OE layers. While mRNA expression in a layer of two to three cells at basal of the OE suggested that both HBCs and GBCs express EGFR (Krishna *et al.*, 1996), subsequent studies have shown EGFR is almost exclusively expressed by HBCs at protein level (Holbrook *et al.*, 1995; Chen *et al.*, 2020). However, low level EGFR protein expression could also be detected in the apical-most layer (Holbrook *et al.*, 1995), which is tightly packed with SC cell bodies in the rodent OE (Vogalis *et al.*, 2005).

Preliminary studies from our group on *egfra* (*erbb1*) expression by in situ hybridization showed that *egfra* expression also localizes to basal and apical layers in the intact zebrafish OE (Güler, 2021). The expression of *egfra* in the basal layers showed a high degree of co-localization with *tp63*, which is exclusively expressed by HBCs (Demirler *et al.*, 2020). However, a low number of *egfra*-expressing *tp63*-negative cells could also be detected in the basal OE. Therefore, HBCs seem to form the majority of EGFR-expressing cells, however, a small number of GBCs or immature neurons might also be included (Güler, 2021). Due to their inverted morphology, SC cell bodies occupy suprabasal layers in the zebrafish OE rather than forming an apical layer. The apical layers on the other hand, is almost exclusively occupied by OSN cell bodies (Demirler *et al.*, 2020). Accordingly, *egfra* expression in apical layers was found to often co-localize with HuC/D, showing that a subpopulation of mature OSNs may also express *egfra*. The nature and exact identity of these cells, however, remains obscure. Suprabasal layers, on the other hand, were found to be negative for *egfra* expression, suggesting that, different from the rodent OE, SCs in the zebrafish OE do not express EGFR.

5.3. pSTAT3 Expression in The OE

JAK/STAT signaling functions as a transducer of several cellular signals downstream of the activation of various cell surface receptors (Bousoik and Montazeri Aliabadi, 2018). Activation of the receptor causes phosphorylation and activation of JAKs (Rawlings *et al.*, 2004). Subsequently, JAKs phosphorylate each other and STATs (Rawlings *et al.*, 2004). Phosphorylation, in addition to certain other types of post-transcriptional modifications cause STATs to become activated and to dimerize (Yuan *et al.*, 2005; Rebe *et al.*, 2013).

Immunostaining against pSTAT3 in the zebrafish OE labels the cytoplasm of structures, which were identified as isolated clusters of cells that include a collection of cellular morphologies under both physiological and injury conditions. While the majority of pSTAT3⁺ cells present with a round morphology, different cell morphologies, for example flattened or irregular profiles, could also be seen.

HBCs in the zebrafish OE have a flat morphology, which can be visualized by cytoplasmic staining against Krt5 or nuclear staining against Sox2 and tp63 (Demirler *et al.*, 2020). Although not as well defined as the HBCs, due to the lack of cytoplasmic markers that are specific to the GBC lineage in zebrafish, Sox2- and Ascl1-expressing GBCs have more spherical morphologies in comparison to HBC-like cells as implicated by their round-shaped nuclei (Demirler *et al.*, 2020, Kocagöz, 2021). In addition to GBCs, a spherical morphology is also characteristic for other cell populations in the zebrafish OE, such as OSNs and SC-like cells (Demirler *et al.*, 2020).

In the intact OE, pSTAT3+ cells are mainly observed at the ILC and SNS and occasional cells can be seen at random positions across the core-sensory region. Interestingly, these cells often form dense clusters of 3 to 10 cells that are tightly connected to each other. In the rodent OE, proliferative activity of GBCs residing in basal layers, give rise to OSNs across all positions of the OE under physiological conditions and result in a homogenous pattern of mitotic activity (Schwob, 2002). Different from the rodent OE, generation of new OSNs takes place at specialized proliferation zones at the ILC and SNS in the intact zebrafish OE where Ascl1- and Sox2-expressing GBCs reside. The core-sensory region on the other hand, is completely devoid of GBCs in the absence of injury and shows no or only little neurogenic mitotic activity (Kocagöz, 2021). However, a small number of HBCs were also found to contribute to low but persistent proliferative activity in more central OE positions (Demirler, 2021). Including non-neurogenic mitotic activity in the nonsensory OE, the zebrafish OE shows a bimodal distribution of proliferative cells, which peaks around the ILC and SNS/nonsensory border (Bayramli *et al.*, 2017). From this perspective, the expression pattern of pSTAT3 resembles the bimodal distribution of proliferating cells and suggests a relationship between pSTAT3-positive cells and GBCs.

In contrast, pSTAT3+ cells randomly occur at radial dimensions of the injured sensory OE during regeneration. Following injury, OSN regeneration takes place across the entire OE with the novel occurrence of increased neurogenic mitotic activity in the core-sensory region (Kocagöz, 2021). The core-sensory is occupied by dormant HBCs, which only self-renew to maintain the availability of their pool in the absence of injury.

After injury, HBCs become activated and generate a transient population of GBCs that restore the OSN population (Kocagöz, 2021). The resemblance between the transitions that occurs in the pSTAT3 staining pattern and the induction of mitotic activity further support a possible relationship between pSTAT3 expression and mitotic activity in GBCs. However, it is not certain at this time whether pSTAT3 occurs in stem and/or progenitor cell populations to work in a direct way to induce their proliferation or in non-stem cell populations to indirectly stimulate the activity of stem and/or progenitor cells.

In the zebrafish sensory OE, different cell types are preferentially distributed within different apical to basal layers. While the apical layers are largely occupied by the cell bodies of different types of HuC/D-expressing mature OSNs, basal layers harbor multiple types of non-neuronal cells. Just underneath the layers formed by OSNs, Sox2- and cytokeratin type II-expressing SCs occupy suprabasal layers (Demirler *et al.*, 2020). In contrast, the basal most layer of the sensory OE is occupied by Krt5-, Sox2- and tp63-expressing HBCs (Demirler *et al.*, 2020). In addition, Sox2- and Ascl1-expressing GBCs can be found slightly more apically oriented and just above the HBCs at the ILC and SNS in the intact OE or across the entire sensory OE after injury (Kocagöz, 2021). The heterogeneous populations of Sox2- and HuC/D-expressing cells together comprise almost every cell type residing in the sensory OE (Demirler *et al.*, 2020). However, a very small number of cells that do not express either Sox2 or HuC/D can also be observed around the ILC and SNS, supposedly representing a transient neuronal precursor subpopulation of the late GBC lineage or immature neurons which lost their Sox2 expression but have not fully matured into OSNs (Demirler *et al.*, 2020). In both the intact and injured OE, only a few basally oriented pSTAT3-expressing cells can be seen to express Sox2, indicating that HBCs and GBCs comprise only a small fraction of the cell populations labeled by pSTAT3. The identity of the majority of pSTAT3 cells remains unknown but could overlap with transient neuronal progenitor cells or early immature neurons based on the absence of marker expression and their basal positions.

One possibility to discriminate between neuronal progenitor cells and immature neurons could be examine their proliferative activity through labelling with markers.

Cells that label positive for pSTAT3 shows very little co-localization with the proliferation marker BrdU. However, antigen retrieval methods were used to successfully visualize pSTAT3+ cells, which appears to reduce the number of BrdU-positive cells. Thus, co-localization of pSTAT3 and BrdU may have been underestimated in this study. Utilizing different methods for labelling of proliferative activity, which sustains antigen retrieval conditions, might help to further characterize the proliferative state of pSTAT3-positive cells directly. In addition to usage of different labelling methods, co-staining with markers for the different stages of neuronal commitment, such as NeuroD1 and Neurogenin-1 could also help to further dissect the exact identity of pSTAT3-expressing cells. Nevertheless, preliminary observations described in this thesis, strongly suggest that pSTAT3-positive cells include late neuronal precursor cells and immature neurons.

5.4. Maintenance vs Repair

The zebrafish OE has the ability to undergo continuous turnover of OSNs (Bayramli *et al.*, 2017) and to regenerate rapidly after acute injury (Kocagöz, 2021). This ability is based on the presence of a dual stem cell system that is comprised of GBC and HBCs (Bayramli *et al.*, 2017; Kocagöz, 2021). GBCs represent a heterogeneous population of cells, whose continuous mitotic activity is responsible for the persistence of maintenance neurogenesis in the intact OE (Bayramli *et al.*, 2017). HBCs on the other hand, are found dormant under physiological conditions and become activated in response to injury and contribute to tissue repair (Kocagöz, 2021). In addition to their dependence on distinct stem cell populations, maintenance and repair neurogenesis also show distinguishable spatial patterns of mitotic activity (Kocagöz, 2021), which can be used to discriminate between these two processes by analyzing the distribution of mitotic activity across the OE under different tissue conditions.

The GBCs are found exclusively in basal and suprabasal layers of the dedicated zones of maintenance neurogenesis at the ILC and the SNS region in the intact tissue (Kocagöz, 2021). The HBCs on the other hand, are located at the basal-most layer across all positions of the whole sensory OE (Kocagöz, 2021; Demirler *et al.*, 2020).

While the continuous mitotic activity of GBCs generates peaks of cell proliferation at ILC and SNS (Bayramlı, 2015; Bayramlı *et al.*, 2017), the core-sensory OE is largely devoid of mitotic activity because of the dormant state of HBCs under physiological conditions (Bayramlı, 2015; Kocagöz, 2021). Continuous mitotic activity at ILC and SNS and the low mitotic activity in the core-sensory OE, collectively generate a bimodal distribution of proliferative cells in the sensory OE (Bayramlı, 2015). Upon injury, HBCs become activated and result in a homogenous distribution of proliferative activity across the entire sensory OE, which is characterized by a dramatic increase in proliferative activity across the core-sensory OE (Kocagöz, 2021). The differential proliferative activity pattern of maintenance and repair neurogenesis allows to discriminate between the GBC and HBC activity without the need of additional markers. While selective changes in proliferative activity at the ILC and SNS can be interpreted as an effect on GBC-driven maintenance neurogenesis, changes in the core-sensory OE could be interpreted as activation of HBCs and repair neurogenesis (Calvo-Ochoa *et al.*, 2021).

Intranasal administration of human recombinant HB-EGF was previously shown to significantly increase cell proliferation and OSN neurogenesis in the core-sensory region (Kocagöz, 2021). The observation that HB-EGF activates Sox2-expressing cells occupying the basal-most layer of the core-sensory OE, which is exclusively occupied by HBCs but not GBCs (this study), supports the hypothesis that HB-EGF activates dormant HBCs and stimulate repair neurogenesis. HB-EGF signals through EGFR (ERBB1 homodimer) and ERBB1/ERBB4 heterodimers (Paria *et al.*, 1999; Iwamoto *et al.*, 1999). Injury selectively upregulates the expression levels of only one member of the EGF receptor family, ERBB1 (Kocagoz, Demirler, and Fuss, unpublished). In order to investigate whether HB-EGF uses the EGFR/JAK/STAT signaling path to induce the activation of HBCs, the effects of EGFR and JAK/STAT signaling inhibition on maintenance and repair neurogenesis has been investigated by utilizing small molecule inhibitors of EGFR and JAK2/STAT3 signaling in the work presented in this thesis.

While EGFR inhibition by PD153035 treatment results in a decrease in overall proliferative activity in the intact OE after a 1 d incubation period, no difference could be detected in the total number of newly generated cells after 5 d. The discrepancy between the early and late time points could result from insufficient inhibition of EGFR signaling by PD153035 since the fish received the inhibitor only at the beginning of the 5 d analysis period. The inhibitory effect of PD153035 on the intact OE is selectively seen on proliferative activity around the SNS after 1 d incubation period. In contrast, no significant decrease was observed in the proliferative activity of the ILC. This difference among the response of the ILC and SNS to the inhibitor suggests an internal heterogeneity among the neurogenic niches of the ILC and SNS, which renders the proliferative activity of the SNS region more susceptible to EGFR inhibition.

For instance, the ILC and SNS have been shown to be non-equivalent in their proliferative activity (Bayramli *et al.*, 2017). Markedly, the neuronal progeny generated in those regions have been shown to have different propensities for OSN subtypes and odorant receptor gene choice. From these findings, it has previously been suggested that the ILC and SNS may contain different subtypes of stem cells contributing preferentially to microvillus and ciliated OSNs. Despite the lack of evidence, this observed selective effect might also suggest a difference in the EGFR expression of GBCs occupying the ILC and SNS regions. In this context, GBCs which are exclusively located at the SNS but not in ILC may express EGFR, which selectively regulates their activity.

However, another argument that could be put forward to explain the observed difference to EGFR inhibition may be technical and results from the looser definition of SNS region compared to the ILC. The analysis of the positions of BrdU⁺ cells was performed on the selected rectangular ROIs of the OEs. Due to the curved nature of the OE, the length of the epithelial folds that are included in the ROIs differ slightly. Since ILC regions of the different epithelial folds are generally located at approximately identical positions relative to the midline raphe, it can be accurately identified and consistently scored by the radial index system. In contrast, location of the SNS and the nonsensory region vary between differently sized epithelial folds and could cause an error when positions of marker-positive cells are projected onto horizontal dimensions.

This inaccuracy may contribute to the observed difference in the inhibitory effects of PD153035 between the neurogenic zones at the ILC and SNS. Repetition of the analysis performed on normalized individual epithelial folds rather than areas including multiple folds of different length would help to accurately identify the positions of BrdU⁺ cells.

Although no difference in the total number of newly generated cells could be observed after 5 d in PD153035-treated fish, the number of newly generated neurons in the ILC was found to be decreased. Therefore, EGFR inhibition appears to affect the ongoing maintenance neurogenesis. Interestingly, however, neither stimulation with HB-EGF (Kocagöz, 2021) nor direct inhibition of HB-EGF (Sireci, unpublished) was found to affect maintenance neurogenesis. Since HB-EGF stimulation would be expected to affect GBCs if they also express EGFR, the observed effect of PD153035 treatment on GBCs seems to be not related with the inhibition of EGFR. PD153035 inhibits the activation of EGFR by preventing the autophosphorylation of ERBB1 (Fry *et al.*, 1994). Therefore, the observed decrease, rather suggested to be resulted from the residual effect of PD153035 on other certain members of the EGFR family since ERBB1 also forms heterodimers with different ERBBs which do not have affinity for HB-EGF (Yarden and Sliwkowski, 2001). In fact, ERBB1 was also shown to be capable of forming heterodimers with RTKs from families that are different from the ERBB family (Wheeler *et al.*, 2008; Tanizaki *et al.*, 2011; Iyer *et al.*, 2016). Usage of different inhibitors targeting different RTKs in similar experimental setups might help to further understand the observed effect of PD153035 treatment on maintenance neurogenesis.

HBCs in the intact OE are quiescent (Kocagöz, 2021) and show very rare proliferative activity (Demirler, 2021). The transition between maintenance and the repair neurogenesis responses can be detected by the substantial increase in proliferative activity in the core-sensory region that goes along with the injury-induced activation of HBCs (Kocagöz, 2021). EGFR inhibition results in a dramatic decrease in the total proliferative activity by 1 dpl. Therefore, it can be suggested that EGFR signaling plays an important role in injury-induced stimulation of the proliferative activity of HBCs.

The low proliferative activity of HBCs in the intact zebrafish OE largely originates from symmetric cell divisions contributing to their self-renewal (Demirler, 2021). In response to injury, HBCs start to proliferate asymmetrically and generate GBCs in the rodent (Schwob *et al.*, 2017) and zebrafish OE (Kocagöz, 2021). GBCs, in turn, give rise to neuronal and non-neuronal cell populations and repopulate the OE after injury (Schwob *et al.*, 2017). The unique appearance of Sox2- and Ascl1-expressing GBCs in the core-sensory region after injury, suggests that the proliferative activity of HBCs in the injured zebrafish OE also includes asymmetric cell divisions (Kocagöz, 2021). Therefore, the transition of the HBC cell divisions from symmetric to asymmetric might be suggested to be one other important aspect of the injury-induced activation of HBCs.

When the distribution profiles of newly generated cell populations in the intact OE is analyzed, EGFR signaling inhibition is found to significantly increase the number of newly generated non-neuronal cell populations that stain positive for the proliferation marker BrdU but not for the neuronal marker HuC/D in the core-sensory region after 5 d incubation period. Although it is not possible to determine the exact identity of these cell populations without the usage of additional markers, their appearance in the basal OE suggests that they might be HBCs. Therefore, EGFR signaling inhibition seems to stimulate the proliferation of HBCs in the intact OE. The lack of neuronal cells in the injured OE in the presence of EGFR inhibition suggests that this expansion does not result from the stimulation of asymmetric cell divisions. The appearance of this expanded population resembling HBCs on the other hand, suggests that they might be the result of an increased rate of symmetric cell divisions. Therefore, a dual role for EGFR signaling in the stimulation of the proliferative activity and suppression of the symmetric cell divisions of HBCs during repair neurogenesis could be suggested.

Despite the dramatic decrease in proliferative activity observed during 1 dpl, the total number of newly generated cells at 5 dpl was found to be only slightly decreased in response to EGFR inhibition. Considering similar discrepancy in the strength of the inhibitory effect of PD153035 treatment observed in the intact OE, the inhibitor treatment might have been insufficient over the entire time course of the experiment.

Nevertheless, the contribution of these newly generated cells to neuronal pool was found to be dramatically decreased. The number of newly generated non-neuronal cells on the other hand, were found to be increased after EGFR inhibition. Since this experiment did not include cell identity markers which could discriminate between stem and non-stem cell populations, the exact identity of these increased number of newly generated non-neuronal cells could not be determined. However, considering the suggested effect of EGFR inhibition in preventing the activation of HBCs during 1 dpl, the decreased number of recovered OSNs might indicate a delay in the regenerative response resulting from postponing the initial generation of neuronal progenitor cells to the later days which the inhibitor becomes ineffective. In this context, the increased number of non-neuronal cells might represent HBCs which become activated with the disappearance of the inhibitory effect and/or neuronal progenitor cells which could only recently start to repopulate the OSNs.

Usage of additional cell identity markers but also examination of later time points is essential to confirm the hypothesis that EGFR signaling results in a delay in the maturation of OSNs. A variety of findings suggest the involvement of EGFR signaling in the activation of HBCs both in the zebrafish (Kocagöz, 2021; Güler, 2021; Sireci unpublished; this study) and in rodent OE (Holbrook *et al.*, 1995; Chen *et al.*, 2020). However, although EGFR signaling inhibition caused a drastic decrease early in regeneration, it did not result in the complete loss of proliferative activity observed during 1 dpl (Figure 4.2) and proliferative activity observed during later phases of regeneration resumed normally in the zebrafish OE (Figure 4.5.B). Since not the exclusive proliferative activity of HBCs but the collective proliferative activity of all cell types were examined, involvement of other cell types, which do not depend on EGFR signaling, to repair neurogenesis might be suggested.

However, even in the rodent OE, where the proliferative activity of HBCs was exclusively examined, EGFR signaling inhibition does not result in a complete loss of HBC activity and although their regeneration is delayed, OSNs eventually arise (Chen *et al.*, 2020). In order to understand whether the insufficient inhibition of EGFR signaling or the involvement of other factors in their activation is the reason behind the incomplete effects and to see to what extent the activity of other cell types overcome the absence of HBC activity during regeneration, additional experiments including longer time period inhibition of EGFR signaling should be performed.

JAK/STAT signaling inhibition with JSI-124 treatment results in an increase in the total proliferative activity in the intact OE at the end of 1 d incubation period. When the distribution profiles of proliferative activity in the intact OE was analyzed, JAK/STAT signaling inhibition was found to significantly increase the proliferative activity observed in the ILC. In contrast, proliferative activity at the SNS was found not to be affected by JAK/STAT signaling inhibition. As mentioned above, the ILC and SNS were suggested to contain different subtypes of GBCs (Bayramli, 2016). Similarly, the differential effect of JAK/STAT signaling inhibition on the ILC and SNS might also suggest the differential distribution of cell surface receptors that activate JAK/STAT signaling in GBCs at the ILC and SNS. In this context, the proliferative activity of GBCs occupying the ILC, which may have a denser expression of cell surface receptors, can be suggested to be negatively by JAK/STAT inhibition.

Again, since selected rectangular ROIs but not individual epithelial folds were used for the analysis of the positions of BrdU⁺ cells, a similar technical error in the identification of the dimensions of the SNS region might have contributed to differences in this experiment. In this context, the increased number of BrdU⁺ cells in the SNS might be falsely assigned from cells within the non-sensory region. Repetition the analysis on normalized individual epithelial folds may help to determine the exact effect of JAK/STAT signaling inhibition on maintenance neurogenesis.

While EGFR and JAK/STAT signaling inhibition seems to have opposing effects on maintenance neurogenesis, they found to similarly suppress the activity at 1 dpl.

Therefore, the activity of EGFR and JAK/STAT signaling might suggested to contribute to related events during repair neurogenesis. The results of the experiments evaluating the effect of EGFR signaling inhibition on OE proliferation and neurogenesis suggested the involvement of EGFR signaling in the activation of HBCs during repair neurogenesis. However, when the proliferative activity of the core-sensory region was analyzed after JSI-124 treatment, no significant difference could be observed. Therefore, it might be suggested that JAK/STAT signaling is not involved in the regulation of HBC activity directly. Yet, this problem rather seems to be resulting from the unusual proliferative activity pattern of the control group. In contrast to the homogeneous distribution pattern which is regularly observed at 1 dpl (Kocagöz, 2021), the control group exhibits a bimodal distribution pattern of proliferative activity which peaks around the ILC and in an intermediate position between the core-sensory and SNS region.

When a second set of control group was prepared in the pursuit of determining if the unusual pattern observed in the first control group was an experimental error, the characteristic homogenous distribution of proliferative activity was seen. However, when the distribution profiles of the intact OEs of the second control group was compared with the JSI-124 treated OEs, the distribution profiles of JSI-124-treated OEs appeared as a flat line below the second control group, showing significant decreases across all positions of the sensory OE. Thus, conflicting results regarding the effect of JSI-124 treatment on maintenance neurogenesis were obtained. Therefore, although no discrepancy observed in the distribution profiles of the proliferative activity, the intact OEs of the first control group also seems to be affected from this suggested experimental error.

Another technical difference is that during the preparation of the first and second control group samples, different batches of the same BrdU antibody was used. Problems that occurred later in the BrdU labelling in other experimental with the same antibody batch which was used for the preparation of the first control group, suggests the existence of a problem in the BrdU labelling also in this experiment.

When the intact OEs of the first and second control group was compared, the total proliferative activity of the second control group was found to be much higher without showing any discrepancy in the characteristic bimodal distribution pattern of proliferative cells. The total number of BrdU⁺ cells observed in the second control group appeared to be similar to the numbers observed previously in the intact OE samples. Consequently, the numbers observed in the first control group also appears to be much lower compared to the intact OE samples.

Therefore, the suggested experimental error seems to result from the low labeling efficiency of BrdU cells in this particular experiment. This relatively low efficiency seems to become even lower when the tissue integrity was compromised, resulting in the formation of an unusual distribution pattern of proliferative activity observed exclusively in the injured OEs. Since the same antibody batch was also used for the preparation of the JSI-124-treated samples, the number of co-labelled cells may be underrepresented. However, it is hard to determine the exact outcome of this inefficient labeling in the JSI-124 treated samples since the tissue conditions resulting from the JAK/STAT signaling inhibition, which might affect the severity of labeling problem remains unknown. Collectively, these observations suggest that the results obtained in this experiment are somewhat unreliable and the effect of JSI-124 treatment on the intact and injured OE remains inconclusive. Repetition of the experiment is necessary to identify the role of JAK/STAT signaling in the proliferative activity of maintenance and repair neurogenesis.

5.4.1. Source of EGFR Ligands and Stimulation

In rodent OE, EGFR is exclusively expressed by HBCs (Holbrook *et al.*, 1995; Chen *et al.*, 2020) and the pharmacological inhibition of EGFR upon injury was shown to significantly suppress the activation of HBCs and resulted in a decrease in their proliferation rate (Chen *et al.*, 2020). Expression of *egfra* in the $tp63^+$ cells (Güler, 2021), suggests the existence of a similar role for EGFR signaling in the injury-induced activation of HBCs. In the same study using EGFR inhibition, injury-induced cleavage of NrCAM by matrix metalloproteases was suggested to be the trigger for dormant HBC activation through the activation of EGFR (Chen *et al.*, 2020). Therefore, in order to provide HBC activation selectively upon injury, the activation of EGFR depends on a ligand which is selectively expressed or activated in the injured zebrafish OE. Among the known ligands of EGFR, transcript levels of one of the paralogs of HB-EGF, *hbegfa*, shows the strongest upregulation during injury along with signaling components that are related to its activation (Kocagöz, 2021). Stimulation with human recombinant HB-EGF increases the proliferative activity of cells (Kocagöz, 2021; this study) which appears to include HBCs according to their position, apicobasal orientation, and marker expression (Demirler, 2021; Kocagöz, 2021; this study). Inhibition of HB-EGF signaling in the injured OE on the other hand, through either direct inhibition of HB-EGF by its sequestration (Mitamura *et al.*, 1995; Dateoka *et al.*, 2012) or by usage of broad spectrum MMP inhibitors, which prevent HB-EGF ectodomain shedding (Higashiyama and Nanba, 2004), resulted in impaired proliferative activity (Kocagöz, 2021; Sireci, unpublished). The overlapping effects of EGFR signaling inhibition and the activation and deactivation of the HB-EGF signaling on the proliferative activity of regions occupied by HBCs suggest an interaction between HB-EGF and EGFR in the injury-induced activation of HBCs in the regenerating zebrafish OE.

5.4.2. Effect of EGFR Signaling Inhibition on OSN Neurogenesis

The proliferative activity of HBCs in the intact zebrafish OE largely contribute to their self-renewal and was shown to be rarely neurogenic (Demirler, 2021). In response to injury, HBCs proliferate and generate GBCs to repopulate the neuronal cell populations of the OE after injury (Schwob *et al.*, 2017). Similarly, the proliferative activity in the injured zebrafish OE is also neurogenic and results from the unique generation of Sox2- and Ascl1-expressing GBCs from activated HBCs (Kocagöz, 2021). As discussed above, the decrease observed in the proliferative activity of zones occupied by HBCs suggests that EGFR signaling might have a role in the activation of HBCs. In order to gain further insight into the role of EGFR signaling in repair neurogenesis, the overall neuronal regeneration efficiency and the contribution of the mitotic activity observed during the 3 dpl to the newly generated neuronal populations found at 5dpl upon EGFR inhibition were examined.

Under normal conditions, OE would regenerate $81.3 \pm 10.1\%$ of its OSNs by 5dpl (Kocagöz, 2021). In PD153035-treated injured OEs, this rate only reaches up to $29.9 \pm 2.9\%$ and majority of the cells that are generated were found to be non-neuronal cells (Figure 4.4). Due to the lack of cell type specific markers these cells comprising the majority of the newly generated cell populations in the PD153035-treated OE could only be identified as non-neuronal cells. Therefore, the possibilities of them to be proliferative stem cells, undifferentiated cells, and also differentiated cell types other than neurons will be discussed. Regardless of the identity of the newly generated cell types, in contrast to the dramatic decrease in the proliferative activity that is seen upon PD153035-treatment at 1 dpl, PD153035-treatment only resulted in a small decrease in total proliferative activity at 5 dpl. Therefore, insufficient inhibition of EGFR signaling also should be considered while evaluating the results.

Although the identity of single BrdU⁺ cells cannot be determined, newly generated OSNs can clearly be seen to comprise majority of the BrdU⁺ cell populations at 5 dpl in controls. Therefore, at the normal pace of regeneration, activity captured at 3 dpl substantially contributes to the generation of fully differentiated cell types at 5dpl.

If the non-neuronal populations observed in the PD153035-treated injured OE at 5dpl are assumed to be proliferative stem cells and/or undifferentiated cells, a delay in the maturation of newly generated cell types can be suggested. The process of regenerating most OSNs takes three to five days in zebrafish OE (Bayramli *et al.*, 2017). The second day of the regeneration is when GBC progenitor cells are generated which can be identified by their *Ascl1* and *Sox2* expression (Kocagöz, 2021). The lack of the *Ascl1* signal in the OE at 1 dpl suggests that this time point defines the differentiation period of HBCs into multipotent progenitor subpopulation of the GBCs. PD153035 treatment, as indicated by the dramatic decline in the cell proliferation across all positions of the sensory region in the injured OE at 1dpi (Figure 4.2), suppresses the progression of a regenerative response to some extent. Therefore, by postponing the initial generation of GBCs, PD153035 treatment might result in a delay in the maturation of OSNs.

If the non-neuronal cells comprise fully differentiated non-neuronal cells or expanded HBC/GBC populations, then an additional role for EGFR signaling in lineage commitment can be suggested. With the usage of multiple single cell techniques, it has been shown that HBCs in the rodent OE acquire a common transitional state after injury, which is unique to regeneration (Fletcher *et al.*, 2018). However, as revealed by gene expression profiles showing the enrichment of different sets of genes in different subsets of HBCs, they start to show heterogeneity in their population early after their activation. When the progeny generated from a subset of HBCs which express *Hopx*, a transcription factor which is implicated to be related with intestinal land hair follicle stem cell identity (Takeda *et al.*, 2011), were traced by inducing *HopxCreER* 1 d post MeBr lesion, the resulting population at 14 dpl were shown to be completely comprised of sustentacular cells and neurons but not of self-renewing HBCs (Gadye *et al.*, 2017). As predicted, lineage committed cells occur early in the activated HBC populations (Gadye *et al.*, 2017).

The appearance of *Ascl1*⁺ GBCs in the core-sensory at 2 dpl (Kocagöz, 2021) also suggests that HBCs which are committed to generate differentiated cell types also occur early in the injured zebrafish OE. Therefore, if EGFR has a role in the regulation of lineage commitment of some subsets of HBCs, it can be affected by the PD153035.

Since EGFR inhibition by PD153035-treatment was shown to be decreased, it might be assumed that EGFR has an additional role in neuronal lineage commitment in a subset of HBCs. In the absence of Sox2, HBCs are found to be defective in neurogenesis since they were not able to differentiate into neuronal lineage restricted GBCs and only show self-renewal and give rise to sustentacular cells (Packard *et al.*, 2016; Gadye *et al.*, 2017). Contrasting to its role in the rodent OE, Sox2 expression is mostly related to maintenance and multipotency of stem cells in other tissues (Pevny and Nicolis, 2010). In the SVZ, Sox2 is essential for the self-renewal of NPCs (Brazel *et al.*, 2005; Kondo and Raff, 2004). A positive feedback loop between EGFR signaling and Sox2 expression was found to positively regulate their self-renewal capacity (Hu *et al.*, 2010). Although the function of Sox2 in OE is different from other tissues, similar feedback loop might explain the observed selective decrease in the formation of neuronal populations.

5.4.3. Effect of JAK/STAT Signaling Inhibition on OSN Neurogenesis

Inhibition of JAK/STAT signaling with JSI-124 treatment also causes a significant decrease in the efficiency of OSN regeneration of injured OEs, in which the area covered by HuC/D⁺ OSNs only reaches up to $26.9 \pm 2.0\%$ of the control values. The decreased number of HuC/D⁺ OSNs was found to be in the range of values that were previously observed between the 1 dpl and 3 dpl (Kocagöz, 2021). Once degeneration is almost complete at 1 dpl, the OE starts to repopulate with OSNs, which result in the recovery of $86.5 \pm 10.2\%$ of the OSN populations by 3 dpl (Kocagöz, 2021; Kocagoz *et al.*, 2022). Thus, JSI-124 treatment seems to either completely prevent the regeneration of OSNs, in which only the degenerating OSN populations could contribute to the relative area covered by HuC/D⁺ cells, or slowed down the recovery rate resulting in a dramatic decrease in the number of newly generated OSNs.

Regardless of the state of the OSNs in JSI-124-treated injured OEs, the recovery appears to be impaired. Therefore, the function of the JAK/STAT signaling in the injured OE could be suggested to be contribute to regeneration of OSNs. Considering the resemblance of the effects of PD153035 and JSI-124 treatment, a relationship between EGFR and JAK/STAT signaling during OE regeneration might be suggested.

Due to the problems that occurred with the BrdU labelling, the effect of JAK/STAT inhibition on the proliferative activity of zones dedicated to maintenance and repair neurogenesis but also the proliferative activity of the cell populations which have activated JAK/STAT signaling could not be determined. Thus, the underlying effect of JAK/STAT signaling inhibition resulting in this dramatic impairment in OE regeneration remains unknown.

5.5. Are EGFR and STAT3 Active in the Same Cell Types?

Intranasal administration of human recombinant HB-EGF results in an increase in the number of pSTAT3+ cells in the core-sensory region. The increased occurrence of pSTAT3+ cells in the core-sensory region also occurs in response to injury and represents an important difference that is characteristic for the transition from maintenance to repair neurogenesis. Observation of a similar transition in the pattern pSTAT3+ cells suggest a relationship between HB-EGF and JAK/STAT signaling in the regulation of regenerative neurogenesis. However, it is not certain if HB-EGF directly activates JAK/STAT signaling as a downstream target to stimulate cell proliferation.

As previously discussed, the basal position and lack of Sox2 expression observed in pSTAT3-positive cells suggest a neuronal lineage committed progenitor/precursor cell or immature neuron identity for these cells. In addition to previous findings suggesting the selective involvement of HB-EGF signaling in the regulation of repair neurogenesis, human recombinant HB-EGF also has been shown to activate Sox2-expressing cells located at the basal most layer of the sensory OE in the work presented in this thesis, further supporting the idea that HB-EGF selectively activates dormant HBC-like cells. Furthermore, the effects of EGFR inhibition on the cell proliferation and neurogenesis suggests a role for EGFR signaling in the propagation of a regenerative response. These findings collectively suggest that HB-EGF stimulated EGFR signaling activation results in the selective activation of HBC-like cells in order to propagate a regenerative response.

Therefore, it can be concluded that JAK/STAT signaling does not work as a direct downstream target of HB-EGF in HBCs. The observed increase in the activation of JAK/STAT signaling in response to HB-EGF stimulation could be explained by the generation of pSTAT3+neuronal lineage-committed cell subpopulation of GBC-like cells resulting from the increased proliferative activity of HBC. Therefore, HB-EGF might suggested to activate JAK/STAT signaling later in the HBC lineage.

5.6. Relationship with Other Niche Factors and Signaling Events

Both the persistence of maintenance and injury-induced propagation of repair neurogenesis are complex in the way that they require the regulation of multiple cellular and molecular events. The results showing the involvement of different signaling pathways in the OSN lineage suggest a relationship between these pathways in order to generate a collective action during different modes of neurogenesis.

To both preserve the dormant state during physiological conditions and to provide the activation of a regenerative response, HBC activity must be under the control of injury-specific cues. In the transcriptome analysis performed on intact and injured OE samples, in addition to HB-EGF (Kocagöz, 2021, Sireci, unpublished), the cytokines IL-6 and Leptin were also found to be uniquely expressed in the injured OE (Demirler, 2021). The stimulatory effect of human recombinant HB-EGF on the proliferation of basally located Sox2 expressing cells (this study) and the stimulatory effect of IL-6 on the HBCs (Demirler, 2021) suggests their synergistic relationship in the injury-induced proliferative activity of HBCs. However, while the increased proliferative activity resulting from the IL-6 largely contribute to the HBC pool expansion (Demirler, 2021), HB-EGF stimulates neurogenic cell proliferations of HBCs (Kocagöz, 2021). Therefore, HB-EGF might suggested to additionally promote asymmetric cell divisions of HBCs contributing to their injury-induced activation.

Among the downstream signaling components which become activated through the activation of EGFR signaling, the transcript levels of the components of MAPK signaling show an injury-induced upregulation in the zebrafish OE (Demirler, 2021).

Inhibition of MAPK signaling impairs the rate of cell proliferation and neurogenesis selectively during repair neurogenesis (Dokuzluoğlu, unpublished). Preliminary results of the experiments evaluating the effect of the inhibition of PI3K-Akt signaling also implicates impairments the cell proliferation observed during repair neurogenesis. Therefore, HB-EGF might suggested to activate MAPK and PI3K-Akt signaling through EGFR to transduce signals related to HBC activation.

Our research group previously identified the effect of Wnt agonists and antagonists on the sites of both maintenance and repair neurogenesis in zebrafish OE. Expression of β -catenin localizes to the maintenance neurogenesis sites under physiological conditions and the expression is found to be dispersed across the sensory OE during regeneration (Eski, 2018). These findings and upregulation of the components of Wnt signaling during the early phases of regeneration suggest a common role for Wnt signaling in the activation of the proliferative activity of both types of stem cell populations located in the OE. Therefore, MAPK and PI3K-Akt signaling together with the downstream components of cytokine signaling might suggested to converge on Wnt/ β -catenin signaling to stimulate the HB-EGF and IL-6-induced proliferation of HBCs during repair neurogenesis. A similar observation has been made in the regenerating zebrafish retina (Wan *et al.*, 2014; Zhao *et al.*, 2014).

5.7. Proposed Model

A dual stem cell system underlies the abilities of the zebrafish OE to facilitate continuous turn-over of OSNs and regenerate fully after acute injury (Bayramli *et al.*, 2017; Demirler *et al.*, 2020; Kocagöz, 2021). This dual stem cell system is comprised of GBCs (Bayramli *et al.*, 2017) and HBCs (Demirler *et al.*, 2020; Kocagöz, 2021). GBCs are found exclusively located in the ILC and SNS and their continuous proliferative activity contribute to the turn-over of OSNs during maintenance neurogenesis (Bayramli, 2016; Bayramli *et al.*, 2017). During maintenance neurogenesis, multipotent progenitor populations of GBCs give rise to neuronal lineage committed GBCs. After the loss of Sox2-expression, later in the lineage commitment, JAK/STAT signaling becomes activated in neuronal lineage-committed GBCs.

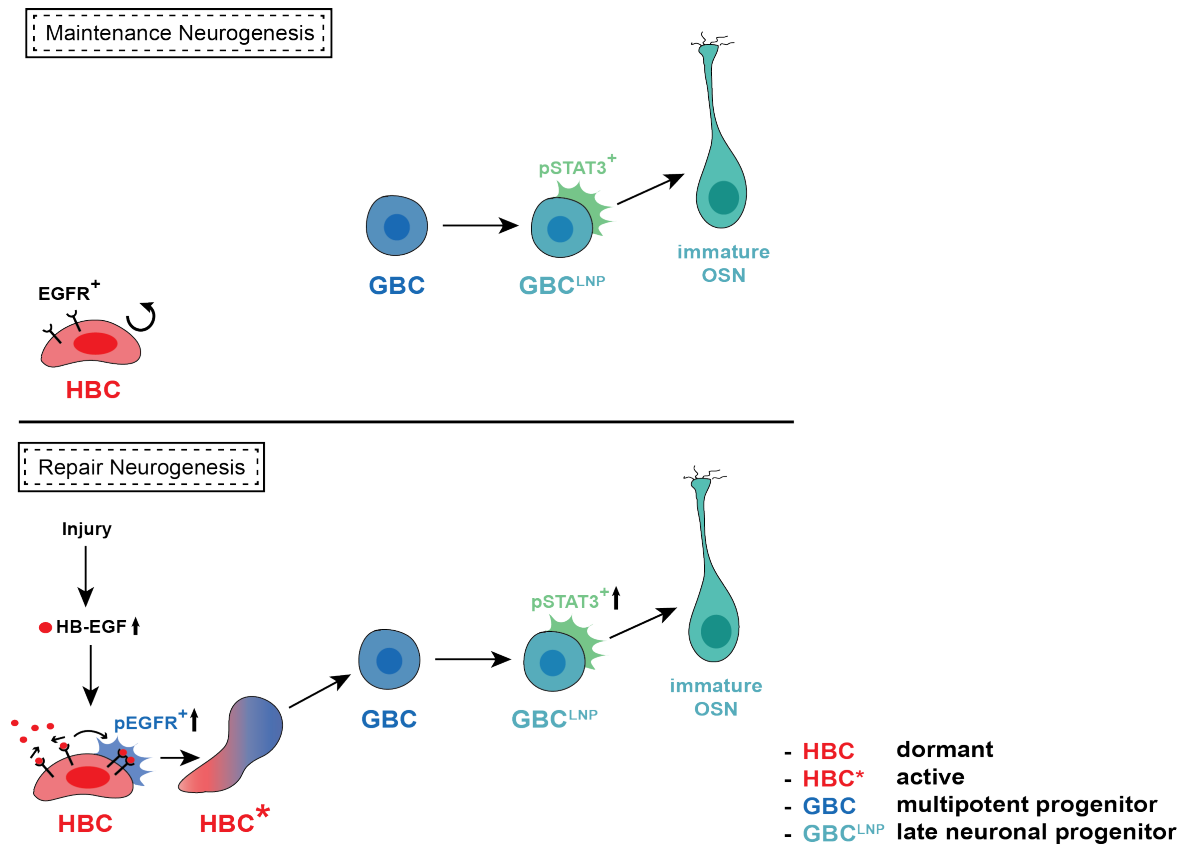


Figure 5.1. Proposed model of maintenance and repair neurogenesis.

Injury to the OE stimulates the expression and secretion of HB-EGF. HB-EGF released from OE cell populations activate dormant HBCs via increasing their proliferative activity and stimulating their asymmetric cell divisions through EGFR signaling. Activated HBCs start to generate multipotent progenitor GBCs. Later in the neuronal lineage commitment, JAK/STAT signaling becomes activated in GBCs and regulate the OSN regeneration during repair neurogenesis.

REFERENCES

- Aaronson, D. S., and C. M. Horvath, 2002, "A Road Map for Those Who Don't Know JAK-STAT", *Science*, 296, no. 5573, pp. 1653-1655.
- Abe, Y., H. Namba, Y. Zheng, and Nawa, H., 2009, "In Situ Hybridization Reveals Developmental Regulation of ErbB1-4 mRNA Expression in Mouse Midbrain: Implication of ErbB Receptors for Dopaminergic Neurons", *Neuroscience*, 161, no. 1, pp. 95-110.
- Aguirre, A., M. E. Zheng, and V. Gallo, 2010, "Notch and EGFR Pathway Interaction Regulates Neural Stem Cell Number and Self-Renewal", *Nature*, 467, no. 7313, pp. 323-327.
- Alexi, T., and F. Hefti, 1993, "Trophic Actions of Transforming Growth Factor Alpha on Mesencephalic Dopaminergic Neurons Developing in Culture", *Neuroscience*, 55, no. 4, pp. 903-918.
- Altman, J., and G. D. Das, 1965, "Autoradiographic and Histological Evidence of Postnatal Hippocampal Neurogenesis in Rats", *The Journal of Comparative Neurology*, 124, no. 3, pp. 319-335.
- Alunni, A., and L. Bally-Cuif, 2016, "A Comparative View of Regenerative Neurogenesis in Vertebrates", *Development*, 143, no. 5, pp. 741-753.
- Alvarez-Buylla, A., and J. R. Kirn, 1997, "Birth, Migration, Incorporation, And Death of Vocal Control Neurons in Adult Songbirds", *Journal of Neurobiology*, 33, no. 5, pp. 585-601.

- Alvarez-Buylla, A., and F. Nottebohm, 1988, "Migration of Young Neurons in Adult Avian Brain", *Nature*, 335, no. 6188, pp. 353-354.
- Alvarez-Buylla, A., C.Y. Ling, W. S. Yu, 1994, "Contribution of Neurons Born During Embryonic and Adult Life to The Brain of Adult Canaries: Regional Specificity and Delayed Birth of Neurons in The Song-Control Nuclei", *The Journal of Comparative Neurology*, 347, no. 2, pp. 233-248.
- Alvarez-Buylla, A., M. Theelen, and F. Nottebohm, 1990, "Proliferation "Hot Spots" in Adult Avian Ventricular Zone Reveal Radial Cell Division", *Neuron*, 5, no. 1, pp. 101-109.
- Andres, K.H., 1965, "Differenzierung und Regeneration von Sinneszellen in Der Regio Olfactoria", *Naturwissenschaften*, 52, no. 17, p. 500.
- Augusto-Oliveira, M., G. Arrifano, J. Malva, and M. Crespo-Lopez, 2019, "Adult Hippocampal Neurogenesis in Different Taxonomic Groups: Possible Functional Similarities and Striking Controversies", *Cells*, 8, no. 2, p. 125.
- Ayati, A., S. Moghimi, S. Salarinejad, M., Safavi, B. Pouramiri, and A. Foroumadi, 2020, "A Review on Progression of Epidermal Growth Factor Receptor (EGFR) Inhibitors as an Efficient Approach in Cancer Targeted Therapy", *Bioorganic Chemistry*, 99, no. 103811.
- Bayer, S. A., 1980, "Quantitative 3H-Thymidine Radiographic Analyses of Neurogenesis on The Rat Amygdala", *The Journal of Comparative Neurology*, 194, no. 4, pp. 845-875.
- Bayramli, X., Y. Kocagöz, U. Sakizli, and S. H. Fuss, 2017, "Patterned Arrangements of Olfactory Receptor Gene Expression in Zebrafish are Established by Radial Movement of Specified Olfactory Sensory Neurons", *Scientific Reports*, 7, no. 1, p. 5572.

- Bayramlı, K., 2016, *Neurogenesis and Migration of Specified Chemosensory Neurons in The Adult Zebrafish Olfactory Epithelium*, Ph.D. Thesis, Boğaziçi University.
- Beauchamp, R. D., R. M. Lyons, E. Y. Yang, R. J. Coffey, Jr, and H. L. Moses, 1990, "Expression of and Response to Growth Regulatory Peptides by Two Human Pancreatic Carcinoma Cell Lines", *Pancreas*, 5, no. 4, pp. 369-380.
- Becker, T. and C.G. Becker, 2014, "Axonal Regeneration in Zebrafish", *Current Opinion in Neurobiology*, 27, pp. 186-191.
- Beecher, M. D., and E. A. Brenowitz, 2005, "Functional Aspects of Song Learning in Songbirds", *Trends in Ecology & Evolution*, 20, no. 3, pp. 143-149.
- Betz, A., H. D. Ryoo, H. Steller, and J. E. Darnell, Jr, 2008, "STAT92E is a Positive Regulator of Drosophila Inhibitor of Apoptosis 1 (DIAP/1) and Protects Against Radiation-Induced Apoptosis", *Proceedings of the National Academy of Sciences of the United States of America*, 105, no. 37, pp. 13805-13810.
- Bingman, V. P., G. E. Hough II, M. C. Kahn, and J. J. Siegel, 2003, "The Homing Pigeon Hippocampus and Space: In Search of Adaptive Specialization", *Brain, Behavior and Evolution*, 62, no. 2, pp. 117-127.
- Blaskovich, M. A., J. Sun, A. Cantor, J. Turkson, R. Jove, and S. M. Sebti, 2003, "Discovery of JSI-124 (Cucurbitacin I), a Selective Janus Kinase/Signal Transducer and Activator of Transcription 3 Signaling Pathway Inhibitor with Potent Antitumor Activity Against Human and Murine Cancer Cells in Mice", *Cancer Research*, 63, no. 6, pp. 1270-1279.
- Bottjer, K. P., P. P. Weinstein, and M. J. Thompson, 1985, "Effects of an Azasteroid on Growth, Development and Reproduction of the Free-Living Nematodes *Caenorhabditis Briggsae* and *Panagrellus Redivivus*", *Comparative Biochemistry and Physiology Part B: Comparative Biochemistry*, 82, no. 1, pp. 99-106.

- Bousoik, E., and H. Montazeri Aliabadi, 2018, "Do We Know Jack" About JAK? A Closer Look at JAK/STAT Signaling Pathway", *Frontiers in Oncology*, 8, no. 287.
- Brazel, C. Y., T. L. Limke, J. K. Osborne, T. Miura, J. Cai, L. Pevny, and M. S. Rao, 2005, "Sox2 Expression Defines a Heterogeneous Population of Neurosphere-Forming Cells in the Adult Murine Brain", *Aging Cell*, 4, no. 4, pp. 197-207.
- Burrows, R. C., D. Wancio, P. Levitt, and L. Lillien, 1997, "Response Diversity and the Timing of Progenitor Cell Maturation are Regulated by Developmental Changes in EGFR Expression in the Cortex", *Neuron*, 19, no. 2, pp. 251-267.
- Buteau, J., S. Foisy, E. Joly, and M. Prentki, 2003, "Glucagon-Like Peptide 1 Induces Pancreatic Beta-Cell Proliferation via Transactivation of the Epidermal Growth Factor Receptor", *Diabetes*, 52, no. 1, pp. 124-132.
- Cajal, S. R. Y., 1913, *Degeneration & Regeneration of the Nervous System.*, Oxford University Press, London.
- Calvo-Ochoa, E., C. A. Byrd-Jacobs, and S. H. Fuss, 2021, "Diving into the Streams and Waves of Constitutive and Regenerative Olfactory Neurogenesis: Insights from Zebrafish", *Cell and Tissue Research*, 383, no. 1, pp. 227-253.
- Carter, L. A., J. L. MacDonald, and A. J. Roskams, 2004, "Olfactory Horizontal Basal Cells Demonstrate a Conserved Multipotent Progenitor Phenotype", *The Journal of neuroscience: the official journal of the Society for Neuroscience*, 24, no. 25, pp. 5670-5683.
- Carver, R. S., M. C. Stevenson, L. A. Scheving, and W. E. Russell, 2002, "Diverse Expression of ErbB Receptor Proteins During Rat Liver Development and Regeneration", *Gastroenterology*, 123, no. 6, pp. 2017-2027.

- Casper, D., C. Mytilineou, and M. Blum, 1991, "EGF Enhances the Survival of Dopamine Neurons in Rat Embryonic Mesencephalon Primary Cell Culture", *Journal of Neuroscience Research*, 30, no. 2, pp. 372-381.
- Castro-Torres, R. D., J. Landa, M. Rabaza, O. Busquets, J. Olloquequi, M. Ettcheto, C. Beas-Zarate, J. Folch, A. Camins, C. Auladell, and E. Verdager, 2019, "JNK Isoforms are Involved in the Control of Adult Hippocampal Neurogenesis in Mice, Both in Physiological Conditions and in an Experimental Model of Temporal Lobe Epilepsy", *Molecular Neurobiology*, 56, no. 8, pp. 5856-5865.
- Catlett-Falcone, R., T. H. Landowski, M. M. Oshiro, J. Turkson, A. Levitzki, R. Savino, G. Ciliberto, L. Moscinski, J. L. Fernández-Luna, G. Nuñez, W. S. Dalton, and R. Jove, 1999, "Constitutive Activation of Stat3 Signaling Confers Resistance to Apoptosis in Human U266 Myeloma Cells", *Immunity*, 10, no. 1, pp. 105-115.
- Cau, E., G. Gradwohl, C. Fode, F. Guillemot, 1997, "Mash1 Activates a Cascade of Bhlh Regulators in Olfactory Neuron Progenitors", *Development*, 124, no. 8, pp. 1611-1621.
- Chen, G.C., P. Guillemot, and J. Settleman, 2004, "Rho-LIM Kinase Signaling Regulates Ecdysone-Induced Gene Expression and Morphogenesis During Drosophila Metamorphosis", *Current Biology*, 14, no. 4, pp. 309-313.
- Chen, Y., M.L. Getchell, X. Ding, and T.V. Getchell, 1992, "Immunolocalization of Two Cytochrome P450 Isozymes in Rat Nasal Chemosensory Tissue", *Neuroreport*, 3, pp. 749-752.
- Chen, J., F. Zeng, S. J. Forrester, S. Eguchi, M. Z. Zhang, and R. C. Harris, 2016, "Expression and Function of the Epidermal Growth Factor Receptor in Physiology and Disease", *Physiological reviews*, 96, no. 3, pp. 1025-1069.
- Chen, Z. H., X. C. Luo, C. R. Yu, and L. Yu, 2020, "Matrix Metalloprotease-Mediated Cleavage of Neural Glial-Related Cell Adhesion Molecules Activates Quiescent

- Olfactory Stem Cells via EGFR”, *Molecular and Cellular Neurosciences*, 108, pp. 1035-1052.
- Cosacak, M. I., C. Papadimitriou, and C. Kizil, 2015, “Regeneration, Plasticity, and Induced Molecular Programs in Adult Zebrafish Brain”, *Biomed Research International*, 2015, pp. 769-763.
- Costanzo, R.M., 1985, “Neural Regeneration and Functional Reconnection Following Olfactory Nerve Transection in Hamster”, *Brain Research Bulletin*, 30, no. 361(1-2), pp. 258-266.
- Craig, C. G., V. Tropepe, C. M. Morshead, B. A. Reynolds, S. Weiss, and D. van der Kooy, 1996, “In Vivo Growth Factor Expansion of Endogenous Subependymal Neural Precursor Cell Populations in the Adult Mouse Brain”, *The Journal of Neuroscience: The Official Journal of The Society for Neuroscience*, 16, no. 8, pp. 2649-2658.
- Cressman, D. E., L. E. Greenbaum, R. A. DeAngelis, G. Ciliberto, E. E. Furth, V. Poli, and R. Taub, 1996, “Liver Failure and Defective Hepatocyte Regeneration in Interleukin-6-Deficient Mice”, *Science*, 274, no. 5291, pp. 1379-1383.
- Dao, D. T., L. Anez-Bustillos, R. M. Adam, M. Puder, and D. R. Bielenberg, 2018, “Heparin-Binding Epidermal Growth Factor-Like Growth Factor as a Critical Mediator of Tissue Repair and Regeneration”, *The American Journal of Pathology*, 188, no. 11, pp. 2446-2456.
- Dateoka, S., Y. Ohnishi, and K. Kakudo, 2012, “Effects of CRM197, a Specific Inhibitor of HB-EGF, in Oral Cancer”, *Medical molecular morphology*, 45, no. 2, pp. 91-97.
- Demirler, M.C., 2021, *Investigation of Molecular Signals Regulating Cell Proliferation and Neurogenesis in the Intact and Injured Zebrafish (Danio Rerio) Olfactory Epithelium*, Ph.D. Thesis, Boğaziçi University.

- Demirler, M.C., U. Sakizli, B. Bali, Y. Kocagöz, S.E. Eski, A. Ergöner, A.S. Alkiraz, X. Bayramli, T. Hassenklöver, I. Manzini, and S.H. Fuss, 2020, “Purinergic Signalling Selectively Modulates Maintenance but not Repair Neurogenesis in the Zebrafish Olfactory Epithelium” *The FEBS Journal*, 287, pp. 2699-2722.
- Ding, X.X., and M.J. Coon, 1988, “Purification and Characterization of Two Unique Forms of Cytochrome P-450 From Rabbit Nasal Microsomes”, *Biochemistry*, 1, no. 27(22), pp. 8330-8337.
- Diotel, N., L. Lübke, U. Strähle, and S. Rastegar, 2020, “Common and Distinct Features of Adult Neurogenesis and Regeneration in the Telencephalon of Zebrafish and Mammals”, *Frontiers in Neuroscience*, 14.
- Eriksson, P. S., E. Perfilieva, T. Björk-Eriksson, A.-M. Alborn, C. Nordborg, D. A. Peterson, and F. H. Gage, 1998, “Neurogenesis in the Adult Human Hippocampus”, *Nature Medicine*, 4, no. 11, pp. 1313-1317.
- Ever, L., and N. Gaiano, 2005, “Radial ‘Glial’ Progenitors: Neurogenesis and Signaling”, *Current Opinion in Neurobiology*, 15, pp. 29-33.
- Fang, J., C. Feng, W. Chen, P. Hou, Z. Liu, M. Zuo, Y. Han, C. Xu, G. Melino, A. Verkhratsky, Y. Wang, C. Shao, and Y. Shi, 2021, “Redressing the Interactions Between Stem Cells and Immune System in Tissue Regeneration”, *Biology Direct*, 16, no. 1, p. 18.
- Fang, Y., V. Gupta, R. Karra, J. E. Holdway, K. Kikuchi, and K. D. Poss, 2013, “Translational Profiling of Cardiomyocytes Identifies an Early Jak1/Stat3 Injury Response Required for Zebrafish Heart Regeneration”, *Proceedings of the National Academy of Sciences of the United States of America*, 110, no. 33, pp. 13416-13421.
- Farbman, A. I., 1990, “Olfactory Neurogenesis: Genetic or Environmental Controls?”, *Trends in Neurosciences*, 13, no. 9, pp. 362-365.

- Farbman, A. I., 1992, *Cell Biology of Olfaction*, Cambridge University Press, Cambridge.
- Farbman A. I., 1994, "Developmental Biology of Olfactory Sensory Neurons", *Seminars in Cell Biology*, 5, no. 1, pp. 3-10.
- Farbman, A. I., and J. A. Poss, 1996, "Transforming Growth Factor-Alpha and Other Growth Factors Stimulate Cell Division in Olfactory Epithelium In Vitro", *Journal of Neurobiology*, 30, no. 2, pp. 267-280.
- Fawcett, J. W., and R. A. Asher, 1999, "The Glial Scar and Central Nervous System Repair", *Brain Research Bulletin*, 49, no. 6, pp. 377-391.
- Fleisch, V. C., B. Fraser, and W. T. Allison, 2011, "Investigating Regeneration and Functional Integration of CNS Neurons: Lessons from Zebrafish Genetics and Other Fish Species", *Biochimica Et Biophysica Acta (BBA) - Molecular Basis of Disease*, 1812, no. 3, pp. 364-380.
- Fitch, M. T., and J. Silver, 2008, "CNS Injury, Glial Scars, and Inflammation: Inhibitory Extracellular Matrices and Regeneration Failure", *Experimental Neurology*, 209, no. 2, pp. 294-301.
- Fry, D. W., A. J. Kraker, A. McMichael, L. A. Ambroso, J. M. Nelson, W. R. Leopold, R. W. Connors, and A. J. Bridges, 1994, "A Specific Inhibitor of the Epidermal Growth Factor Receptor Tyrosine Kinase" *Science*, 265, no. 5175, pp. 1093-1095.
- Gadye, L., D. Das, M. A. Sanchez, K. Street, A. Baudhuin, A. Wagner, M. B. Cole, Y. G. Choi, N. Yosef, E. Purdom, S. Dudoit, D. Risso, J. Ngai, and R. B. Fletcher, 2017, "Injury Activates Transient Olfactory Stem Cell States with Diverse Lineage Capacities", *Cell Stem Cell*, 21, no. 6, pp. 775-790.

- Ganz, J., J. Kaslin, S. Hochmann, D. Freudenreich, and M. Brand, 2010, “Heterogeneity and FGF Dependence of Adult Neural Progenitors in The Zebrafish Telencephalon”, *Glia*, 58, no. 11, pp. 1345-1363.
- Garcia-Verdugo, J.M., S. Ferron, N. Flames, L. Collado, E. Desfilis, and E. Font, 2002, “The Proliferative Ventricular Zone in Adult Vertebrates: A Comparative Study Using Reptiles, Birds, and Mammals”, *Brain Research Bulletin*, 57, pp. 765-775.
- Garcia-Verdugo, J.M., S. Llahi, I. Ferrer, and C. Lopez-Garcia, 1989, “Postnatal Neurogenesis in The Olfactory Bulbs of a Lizard: A Tritiated Thymidine Autoradiographic Study” *Neuroscience Letters*, 98, pp. 247-252.
- Gaze, R. M., and M. J. Keating, 1972, “The Visual System and “Neuronal Specificity””, *Nature*, 237, no. 5355, pp. 375-378.
- Getchell, M.L., and T.K. Mellert, 1991, “Olfactory Mucus Secretion. In: Smell and Taste in Health and Disease”, *New York: Raven Press*, pp. 83-95.
- Getchell, T.V., and M.L. Getchell, 1982, “Physiology of vertebrate olfactory chemoreception”, *Fragrance Chemistry*, pp. 1-25.
- Gilbert, M. A., B. Lin, J. Peterson, W. Jang, and J. E. Jang, 2015, “Neuregulin1 and ErbB Expression in the Uninjured and Regenerating Olfactory Mucosa”, *Gene expression patterns: GEP*, 19, no. 1-2, pp. 108-119.
- Goldman, S., 2005, “Stem and Progenitor Cell–Based Therapy of The Human Central Nervous System”, *Nature Biotechnology*, 23, no. 7, pp. 862-871.
- Goldstein, A.M. and M.C. Fishman, 1998, “Notochord Regulates Cardiac Lineage in Zebrafish Embryos”, *Developmental Biology*, 201, pp. 247-252.

- Goodyer, P. R., J. Fata, L. Mulligan, D. Fischer, R. Fagan, H. J. Guyda, and C. G. Goodyer, 1991, "Expression of Transforming Growth Factor-Alpha and Epidermal Growth Factor Receptor in Human Fetal Kidneys", *Molecular and cellular endocrinology*, 77, no. 1-3, pp. 199-206.
- Gómez-Nicola, D., B. Valle-Argos, N. Pallas-Bazarra, and M. Nieto-Sampedro, 2011, "Interleukin-15 Regulates Proliferation and Self-Renewal of Adult Neural Stem Cells", *Molecular Biology of The Cell*, 22, no. 12, pp. 1960-1970.
- Götz, M., and Y.A. Barde, 2005, "Radial Glial Cells Defined and Major Intermediates Between Embryonic Stem Cells and CNS Neurons", *Neuron*, 46, pp. 369-372.
- Götz, M., E. Hartfuss, and P. Malatesta, 2002, "Radial Glial Cells as Neuronal Precursors: A New Perspective on the Correlation of Morphology and Lineage Restriction in the Developing Cerebral Cortex of Mice", *Brain Research Bulletin*, 57, pp. 777-788.
- Gould, E., A. J. Reeves, M. Fallah, P. Tanapat, C. G. Gross, and E. Fuchs, 1999, "Hippocampal Neurogenesis in Adult Old World Primates", *Proceedings of the National Academy of Sciences of the United States of America*, 96, no. 9, pp. 5263-5267.
- Graziadei, P.P.C. and G.A.M. Graziadei, 1979, "Neurogenesis and Neuron Regeneration in The Olfactory System of Mammals: Morphological Aspects of Differentiation and Structural Organization of The Olfactory Sensory Neurons", *Journal of Neurocytology*, 8, pp. 1-18.
- Green, P. A., B. Van Valkenburgh, B. Pang, D. Bird, T. Rowe, and A. Curtis, 2012, "Respiratory and Olfactory Turbinal Size in Canid and Arctoid Carnivorans", *Journal of Anatomy*, 221, no. 6, pp. 609-621.

- Guo, G., M. Huss, G.Q. Tong, C. Wang, L. Li Sun, N.D. Clarke, and P. Robson, 2010, “Resolution of Cell Fate Decisions Revealed by Single-Cell Gene Expression Analysis from Zygote to Blastocyst”, *Developmental Cell*, 20, no. 18(4), pp. 675-85.
- Guo, Y. J., W. W. Pan, S. B. Liu, Z. F. Shen, Y. Xu, and L. L. Hu, 2020, “ERK/MAPK Signalling Pathway and Tumorigenesis”, *Experimental and Therapeutic Medicine*, 19, no. 3, pp. 1997-2007.
- Hansen, L. A., N. Alexander, M. E. Hogan, J. P. Sundberg, A. Dlugosz, D. W. Threadgill, T. Magnuson, and S. H. Yuspa, 1997, “Genetically Null Mice Reveal a Central Role for Epidermal Growth Factor Receptor in the Differentiation of the Hair Follicle and Normal Hair Development”, *The American Journal of Pathology*, 150, no. 6, pp. 1959-1975.
- Hardy, K., and S. Spanos, 2002, “Growth Factor Expression and Function in The Human and Mouse Preimplantation Embryo”, *The Journal of Endocrinology*, 172, no. 2, pp. 221-236.
- Hasan, S., P. Hétié, and E. L. Matunis, 2015, “Niche Signaling Promotes Stem Cell Survival in The Drosophila Testis via the JAK-STAT Target DIAP1”, *Developmental biology*, 404, no. 1, pp. 27-39.
- Hemmings, B. A., and D. F. Restuccia, 2012, “PI3K-PKB/Akt Pathway”, *Cold Spring Harbor Perspectives in Biology*, 4, no. 9.
- Herrera, S. C., and E. A. Bach, 2019, “JAK/STAT Signaling in Stem Cells and Regeneration: from Drosophila to Vertebrates”, *Development*, 146, no. 2.
- Herrick, D. B., B. Lin, J. Peterson, N. Schnittke, and J. E. Schwob, 2017, “NOTCH1 Maintains Dormancy of Olfactory Horizontal Basal Cells, A Reserve Neural Stem Cell”, *Proceedings of the National Academy of Sciences*, 114, no. 28.

- Higashiyama, S., H. Iwabuki, C. Morimoto, M. Hieda, H. Inoue, and N. Matsushita, 2008, "Membrane-Anchored Growth Factors, The Epidermal Growth Factor Family: Beyond Receptor Ligands", *Cancer Science*, 99, no. 2, pp. 214-220.
- Higashiyama, S., and D. Nanba, 2005, "ADAM-Mediated Ectodomain Shedding of HB-EGF in Receptor Cross-Talk", *Biochimica et Biophysica Acta*, 1751, no. 1, pp. 110-117.
- Hitoshi, S., T. Alexson, V. Tropepe, D. Donoviel, A. J. Elia, J. S. Nye, R. A. Conlon, T. W. Mak, A. Bernstein, and D. van der Kooy, 2002, "Notch Pathway Molecules are Essential for the Maintenance, but not the Generation, of Mammalian Neural Stem Cells", *Genes & Development*, 16, no. 7, pp. 846-858.
- Holbrook, E. H., K. E. Szumowski, and J. E. Schwob, 1995, "An Immunochemical, Ultrastructural, and Developmental Characterization of the Horizontal Basal Cells of Rat Olfactory Epithelium", *The Journal of Comparative Neurology*, 363, no. 1, pp. 129-146.
- Hu, Q., L. Zhang, J. Wen, S. Wang, M. Li, R. Feng, X. Yang, and L. Li, 2010, "The EGF Receptor-Sox2-EGF Receptor Feedback Loop Positively Regulates the Self-Renewal of Neural Precursor Cells", *Stem Cells*, 28, no. 2, pp. 279-286.
- Huard, J. M., and J. E. Schwob, 1995, "Cell Cycle of Globose Basal Cells in Rat Olfactory Epithelium", *Developmental Dynamics*, 203, no. 1, pp. 17-26.
- Ishibe, S., A. Karihaloo, H. Ma, J. Zhang, A. Marlier, M. Mitobe, A. Togawa, R. Schmitt, J. Czyczk, M. Kashgarian, D. S. Geller, S. S. Thorgeirsson, and L. G. Cantley, 2009, "Met and the Epidermal Growth Factor Receptor Act Cooperatively to Regulate Final Nephron Number and Maintain Collecting Duct Morphology", *Development*, 136, no. 2, pp. 337-345.

- Ito, T., H. Ando, T. Suzuki, T. Ogura, K. Hotta, Y. Imamura, Y. Yamaguchi, and H. Handa, 2010, "Identification of a Primary Target of Thalidomide Teratogenicity" *Science*, 327, no. 5971, pp. 1345-1350.
- Iqbal, T., and C. Byrd-Jacobs, 2010, "Rapid Degeneration and Regeneration of The Zebrafish Olfactory Epithelium After Triton X-100 Application", *Chemical Senses*, 35, no. 5, pp. 351-361.
- Iwamoto, R., N. Mine, H. Mizushima, and E. Mekada, 2017, "ErbB1 and ErbB4 Generate Opposing Signals Regulating Mesenchymal Cell Proliferation During Valvulogenesis", *Journal of Cell Science*, 130, no. 7, pp. 1321-1332.
- Iwamoto, R., S. Yamazaki, M. Asakura, S. Takashima, H. Hasuwa, K., Miyado, S. Adachi, M. Kitakaze, K. Hashimoto, G. Raab, D. Nanba, S. Higashiyama, M. Hori, M. Klagsbrun, and E. Mekada, 2003, "Heparin-Binding EGF-Like Growth Factor and ErbB Signaling is Essential for Heart Function", *Proceedings of the National Academy of Sciences of the United States of America*, 100, no. 6, pp. 3221-3226.
- Iyer, G., J. Price, S. Bourgeois, E. Armstrong, S. Huang, and P. M. Harari, 2016, "Insulin-Like Growth Factor 1 Receptor Mediated Tyrosine 845 Phosphorylation of Epidermal Growth Factor Receptor in The Presence of Monoclonal Antibody Cetuximab", *BioMed Central*, 16, no. 1, p. 773.
- Kalman, M., 2002, "GFAP Expression Withdraws-A Trend of Glial Evolution?", *Brain Research Bulletin*, 57, pp. 509-511.
- Kaplan, M. S., 1981, "Neurogenesis in the 3-Month-Old Rat Visual Cortex", *The Journal of Comparative Neurology*, 195, no. 2, pp. 323-338.
- Kaplan, M. S., 1983, "Proliferation of Subependymal Cells in The Adult Primate CNS: Differential Uptake of DNA Labelled Precursors", *Journal of Hirnforsch*, 24, no. 1, pp. 23-33.

- Kaplan, M. S., and J. W. Hinds, 1977, "Neurogenesis in the Adult Rat: Electron Microscopic Analysis of Light Radioautographs", *Science*, 197, no. 4308, pp. 1092-1094.
- Kaslin, J., J. Ganz, M. Geffarth, H. Grandel, S. Hans, and M. Brand, 2008, "Stem Cells in the Adult Zebrafish Cerebellum: Initiation and Maintenance of a Novel Stem Cell Niche", *Journal of Neuroscience*, 29, no. 19, pp. 6142-6153.
- Kaslin, J., J. Ganz, and M. Brand, 2008, "Proliferation, Neurogenesis and Regeneration in the Non-Mammalian Vertebrate Brain", *Philosophical Transactions of The Royal Society of London. Series B, Biological Sciences*, 363, no. 1489, pp. 101-122.
- Katsuyama, T., F. Comoglio, M. Seimiya, E. Cabuy, and R. Paro, 2015, "During Drosophila Disc Regeneration, JAK/STAT Coordinates Cell Proliferation with Dilp8-Mediated Developmental Delay", *Proceedings of the National Academy of Sciences of the United States of America*, 112, no. 18, pp. 2327-2336.
- Kempermann, G., H. Song, and F. H. Gage, 2015, "Neurogenesis in the Adult Hippocampus", *Cold Spring Harbor Perspectives in Biology*, 7, no. 9.
- Kirn, J. R., A. Alvarez-Buylla, and F. Nottebohm, 1991, "Production and Survival of Projection Neurons in A Forebrain Vocal Center of Adult Male Canaries", *The Journal of Neuroscience*, 11, no. 6, pp. 1756-1762.
- Kleppe, M., M. H. Spitzer, S. Li, C. E. Hill, L. Dong, E. Papalex, S. De Groote, R. L. Bowman, M. Keller, P. Koppikar, F. T. Rapaport, J. Teruya-Feldstein, J. Gandara, C. E. Mason, G. P. Nolan, and R. L. Levine, 2017, "Jak1 Integrates Cytokine Sensing to Regulate Hematopoietic Stem Cell Function and Stress Hematopoiesis", *Cell, Stem Cell*, 21, no. 4, pp. 489-501.

- Kocagoz, Y., M. C. Demirler, S. E. Eski, K. Guler, Z. Dokuzluoglu, and S. H. Fuss, 2022, “Disparate Progenitor Cell Populations Contribute to Maintenance and Repair Neurogenesis in the Zebrafish Olfactory Epithelium”, *Cell and Tissue Research*.
- Kocagöz, Y., 2021, *Cellular and Molecular Analysis of Regenerative Neurogenesis in The Zebrafish (Danio Rerio) Olfactory Epithelium*, Ph.D. Thesis, Bogazici University.
- Kondo, T., and M. Raff, 2004, “Chromatin Remodeling and Histone Modification in the Conversion of Oligodendrocyte Precursors to Neural Stem Cells”, *Genes & Development*, 18, no. 23, pp. 2963-2972.
- Kornblum, H. I., H. K. Raymon, R. S. Morrison, K. P. Cavanaugh, R. A. Bradshaw, and F. M. Leslie, 1990, “Epidermal Growth Factor and Basic Fibroblast Growth Factor: Effects on an Overlapping Population of Neocortical Neurons In Vitro”, *Brain Research*, 535, no. 2, pp. 255-263.
- Knudsen, S. L., A. S. Mac, L. Henriksen, B. van Deurs, and L. M. Grøvdal, 2014, “EGFR Signaling Patterns Are Regulated by Its Different Ligands”, *Growth Factors*, 32, no. 5, pp. 155-163.
- Krishna, N. S., S. S. Little, and T. V. Getchell, 1996, “Epidermal Growth Factor Receptor mRNA and Protein Are Expressed in Progenitor Cells of the Olfactory Epithelium”, *The Journal of Comparative Neurology*, 373, no. 2, pp. 297-307.
- Krolewski, R. C., A. Packard, W. Jang, H. Wildner, and J. E. Schwob, 2012, “ASCL1 (Mash1) Knockout Perturbs Differentiation of Nonneuronal Cells in Olfactory Epithelium”, *Plos One*, 7, p. 12.
- Kyriakis, J. M., and J. Avruch, 2012, “Mammalian MAPK Signal Transduction Pathways Activated by Stress and Inflammation: A 10-Year Update”, *Physiological Reviews*, 92, no. 2, pp. 689-737.

- La Fortezza, M., M. Schenk, A. Cosolo, A. Kolybaba, I. Grass, and A. K. Classen, 2016, "JAK/STAT Signalling Mediates Cell Survival in Response to Tissue Stress", *Development*, 143, no. 16, pp. 2907-2919.
- Labusch, M., L. Mancini, D. Morizet, and L. Bally-Cuif, 2020, "Conserved and Divergent Features of Adult Neurogenesis in Zebrafish", *Frontiers in Cell and Developmental Biology*, 8, p. 525.
- Leung, Y.F., P. Ma, and J.E. Dowling, 2007, "Gene Expression Profiling of Zebrafish Embryonic Retinal Pigment Epithelium in Vivo", *Investigative Ophthalmology & Visual Science*. 48, no. 2, pp. 881-890.
- Levison, S.W., and J.E. Goldman, 1993, "Both Oligodendrocytes and Astrocytes Develop from Progenitors in The Subventricular Zone of Postnatal Rat Forebrain", *Neuron*, 10, no. 2, pp. 201-12.
- Liang, J., D. Wang, G. Renaud, T. G. Wolfsberg, A. F. Wilson, and S. M. Burgess, 2012, "The Stat3/Socs3a Pathway Is a Key Regulator of Hair Cell Regeneration in Zebrafish", *Neuroscience*, 32, no. 31, pp. 10662-10673.
- Linggi, B., and G. Carpenter, 2006, "ErbB Receptors: New Insights on Mechanisms and Biology", *Trends in Cell Biology*, 16, no. 12, pp. 649-656.
- Lopez-Garcia, C., and F.J. Martinez-Guijarro, 1988, "Neurons in The Medial Cortex Give Rise to Timmpositive Boutons in The Cerebral Cortex of Lizards", *Brain Research*, 463, pp. 205-217.
- Lopez-Garcia, C., P. Tineo, and J. Del Corral, 1984, "Increase of The Neuron Number in Some Cerebral Cortical Areas of a Lizard, *Podarcis Hispanica* (Steind; 1870) During Postnatal Periods of Life", *Journal of Hirnforsch.* 25255, pp. 259.

- Mackay-Sim, A., and P. Kittel, 1991, "Cell Dynamics in The Adult Mouse Olfactory Epithelium: A Quantitative Autoradiographic Study", *Journal of Neuroscience*, 11, no. 4, pp. 979-84.
- Mahanthappa, N. K., and G. A. Schwarting, 1993, "Peptide Growth Factor Control of Olfactory Neurogenesis and Neuron Survival In Vitro: Roles of EGF And TGF-Betas", *Neuron*, 10, no. 2, pp. 293-305.
- Manglapus, G.L., S.L. Youngentob, and J.E. Schwob, 2004, "Expression Patterns of Basic Helix-Loop-Helix Transcription Factors Define Subsets of Olfactory Progenitor Cells", *The Journal of Comparative Neurology*, 479, no. 2, pp. 216-233.
- Mannon, P. J., and J. M. Mele, 2000, "Peptide YY Y1 Receptor Activates Mitogen-Activated Protein Kinase and Proliferation in Gut Epithelial Cells Via the Epidermal Growth Factor Receptor", *The Biochemical Journal*, 350, no. 3, pp. 655-661.
- Marchioro, M., J.M. de Azevedo Mota Nunes, A.M. Rabelo Ramalho, A. Molowny, E. Perez-Martinez, X. Ponsoda, C. Lopez-Garcia, 2005, "Postnatal Neurogenesis in The Medial Cortex of the Tropical Lizard *Tropidurus hispidus*", *Neuroscience*, 134, pp. 407-413.
- Margotta, V., A. Morelli, 1997, "Contribution of Radial Glial Cells to Neurogenesis and Plasticity of Central Nervous System in Adult Vertebrates", *Animal Biology*, 6, pp. 101-108.
- Mazzoni, I. E., and R. L. Kenigsberg, 1994, "Localization and Characterization of Epidermal Growth-Factor Receptors in the Developing Rat Medial Septal Area in Culture.", *Brain Research*, 656, no. 1, pp. 115-126.
- Mascia, F., V. Mariani, G. Girolomoni, and S. Pastore, 2003, "Blockade of the EGF Receptor Induces a Deranged Chemokine Expression in Keratinocytes Leading to Enhanced Skin Inflammation", *The American Journal of Pathology*, 163, no. 1, pp. 303-312.

- Miettinen, P. J., D. Warburton, D. Bu, J. S. Zhao, J. E. Berger, P. Minoo, T. Koivisto, L. Allen, L. Dobbs, Z. Werb, and R. Derynck, 1997, "Impaired Lung Branching Morphogenesis in the Absence of Functional EGF Receptor", *Developmental Biology*, 186, no. 2, pp. 224-236.
- Mitamura, T., S. Higashiyama, N. Taniguchi, M. Klagsbrun, and E. Mekada, 1995, "Diphtheria Toxin Binds to The Epidermal Growth Factor (EGF)-Like Domain of Human Heparin-Binding EGF-Like Growth Factor/Diphtheria Toxin Receptor and Inhibits Specifically Its Mitogenic Activity", *The Journal of Biological Chemistry*, 270, no. 3, pp. 1015-1019.
- Miyata, T., A. Kawaguchi, H. Okano, and M. Ogawa, 2001, "Asymmetric Inheritance of Radial Glial Fibers by Cortical Neurons", *Neuron*, 31, no. 5, pp. 727-741.
- Miyata, T., A. Kawaguchi, K. Saito, M. Kawano, T. Muto, M. Ogawa, 2004, "Asymmetric Production of Surface-Dividing and Non-Surface-Dividing Cortical Progenitor Cells", *Development*, 131, no. 13, pp. 3133-45.
- Mombaerts P., 2004, "Genes and Ligands for Odorant, Vomeronasal and Taste Receptors", *Nature Reviews. Neuroscience*, 5, no. 4, pp. 263-278.
- Moulton, D. G., 1974, "Dynamics of Cell Populations in the Olfactory Epithelium". *Annals of the New York Academy of Sciences*, 237, no. 1, pp. 52-61.
- Mombaerts P., 2006, "Axonal Wiring in The Mouse Olfactory System", *Annual Review of Cell and Developmental Biology*, 22, pp. 713-737.
- Nakamura, K., R. Ogawa, and E. Mekada, 1995, "Membrane-Anchored Heparin-Binding EGF-Like Growth Factor (HB-EGF) And Diphtheria Toxin Receptor-Associated Protein (DRAP27)/CD9 Form a Complex with Integrin Alpha 3 Beta 1 At Cell-Cell Contact Sites", *The Journal of Cell Biology*, 129, no. 6, pp. 1691-1705.

- Nicolas, C. S., M. Amici, Z. A. Bortolotto, A. Doherty, Z. Csaba, A. Fafouri, P. Dournaud, P. Gressens, G. L. Collingridge, and S. Peineau, 2013, "The Role of JAK-STAT Signaling Within The CNS", *Jak-Stat*, 2, no. 1.
- Nielsen, B. L., T. Jezierski, J. E. Bolhuis, L. Amo, F. Rosell, M. Oostindjer, J. W. Christensen, D. McKeegan, D. L. Wells, and P. Hepper, 2015, "Olfaction: An Overlooked Sensory Modality in Applied Ethology and Animal Welfare", *Frontiers in Veterinary Science*, 2.
- Noctor, S. C., A. C. Flint, T. A. Weissman, R. S. Dammerman, and A. R., Kriegstein, 2001, "Neurons Derived from Radial Glial Cells Establish Radial Units in Neocortex", *Nature*, 409, no. 6821, pp. 714-720.
- Noma, T., A. Lemaire, S. V. Naga Prasad, L. Barki-Harrington, D. G. Tilley, J. Chen, P. Le Corvoisier, J. D. Violin, H. Wei, R. J. Lefkowitz, and H. A. Rockman, 2007, "1Beta-Arrestin-Mediated Beta1-Adrenergic Receptor Transactivation of The EGFR Confers Cardioprotection", *The Journal of Clinical Investigation*, 117, no. 9, pp. 2445-2458.
- Nomura, T., S. Takahashi, and T. Ushiki, 2004, "Cytoarchitecture of The Normal Rat Olfactory Epithelium: Light and Scanning Electron Microscopic Studies", *Archives of Histology and Cytology*, 67, pp. 159-170.
- Nottebohm, F., 1985, "Neuronal Replacement in Adulthood: Hope for A New Neurology.", *Annals of the New York Academy of Sciences*, 457, pp. 143-161.
- O'Loughlin, E. V., M. Chung, M. Hollenberg, J. Hayden, I. Zahavi, and D. G. Gall, 1985, "Effect of Epidermal Growth Factor on Ontogeny of The Gastrointestinal Tract", *The American Journal of Physiology*, 249, no. 6.1, pp. 674-678.
- Ohlsson, B., C. Jansen, I. Ihse, and J. Axelson, 1997, "Epidermal Growth Factor Induces Cell Proliferation in Mouse Pancreas and Salivary Glands", *Pancreas*, 14, no. 1, pp. 94-98.

- Onishi, K., And P. W. Zandstra, 2015, “LIF Signaling in Stem Cells and Development”, *Development*, 142, No. 13, Pp. 2230-2236.
- Ottoson, D., and G. M. Shepherd, 1966, “Experiments and Concepts in Olfactory Physiology”, *Progress in Brain Research*, pp. 83-138.
- Owens, D. M., and S. M. Keyse, 2007, “Differential Regulation of MAP Kinase Signalling by Dual-Specificity Protein Phosphatases”, *Oncogene*, 26, no. 22, pp. 3203-3213.
- Owji, S., and M. M. Shoja, 2019, “The History of Discovery of Adult Neurogenesis”, *Clinical Anatomy*, 33, no. 1, pp. 41-55.
- Packard, A. I., B. Lin, and J. E. Schwob, 2016, “Sox2 and Pax6 Play Counteracting Roles in Regulating Neurogenesis within the Murine Olfactory Epithelium”, *Plos One*, 11, no. 5.
- Packard, A., N. Schnittke, R.-A. Romano, S. Sinha, and J. E. Schwob, (2011), “NP63 Regulates Stem Cell Dynamics in The Mammalian Olfactory Epithelium”, *Journal of Neuroscience*, 31, no. 24, pp. 8748-8759.
- Paria, B. C., K. Elenius, M. Klagsbrun, and S. K. Dey, 1999, “Heparin-Binding EGF-Like Growth Factor Interacts with Mouse Blastocysts Independently of ErbB1: A Possible Role for Heparan Sulfate Proteoglycans and ErbB4 in Blastocyst Implantation”, *Development*, 126, no. 9, pp. 1997-2005.
- Pekny, M. and M. Pekna, 2004, “Astrocyte Intermediate Filaments in CNS Pathologies and Regeneration”, *Journal of Pathology*, 204, pp. 428-437.

- Peltier, J., A. O'Neill, and D. V. Schaffer, 2007, "PI3K/Akt and CREB Regulate Adult Neural Hippocampal Progenitor Proliferation and Differentiation", *Developmental Neurobiology*, 67, no. 10, pp. 1348-1361.
- Pereira, L., M. Font-Nieves, C. Van den Haute, V. Baekelandt, A. M. Planas, and E. Pozas, 2015, "IL-10 Regulates Adult Neurogenesis by Modulating ERK and STAT3 Activity", *Frontiers in Cellular Neuroscience*, 9, no. 57.
- Perez-Sanchez, F., A. Molowny, J.M. Garcia-Verdugo, C. Lopez-Garcia, 1989, "Postnatal Neurogenesis in The Nucleus Sphericus of the Lizard, *Podarcis hispanica*", *Neuroscience Letters*, 106, pp. 71-75.
- Peus, D., R. A. Vasa, A. Meves, A. Beyerle, and M. R. Pittelkow, 2000, "UVB-Induced Epidermal Growth Factor Receptor Phosphorylation Is Critical for Downstream Signaling and Keratinocyte Survival", *Photochemistry and Photobiology*, 72, no. 1, pp. 135-140.
- Pevny, L. H., and S. K. Nicolis, 2010, "Sox2 Roles in Neural Stem Cells", *The International Journal of Biochemistry & Cell Biology*, 42, no. 3, pp. 421-424.
- Piepkorn M., 1996, "Overexpression of Amphiregulin, A Major Autocrine Growth Factor for Cultured Human Keratinocytes, In Hyperproliferative Skin Diseases", *The American Journal of Dermatopathology*, 18, no. 2, pp. 165-171.
- Poulsen, S. S., E. Nexø, P. S. Olsen, J. Hess, and P. Kirkegaard, 1986, "Immunohistochemical Localization of Epidermal Growth Factor in Rat and Man", *Histochemistry*, 85, no. 5, pp. 389-394.
- Post, Y., and H. Clevers, 2019, "Defining Adult Stem Cell Function at Its Simplest: The Ability to Replace Lost Cells Through Mitosis", *Cell Stem Cell*, 25, no. 2, pp. 174-183.

- Puehringer, D., N. Orel, P. Lüningschrör, N. Subramanian, T. Herrmann, M. V. Chao, and M. Sendtner, 2013, “EGF Transactivation of Trk Receptors Regulates the Migration of Newborn Cortical Neurons”, *Nature Neuroscience*, 16, 4, pp. 407-415.
- Rawlings, J. S., K. M. Rosler, and D. A. Harrison, 2004, “The JAK/STAT Signaling Pathway”, *Journal of Cell Science*, 117, no. 8, pp. 1281-1283.
- Rébé, C., F. Végran, H. Berger, and F. Ghiringhelli, 2013, “STAT3 Activation: A Key Factor in Tumor Immunoescape”, *Jak-Stat*, 2, no. 1.
- Recasens-Alvarez, C., A. Ferreira, and M. Milán, 2017, “JAK/STAT Controls Organ Size and Fate Specification by Regulating Morphogen Production and Signalling”, *Nature Communications*, 8, no. 13815.
- Rescan, C., S. Milán, V. H. Lefebvre, U. Frandsen, T. Klein, M. Foschi, D. G. Pipeleers, R. Scharfmann, O. D. Madsen, and H. Heimberg, 2005, “EGF-Induced Proliferation of Adult Human Pancreatic Duct Cells Is Mediated by the MEK/ERK Cascade”, *Laboratory Investigation: A Journal of Technical Methods and Pathology*, 85, no. 1, pp. 65-74.
- Richter K. S., 2008, “The Importance of Growth Factors for Preimplantation Embryo Development and In-Vitro Culture”, *Current Opinion in Obstetrics & Gynecology*, 20, no. 3, pp. 292-304.
- Rhim, J. H., X. Luo, D. Gao, X. Xu, T. Zhou, F. Li, P. Wang, S. T. Wong, and X. Xia, 2016, “Cell Type-Dependent Erk-Akt Pathway Crosstalk Regulates the Proliferation of Fetal Neural Progenitor Cells”, *Scientific Reports*, 6, no. 26547.
- Rogers, S. A., G. Ryan, and M. R. Hammerman, 1992, “Metanephric Transforming Growth Factor-Alpha Is Required for Renal Organogenesis in Vitro” *The American Journal of Physiology*, 262, no. 4.2, pp. 533-539.

- Qiu, J., D. Cai, M.T. Filbin, 2000, "Glial Inhibition of Nerve Regeneration in The Mature Mammalian CNS", *Glia*, 29, pp. 166-174.
- Rakic. P., 2002, "Neurogenesis in Adult Primate Neocortex: An Evaluation of the Evidence", *Nature Reviews Neuroscience.*, 3, pp. 65-71.
- Raymond, P.A., and S.S. Easter, Jr., 1983, "Postembryonic Growth of the Optic Tectum in Goldfish. I. Location of Germinal Cells and Numbers of Neurons Produced" *Journal of Neuroscience*, 3, no. 5, pp. 1077-1091.
- Reimer, M. M., I. Sorensen, V. Kuscha, R. E. Frank, C. Liu, C. G. Becker, and T. Becker, 2008, "Motor Neuron Regeneration in Adult Zebrafish", *Journal of Neuroscience*, 28, no. 34, pp. 8510-8516.
- Repertinger, S. K., E. Campagnaro, J. Fuhrman T. El-Abaseri, S. H. Yuspa, and L. A. Hansen, 2004, "EGFR Enhances Early Healing After Cutaneous Incisional Wounding", *The Journal of Investigative Dermatology*, 123, no. 5, pp. 982-989.
- Robson, J. P., B. Wagner, E. Gltzner, F. L. Heppner, T. Steinkellner, D. Khan, C. Petritsch, D. D. Pollak, H. H. Sitte, and M. Sibilica, 2018, "Impaired Neural Stem Cell Expansion and Hypersensitivity to Epileptic Seizures in Mice Lacking The EGFR in The Brain", *The FEBS journal*, 285, no. 17, pp. 3175-3196.
- Romano, R., and Bucci, C., 2020, "Role of EGFR in the Nervous System", *Cells*, 9, no. 8, p. 1887.
- Scharff, C., J. R. Kirn, M. Grossman, J. D. Macklis, and F. Nottebohm, 2000, "Targeted Neuronal Death Affects Neuronal Replacement and Vocal Behavior in Adult Songbirds", *Neuron*, 25, no. 2, pp. 481-492.

- Schindelin, J., I. Arganda-Carreras, E. Frise, V. Kaynig, M. Longair, T. Pietzsch, S. Preibisch, C. Rueden, S. Saalfeld, B. Schmid, J. Y. Tinevez, D. J. White, V. Hartenstein, K. Eliceiri, P. Tomancak, and A. Cardona, 2012, "Fiji: An Open-Source Platform for Biological-Image Analysis", *Nature Methods*, 9, no. 7, pp. 676-682.
- Schlessinger J., 2002, "Ligand-Induced, Receptor-Mediated Dimerization and Activation of EGF Receptor", *Cell*, 110, no. 6, pp. 669-672.
- Schwartz Levey, M., D. M. Chikaraishi, and J. S. Kauer, 1991, "Characterization of Potential Precursor Populations in The Mouse Olfactory Epithelium Using Immunocytochemistry and Autoradiography", *The Journal of Neuroscience*, 11, no. 11, pp. 3556-3564.
- Schwob, J.E., W. Jang, E.H. Holbrook, B. Lin, D.B. Herrick, J.N. Peterson, J. Hewitt Coleman, 2017, "Stem and Progenitor Cells of the Mammalian Olfactory Epithelium: Taking Poietic License", *The Journal of Comparative Neurology*, 525, no. 4, pp. 1034-1054.
- Schwob J. E., 2002, "Neural Regeneration and The Peripheral Olfactory System", *The Anatomical Record*, 269, no. 1, pp. 33-49.
- Sibilia, M., J. P. Steinbach, L. Stingl, A. Aguzzi, and E. F. Wagner, 1998, "A Strain-Independent Postnatal Neurodegeneration in Mice Lacking the EGF Receptor", *The EMBO Journal*, 17, no. 3, pp. 719-731.
- Sibilia, M., and E. F. Wagner, 1995, "Strain-Dependent Epithelial Defects in Mice Lacking the EGF Receptor", *Science*, 269, no. 5221, pp. 234-238.
- Simpson, D. L., R. Morrison, J. de Vellis, and H. R. Herschman, 1982, "Epidermal Growth Factor Binding and Mitogenic Activity on Purified Populations of Cells from The Central Nervous System", *Journal of Neuroscience Research*, 8, no. 2-3, pp. 453-462.

- Singh, B., G. Carpenter, and R. J. Coffey, 2016, "EGF Receptor Ligands: Recent Advances", *F1000Research*, 5, p. 2270.
- Song, Y., K.D. Cygnar, B. Sagdullaev, M. Valley, S. Hirsh, A. Stephan, J. Reisert, H. Zhao, 2008, "Olfactory CNG Channel Desensitization by Ca²⁺/Cam Via the B1b Subunit Affects Response Termination but Not Sensitivity to Recurring Stimulation", *Neuron*, 58, pp. 374-386.
- Stoll, S. W., S. Kansra, S. Peshick, D. W. Fry, W. R. Leopold, J. F. Wiesen, M. Sibia, T. Zhang, Z. Werb, R. Derynck, E. F. Wagner, and J. T. Elder, 2001, "Differential Utilization and Localization of ErbB Receptor Tyrosine Kinases in Skin Compared to Normal and Malignant Keratinocytes", *Neoplasia*. 3, no. 4, pp. 339-350.
- Sun, Y., S. K. Goderie, and S. Temple, 2005, "Asymmetric Distribution of EGFR Receptor During Mitosis Generates Diverse CNS Progenitor Cells", *Neuron*, 45, no. 6, pp. 873-886.
- Sung, S. M., D. S. Jung, C. H. Kwon, J. Y. Park, S. K. Kang, and Y. K. Kim, 2007, "Hypoxia/Reoxygenation Stimulates Proliferation Through PKC-Dependent Activation of ERK and Akt in Mouse Neural Progenitor Cells", *Neurochemical Research*, 32, no. 11, pp. 1932-1939.
- Tanizaki, J., I. Okamoto, S. Fumita, W. Okamoto, K. Nishio, and K. Nakagawa, 2011, "Roles of BIM Induction and Survivin Downregulation in Lapatinib-Induced Apoptosis in Breast Cancer Cells with HER2 Amplification", *Oncogene*, 30, no. 39, pp. 4097-4106.
- Taub R., 2004, "Liver Regeneration: From Myth to Mechanism", *Nature Reviews. Molecular Cell Biology*, 5, no. 10, pp. 836-847.
- Threadgill, D. W., A. A. Dlugosz, L. A. Hansen, T. Tennenbaum, U. Lichti, D. Yee, C. LaMantia, T. Mourton, K. Herrup, and R. C. Harris, 1995, "Targeted Disruption of

- Mouse EGF Receptor: Effect of Genetic Background on Mutant Phenotype”, *Science*, 269, no. 5221, pp. 230-234.
- Tsujioka, H., T. Kunieda, Y. Katou, K. Shirahige, T. Fukazawa, and T. Kubo, 2017, “Interleukin-11 Induces and Maintains Progenitors of Different Cell Lineages During *Xenopus* Tadpole Tail Regeneration”, *Nature Communications*, 8, no. 1, p. 495.
- Tucker, M. S., I. Khan, R. Fuchs-Young, S. Price, T. L. Steininger, G. Greene, B. H. Wainer, and M. R. Rosner, 1993, “Localization of Immunoreactive Epidermal Growth Factor Receptor in Neonatal and Adult Rat Hippocampus”, *Brain Research*, 631, no. 1, pp. 65-71.
- Vogalis, F., C. C. Hegg, and M. T. Lucero, 2005, “Ionic Conductances in Sustentacular Cells of the Mouse Olfactory Epithelium”, *The Journal of Physiology*, 562, no. 3, pp. 785-799.
- Wan, J., R. Ramachandran, and D. Goldman, 2012, “HB-EGF Is Necessary and Sufficient for Müller Glia Dedifferentiation and Retina Regeneration”, *Developmental Cell*, 22, no. 2, pp. 334-347.
- Wang, H., K. Gambosova, Z. A. Cooper, M. P. Holloway, A. Kassai, D. Izquierdo, K. Cleveland, C. M. Boney, and R. A. Altura, 2010, “EGF Regulates Survivin Stability Through the Raf-1/ERK Pathway in Insulin-Secreting Pancreatic β -Cells”, *BioMed Central*, 11, p. 66.
- Wang, T., W. Yuan, Y. Liu, Y. Zhang, Z. Wang, X. Zhou, G. Ning, L. Zhang, L. Yao, S. Feng, and X. Kong, 2015, “The Role of the JAK-STAT Pathway in Neural Stem Cells, Neural Progenitor Cells and Reactive Astrocytes After Spinal Cord Injury”, *Biomedical Reports*, 3, no. 2, pp. 141-146.

- Wee, P., and Z. Wang, 2017, “Epidermal Growth Factor Receptor Cell Proliferation Signaling Pathways”, *Cancers*, 9, no. 5, p. 52.
- Wells A., 1999, “EGF Receptor.”, *The International Journal of Biochemistry & Cell Biology*, 31, no. 6, pp. 637-643.
- Wieduwilt, M. J., and M. M. Moasser, 2008, “The Epidermal Growth Factor Receptor Family: Biology Driving Targeted Therapeutics”, *Cellular and Molecular Life Sciences: CMLS*, 65, no. 10, pp. 1566-1584.
- Wilson, K. C. P., and G. Raisman, 1980, “Age-Related Changes in The Neurosensory Epithelium of the Mouse Vomeronasal Organ: Extended Period of Post-Natal Growth in Size and Evidence for Rapid Cell Turnover in The Adult”, *Brain Research*, 185, no. 1, pp. 103-113.
- Wheeler, D. L., S. Huang, T. J. Kruser, M. M. Nechrebecki, E. A. Armstrong, S. Benavente, V. Gondi, K. T. Hsu, and P. M. Harari, 2008, “Mechanisms of Acquired Resistance to Cetuximab: Role of HER (ErbB) Family Members”, *Oncogene*, 27, no. 28, pp. 3944-3956.
- Yang, T., Y. J. Dai, G. Chen, and S. S. Cui, 2020, “Dissecting the Dual Role of The Glial Scar and Scar-Forming Astrocytes in Spinal Cord Injury”, *Frontiers in Cellular Neuroscience*, 14.
- Yarden, Y., and M. X. Sliwkowski, 2001, “Untangling the ErbB Signalling Network”, *Nature Reviews. Molecular Cell Biology*, 2, no. 2, pp. 127-137.
- Yoshida, K., T. Taga, M. Saito, S. Suematsu, A. Kumanogoh, T. Tanaka, H. Fujiwara, M. Hirata, T. Yamagami, T. Nakahata, T. Hirabayashi, Y. Yoneda, K. Tanaka, W. Z. Wang, C. Mori, K. Shiota, N. Yoshida, and T. Kishimoto, 1996, “Targeted Disruption of Gp130, A Common Signal Transducer for the Interleukin 6 Family of Cytokines,

- Leads to Myocardial and Hematological Disorders”, *Proceedings of the National Academy of Sciences of the United States of America*, 93, no. 1, pp. 407-411.
- Yuan, Z. L., Y. J. Guan, D. Chatterjee, and Y. E. Chin, 2005, “Stat3 Dimerization Regulated by Reversible Acetylation of a Single Lysine Residue”, *Science*, 307, no. 5707, pp. 269-273.
- Yusta, B., D. Holland, J. A. Koehler, M. Maziarz, J. L. Estall, R. Higgins, and D. J. Drucker, 2009, “ErbB signaling Is Required for The Proliferative Actions of GLP-2 In the Murine Gut”, *Gastroenterology*, 137, no. 3, pp. 986-996.
- Zeng, F., and R. C. Harris, 2014, “Epidermal Growth Factor, From Gene Organization to Bedside”, *Seminars in Cell & Developmental Biology*, 28, 2-11.
- Zhang, R. L., Z. G. Zhang, and M. Chopp, 2005, “Neurogenesis in the Adult Ischemic Brain: Generation, Migration, Survival, and Restorative Therapy”, *The Neuroscientist*, 11, no. 5, pp. 408-416.
- Zhang, X., V. A. Siclari, S. Lan, J. Zhu, E. Koyama, H. L. Dupuis, M. Enomoto-Iwamoto, F. Beier, and L. Qin, 2011, “The Critical Role of The Epidermal Growth Factor Receptor in Endochondral Ossification”, *Journal of Bone and Mineral Research: The Official Journal of The American Society for Bone and Mineral Research*, 26, no. 11, pp. 2622-2633.
- Zhao, X. F., J. Wan, C. Powell, R. Ramachandran, M. G. Myers, Jr, and D. Goldman, 2014, “Leptin and IL-6 Family Cytokines Synergize to Stimulate Müller Glia Reprogramming and Retina Regeneration”, *Cell Reports*, 9, no. 1, pp. 272-284.
- Zupanc, G. K., and R. F. Sîrbulescu, 2013, “Teleost Fish as A Model System to Study Successful Regeneration of the Central Nervous System”, *Current Topics in Microbiology and Immunology*, 367, pp. 193-233.

APPENDIX A: Chemicals and Reagents

Table A.1. List of chemicals and reagents

Chemical / Reagent	Manufacturer
5- Bromo-2'- Deoxyuridine (BrdU) BioChemica A2139, 0005	AppliChem, Germany
Anti-rabbit Alexa Flour® 555	Life Technologies, USA
Anti-mouse-HuC/D antibody, 1661237	Life Technologies, USA
Anti-mouse-phospho-STAT3 (Tyr708) Antibody, D128-3	MBL Life Science, Japan
Anti-rabbit-Sox2 antibody	Life Technologies, USA
Bovine Serum Albumin (BSA)	New England Biolabs, USA
Calcium Sulfate (CaSO ₄)	Alfa Aesar, Germany
Dimethyl Sulphoxide (DMSO)	Sigma-Aldrich, USA
Hydrochloric Acid (HCl)	Merck, Germany
Human recombinant HB-EGF	R&D Systems, USA
JSI-124, 1571	Tocris, UK
Optimum Cutting Temperature Compound (OCT), 4583	Sakura Finetek, USA
Paraformaldehyde (PFA), P6148-1kg	Sigma-Aldrich, USA
PD153035, SML0564	Sigma-Aldrich, USA
Phenol Red, A7615,01001	AppliChem, USA

Table A.2. List of chemicals and reagents (cont.)

Potassium Chloride (KCl), P9541	Sigma-Aldrich, USA
Potassium Sulfate Monobasic (KH ₂ PO ₄)	Sigma-Aldrich, USA
Sodium Bicarbonate (NaHCO ₃)	Aquatic Habitats, USA
Sodium Chloride (NaCl), S7653	Sigma-Aldrich, USA
Sodium Citrate Tribasic Dihydrate	Sigma-Aldrich, USA
Sodium Phosphate Dibasic	Sigma-Aldrich, USA
Triton X-100, A4975	AppliChem, Germany
Tricane (MS-222)	Sigma-Aldrich, USA
Trizma® Base, T6066	Sigma-Aldrich, USA
Tween®20, 11332465001	Roche, Germany

Table A.3. Solutions and Buffers

Buffer / Solution	Preparation / Content
10X PBS Stock Solution	<ul style="list-style-type: none"> - Dissolve 80g NaCl, 14.4g Na₂PO₄, 2.4g KH₂PO₄, and 2g KCl in ddH₂O to a final 1.0 L volume - Stir until the all the components are dissolved - Sterilize by autoclaving - Adjust pH to 7.4

Table A.4. Solutions and buffers (cont.)

1X PBST	<ul style="list-style-type: none"> - Filtrate 100 ml 10X PBS solution via vacuum filtration - Adjust final volume to 1.0 L by adding ddH₂O - Add 5 ml Tween-20
10X TBS Stock Solution	<ul style="list-style-type: none"> - Dissolve 80.1g NaCl, 60.6g Trizma® base, and 2.g KCl in ddH₂O to a final 1.0 L volume - Stir until the all the components are dissolved - Sterilize by autoclaving - Adjust pH to 7.4
1X TBST	<ul style="list-style-type: none"> - Filtrate 100 ml 10X TBS solution via vacuum filtration - Adjust final volume to 1.0 L by adding ddH₂O - Add 5 ml Tween-20
1M Tris Buffer Solution	<ul style="list-style-type: none"> - Dissolve 30.3 g Trizma® base in ddH₂O to a final volume of 250 ml. - Adjust pH to 9.0

Table A.5. Solutions and buffers (cont.)

4% Paraformaldehyde (PFA) Solution	<ul style="list-style-type: none"> - Add 4 g PFA in 75 ml ddH₂O preheated to 60°C in water bath - To dissolve PFA, raise the pH by adding a few droplets of NaOH until a clear solution is formed - Add 10 ml 10X PBS and mix until there is no precipitation <ul style="list-style-type: none"> - Adjust pH to 7.4 - Complete the solution to a final volume of 100 ml by adding ddH₂O - Filtrate the solution using vacuum filtration <ul style="list-style-type: none"> - Store at 4°C
10 mM Sodium Citrate Buffer Solution	<ul style="list-style-type: none"> - Dissolve 2.9g Na₃C₆H₅O₇ in ddH₂O to a final volume of 1.0 L <ul style="list-style-type: none"> - Adjust pH to 6 - Add 5 ml Tween-20
3% BSA Solution	<ul style="list-style-type: none"> - Dissolve 3g BSA in 100 ml 1X PBST solution - Mix well until a clear solution is formed - Filtrate the solution with a 0.22 µl syringe filter <ul style="list-style-type: none"> - Store at -20°C

Table A.6. Solutions and buffers (cont.)

5% Goat Serum Solution	<ul style="list-style-type: none"> - Heat inactivate the serum for 30 min at 56°C - Take 5 ml serum and complete the volume to 100 ml with 1X TBST and mix well <ul style="list-style-type: none"> - Store at -20°C
1% Triton X-100 Solution	<ul style="list-style-type: none"> - Add 10 μ Triton X-100 to 790 μl 1X PBS and mix well - After the detergent is completely dissolved add 200 μl Phenol Red <ul style="list-style-type: none"> - Mix until you get a reddish solution
10 mM PD153035 Stock Solution	<ul style="list-style-type: none"> - Dissolve 5 mg PD153035 in 1250 ml DMSO - Mix to dissolve and heat briefly if necessary <ul style="list-style-type: none"> - Store at 4°C
1mM JSI-124 Stock Solution	<ul style="list-style-type: none"> - Dissolve 1 mg JSI-124 in 1.94 ml DMSO and mix to dissolve <ul style="list-style-type: none"> - Store at -20°C
PD153035 IP Injection Solution	<ul style="list-style-type: none"> - Take 10 μl of 10mM PD153035 Stock Solution and dissolve in 1X PBS to a final volume of 30 μl
JSI-124 IP Injection Solution	<ul style="list-style-type: none"> - Take 2 μl of 1mM JSI-124 Stock Solution and dissolve in 1X PBS to a final volume of 30 μl

APPENDIX B: Disposable And Non-disposable Equipment

Table B. 1. List of disposable and non-disposable equipment

Equipment	Manufacturer
-20°C Freezer	Uğur, Turkey
-80°C Freezer, Farma 723	Thermo Elektron Corp., USA
4°C Room	Birikim Elektrik, Turkey
Aquatic Habitats	Pentair Aquatic Eco-systems, Inc., USA
Beaker	IsoLab, Germany
Capillary glass (1.00 mm × 0.75 mm × 10'')	Warner Instruments, USA
Coplin Staining Jar with Cover	VWR, USA
Confocal Microscope, SP5-AOBS	Leica Microsystems, USA
Confocal Microscope, SP5-AOBS Software LAS AF	Leica Microsystems, USA
Confocal Microscope, TCS SP8	Leica Microsystems, USA
Confocal Microscope, TCS SP8 Software LAS AF	Leica Microsystems, USA
Cryostat CM3050S	Leica Biosystems, Germany
Dishwasher, Melabor G 7783	Miele, Germany
Fiji Image J Software	Developed at NIH
Forceps, FST	Dumont, Switzerland
GELoader tips, 0.5-20 µl	Eppendorf, Germany
Glass bottle	Isolab, Germany
Glass Slides - Superfrost® Plus	Thermo Scientific, USA

Table B.2. List of disposable and non-disposable equipment (cont.)

Graduate cylinder	Isolab, Germany
Ice Flaker	Brema, Italy
IKA Color Squid magnetic stirrer	IKA works, Inc., USA
Incubator	Nüve, Turkey
Magnetic stirrer and heater, MK 318	Nüve, Turkey
Microinjector, FemtoJet	Eppendorf, Germany
Micropipette tips (2-1000 µl)	CAPP, Germany
Micropipettes (2-1000 µl)	Eppendorf, Germany
Nutator, Polymax 2040	Heidolph, Germany
Orbital shaker, Rotamax 120	Heidolph, Germany
P-97 Micropipette Puller	Sutter Instrument, Co., USA
Parafilm™	Parafilm, USA
pH-meter, pH315i	WTW, Germany
Refrigerator	Arçelik, Turkey
Stereomicroscope	Zeiss, Germany
Super PAP Pen	Liquid Blocker, Japan
Swiftlock Front loading Autoclave	Astell, UK
Syringe filter, 0.22 µm, 99722	TPP, Switzerland
Vortex- Genie 2	Scientific Industries, Inc., USA
Water Bath, WNB 10	Memmert, Germany
U-100 insulin needle (30G)	Beckon Dickinson, USA